Faculty of Aerospace Engineering

Quantifying ageing effect on gaze dynamics

By using identification techniques with an eye-only and an eye-hand pursuit tracking task

J. Büskens

16 April 2018

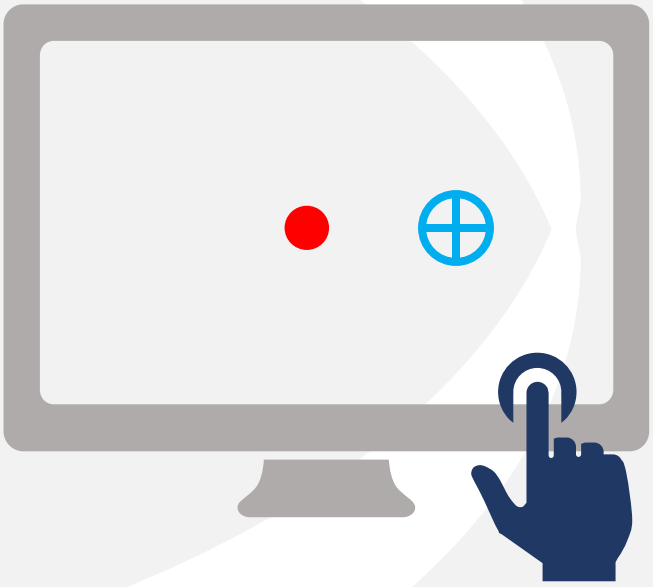

TU Delft Delft University of Technology

Challenge the future

Quantifying ageing effect on gaze dynamics

By using identification techniques with an eye-only and an eye-hand pursuit tracking task

Master of Science Thesis

For obtaining the degree of Master of Science in Aerospace Engineering
at Delft University of Technology

J. Büskens

16 April 2018

Faculty of Aerospace Engineering · Delft University of Technology

Delft University of Technology

Delft University Of Technology
Department Of
Control and Simulation

The undersigned hereby certify that they have read and recommend to the Faculty of Aerospace Engineering for acceptance a thesis entitled **"Quantifying ageing effect on gaze dynamics"** by **J. Büskens** in partial fulfillment of the requirements for the degree of **Master of Science**.

Dated: 16 April 2018

Readers:

prof.dr.ir. M. Mulder

dr.ir. D. M. Pool

dr.ir. J. J. M. Pel (EMC)

dr.ir. M. A. Mitici

Acknowledgements

This thesis report contains my work of the past nine months and also concludes my studies in Delft. It was during these months that I enjoyed my studies not because I learned something for myself, but got to contribute to existing work. Where initially not having an answering sheet when doing research was unknown to me, it turned out this was a lot more fun because of the appreciation of doing something new. This work would not have been completed as such, had it not been for my supervisors.

First of al I would therefore like to thank my daily supervisors Daan Pool and Johan Pel for giving me the oppurtunity to do my thesis project at the Erasmus Medical Center. I enjoyed applying the aerospace knowledge to a for me completely new field. Thank you for all the meetings we had together and I appreciate all your time, guidance and enthusiasm. Secondly I would like to thank Max Mulder, who helped me choose the direction of my thesis which could not have been better.

Of course I would also like to thank the people I spend most of my days with for the past few months, the people from SIM008. I enjoyed the laughs we had together and the discussions that often followed to help each other.

Finally, I would also like to thank my family and friends for all their support. Thank you for either particpating (sometimes twice) in my experiments, or else helping me find suitable participants. It was a privilege to meet so many enthusiastic people willing to contribute to my final thesis.

Contents

List of Figures

List of Tables

Acronyms

CNS	Central Nervous System
DRT	Disjunction Reaction Time
EMC	Erasmus Medical Center
ESC	EyeSeeCam
FCM	Fourier Coefficient Method
FRF	Frequency Response Function
HC	Human Controller
NMS	neuromuscular system
OKR	Optokinetic Response
PPRF	Paramedian Pontine Reticular Formation
SOP	Succesive Organization of Perception
SRT	Simple Reaction Time
VAF	Variance Accounted For
VOR	Vestibulo-ocular Reflex

List of Symbols

Greek Symbols

ω_f	Frequencies of forcing function
ω_g	Frequencies of gaze dynamics
ω_{nms}	Frequencies of neuromuscular system
ϕ_f	Phase shifts of forcing function
π	Ratio of the circumference of a circle to the diameter
τ_e	Time constant of delay
τ_g	Time constant of delay in gaze dynamics
ζ_g	Damping coefficient of gaze dynamics
ζ_{nms}	Damping coefficient of neuromuscular system

Roman Symbols

A_f	Amplitudes of forcing function
K_e	Gain
K_g	Gain for gaze dynamics
N_f	Number of sinusoids in target function

Chapter 1

Introduction

Everyday humans perform hundreds of actions. These actions can be simple daily tasks such as reaching for objects, but they can also be controlling tasks such as driving a car. These actions start with observing and perceiving information that is needed. In order to grab an object, its location needs to be known so it can be grabbed with your hand. The eyes are one of the most important sensory organs to obtain this information. Next, the brains will process this information in different brain regions such that the eye muscles and limb muscles can act accordingly.

Unfortunately there are numerous neurodegenerative diseases that can cause different brain parts to degenerate which can also cause eye symptoms. This can make these simple daily tasks a challenge for people with neurodegenerative diseases. Even though knowledge about neurodegenerative diseases expands everyday, it is still a challenge to diagnose these diseases at an early stage. This is partly because initial symptoms of different neurodegenerative diseases can be similar. Low-level cognitive tests exist to evaluate the basic state of the cognition and eye-hand coordination of the patients (Dubois, Slachevsky, Litvan, and Pillon (2000); Fahn and Elton (1987); Folstein, Folstein, and McHugh (1975); Goetz et al. (2007); Hoehn and Yahr (1998)). The downside of these tests is obvious, they are not accurate enough to monitor degredation in the disease and to distinguish between the different diseases at an early stage. For that reason a lot of research has been performed in finding different tools to classify specific neurodegenerative diseases accurately. One way is gaining more insight into eye-hand coordination. This can be done by having the patient perform certain eye-hand coordination tasks. Insight can be gained by quantifying the dynamics of the tracking performance of the patient. A tracking task is very suitable for this means (D. McRuer et al. (1965)).

A lot of research has been done already on identifying the Human Controller (HC) inside the control loop (D. T. McRuer and Jex (1967)). However, the focus has primarily been on identifying the hand dynamics and knowledge about the ocular motor dynamics during tracking tasks is largely unknown. Before investigating the ocular motor dynamics in patients to use as a clinical tool, more knowledge is needed on the ocular motor dynamics in

healthy people. How does this behavior change when people age? Since neurodegeneration occurs more often in older people, it is important to quantify this ageing effect in the ocular motor dynamics. When this effect is quantified, research can be extended to patients in order to investigate whether the same methods can be used as a classification tool for neurodegenerative diseases.

Previous research performed tracking tasks and compared identified hand dynamics of the HC for people with neurological diseases, with healthy people (de Vries (2015), Haartsen (2017)). The results however also suggested that the same analysis could be done for the ocular motor dynamics by investigating the gaze of the human eye. A tracking task would therefore also be suitable when the gaze can be measured, to identify the gaze dynamics. It is obvious that the gaze influences the tracking performance, since the sensory information is used to activate the muscles. (Niehorster and Siu (2015)) found there was also an influence of manual tracking on the gaze signal. This would also make it interesting to perform a tracking task without manual tracking, to compare the two conditions.

The research objective of this research is thus as stated below.

System identification of the gaze dynamics during an eye-only and an eye-hand pursuit tracking task to differentiate between age groups

The goal of this research therefore is to quantify the ageing effect in the gaze dynamics. The data gathered in this research can be used in the future as a normative database, if the research was to continue and extend to patients. This research can therefore also be seen as a proof of concept of applying the tracking task technique to quantify the gaze dynamics.

The remainder of this report will be structured as follows. Part I will present the scientific paper which is the main deliverable of this research. The paper contains the main work, including the methods used, experiments conducted and results obtained. It will discuss the main findings and report the conclusions. Part II contains the preliminary report, which describes the work that has been performed during the first stage of the thesis work. It contains literature and an initial experiment of which the results will be discussed, which determined the design of the final experiment. Finally, part III contains the appendices. These include the experiment consent form used, the experiment brieing, all FRF models of the participants and the phase margins.

Part I

Paper

Quantifying ageing effect on gaze dynamics using an eye-only and an eye-hand tracking pursuit task

J. Büskens (MSc Student)
Supervisors: dr. ir. D.M. Pool*, dr. ir. J.J.M. Pel**, Prof. dr. ir. M. Mulder*
*Control & Simulation, Department Control and Operations, Faculty of Aerospace Engineering, Delft University of Technology, Delft, Netherlands
**Erasmus MC department of Neuroscience, Rotterdam, Netherlands

***Abstract*— In an effort to develop new tools for the classification of neurodegenerative diseases, the effect on the ocular motor system and specifically the visuomotor integration has been a field of interest for more than a decade. Where tracking tasks have shown the potential to quantify fine motor skills of the hand, too little is known about the ocular motor behavior during tracking tasks to make it clinically applicable. This paper therefore studies the gaze of the human eye and will quantify the ageing effect on the gaze dynamics in healthy controls, as neurodegenerative diseases can be age-related. Experiments were conducted with 40 participants divided in two groups of 20-30 yrs and 55-70 yrs old. The tracking tasks designed involved an eye-only tracking task where a target had to be followed by the eyes alone and an eye-hand tracking task involving the hand to track an element as well. As an addition to the gaze dynamics, the hand dynamics during the eye-hand tracking task has been analyzed too. Two quasi-random forcing functions of increasing bandwidth (increasing difficulty) were used, making it possible to create models for the gaze dynamics and the hand dynamics. Overall, the gaze performance of the older group was worse than the gaze performance of the younger group, apparent in a lower gain parameter K_g when changing task condition and a higher time constant in the eye-hand tracking condition for older people. The second-order model parameters did not show the expected differences. Additionaly, similar yet not significant results were found in the hand dynamics. This research was able to identify an ageing effect in the gaze dynamics and the experiments can therefore be extended to research with patients, using the generated results as normative database.**

***Index Terms*—Eye movements, gaze dynamics, ageing, EyeSeeCam, pursuit tracking tasks, manual tracking, cybernetic approach, system identification**

I. Introduction

THE eyes are one of the most important sensory organs for humans and are vital in many daily tasks. During most of these tasks, the eyes precede the hands, e.g., grabbing an object or pointing somewhere. Eye-hand coordination is thus important to be able to function well at those activities. For people with neurodegenerative diseases, simple activities can become a challenge. Neurodegeneration starts with the damaging or death of pathways of the neurons or of the neurons itself. Neurons are the cells that receive, process and transmit information by making use of electrical or chemical signals and cannot be replaced once damaged [1]. Since neurons are the building blocks of the brain and spinal cord, it is apparent that the brain will lose some functionality when neurons are damaged. The location where the damage occurs, influences the different symptoms that come with the disease. Examples of these symptoms can become apparent in the ocular motor system, thus affecting eye-hand coordination [2]. Where low-level motor tasks exist to help diagnose diseases [3]–[7], more insight into eye-hand coordination could help catch early symptoms. Tracking tasks have shown the potential to outperform these low-level motor tasks, however tracking tasks have primarily been studied for hand dynamics. More knowledge is therefore needed on the ocular motor behavior during tracking tasks. Before studying this behavior in patients however, the variabilty in healthy people needs to be quantified. Some symptoms caused by neurodegeneration can also occur to some degree because of ageing [8]–[11]. Additionally, neurodegeneration occurs more often in older people. Therefore variability can be caused by the ageing effect on which this paper will focus. Symptoms caused by ageing can involve a decrease in brain volume, slower reaction times and an impairment in sensory and perceptual functions [8]. As such the goal of this research is to quantify differences in eye-hand coordination for the different age groups. A positive result would be promising for future research to use the same method to quantify changes in eye-hand coordination for people with neurodegenerative diseases and would make it possible to separate ageing effects from neurodegenerative effects in the future.

Previous research attempted to quantify hand dynamics of people suffering from Parkinson's Disease [12] and people who experienced a cerebellar stroke [13]. This was done by taking a cybernetic approach and using tracking tasks to quantify the dynamics of the patients, which has been an effective method for different applications for decades [14]–[20]. A tracking task is a task where the Human Controller (HC) tries to control a system perturbed by a multi-sine function by minimizing the error between the target and the to be controlled element. As such, a transfer function can be obtained by means of a Fourier transform of the input and output of the participant. The multi-sine signal used to describe the target forcing function has a great effect on the behavior induced in the participant. One of the variables that can be tuned is the shape of the amplitude spectrum affecting the bandwidth of the forcing function [14]. The bandwidth is defined as the frequency up to which the forcing function has significant power. By changing this, the forcing function is thus influenced and thereby the behavior induced. Another

research topic in the field of eye-hand coordination research has been the effect of manual tracking on eye movements [21]–[23]. Experiments were conducted involving both a tracking pursuit task and a task where the same multi-sine signal was used for the target but no element needed to be controlled. During the latter experiment, the participant thus only had to move the eyes to follow the target. Manual tracking was found to have an enhancing effect on the eye movements [22].

The focus of both researches [12] and [13] was on quantifying the tracking performance of the hand. As described above, knowledge about the gaze dynamics is lacking, even though the eyes play such an important role during the tracking. To quantify the gaze dynamics, the same methods can be applied as are used when quantifying hand dynamics. Instead of using the hand input, the gaze input is taken as output signal for the transfer function. The gaze signal can be recorded during the tracking task with an eye tracker. In past research, the effect of bandwidths has been studied for the hand dynamics [14], however the effect on the gaze dynamics is unknown. Additionally, this effect could be different for the two age groups. Therefore two different bandwidths will be used to create two target forcing functions. We are also interested in the influence of manual tracking on eye movements. Although similar experiments were conducted to study the effect of manual tracking [21]–[23], the fitting of a model in order to quantify the gaze dynamics has not been studied. In conclusion, it is not known whether the influence of both the bandwidth and manual tracking on eye movements is existent and/or age dependent, which would result in different effects for different age groups. Therefore both an eye-only and eye-hand tracking task will be used in the experiment. The eye-hand tracking task is a pursuit tracking task involving an element that needs to be controlled by the participant by minimizing the error between the target and the element. The eye-only tracking task will only involve a moving target that the participant will need to follow with the eyes.

We are interested in finding differences in gaze dynamics for the two age groups under different conditions. Therefore this research proposes an experiment with both an eye-only and eye-hand tracking task, each performed for two forcing functions of increasing bandwidth. Two age groups of 20-30 yrs and 55-70 yrs old, each consisting of 20 participants were recruited and performed tracking tasks in these four conditions. The four different conditions were each performed eight times by the participants. The gaze signal was recorded analyzed by using a Fourier transform. The resulting Frequency Response Function (FRF) was used to fit a model for each participant in each condition. The resulting parameters describing the gaze models for the two age groups were compared. The hand data were also recorded during the experiments and these results were also analyzed to accompany the gaze results.

The remainder of this paper will discuss the methods used for the experiment and the analyses in Section II. It will continue with presenting the results in Section III and these will be discussed together with the recommendations in Section IV. Finally, the paper will conclude with the main findings in Section V.

II. Methods

A. Control task

Different control tasks can be selected to induce the desired behavior of the HC and for this study an eye-only an an eye-hand tracking pursuit task were selected. A pursuit display was chosen, as previous research in the field of system identification of the HC with neurodegenerative diseases has shown this to be a succesful display [12], [24].

The eye-only task is similar to a regular pursuit tracking task except for the fact that the controlled element is missing. During this task the participant therefore does not have to control anything but only has to follow the target with the eyes. So the hand is not used in this task. This task was designed to investigate the effect of manual tracking on eye movement performance and whether this has an effect on both groups [22]. The block diagram and display of the eye-only task are shown in Figure 1 and 3a. The gaze signal g can be seen in the block diagram. In this task there is no input of the hand and therefore no u signal in the block diagram. No assumption is done on what the dynamics is inside the control loop, therefore the entire closed loop is defined as the gaze dynamics.

The eye-hand task was a regular pursuit task and the corresponding block diagram and display are shown in Figure 2 and 3b respectively. The eye-hand task contains an element that needs to be controlled by the participant, depicted by the H_c block in Figure 2. The dynamics of this element is a gain approximated by a low-pass filter described by $\frac{1}{0.1j\omega+1}$, since this was previously used in research with patients and people without tracking task experience and was found to be challenging enough [13]. The low-pass filter ensures that higher frequencies have less effect on the position of the element, which makes it more comfortable to control. As can be seen from the block diagram, the participant can deduce the error between the system output and the target, $e = f_t - x$ and using this information try to minimize the error. The behavior that is therefore induced is compensatory behavior [14]. The signal used for the gaze analysis is the gaze signal g. For the analysis of the hand, the hand input signal u is used. As can be seen in the block diagram, the open loop dynamics is defined, since it is known from previous research what is inside the control loop [14].

In both tasks, the gaze block identified has the same input, which is the forcing function f_t.

B. Target forcing function

To quantify the gaze dynamics, the identification method based on Fourier coefficients is used. Therefore the eye-only and eye-hand tracking tasks performed were designed with a quasi-random multisine forcing function. The forcing function consisted of 11 sinusoids with frequencies ranging from 0.6-24 rad/s. The target signal f_t is given by:

$$f_t(t) = \sum_{k=1}^{11} A_{t_k} \sin\left(\omega_{t_k} t + \phi_{t_k}\right) \tag{1}$$

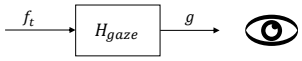

Fig. 1: Block diagram of eye-only tracking task

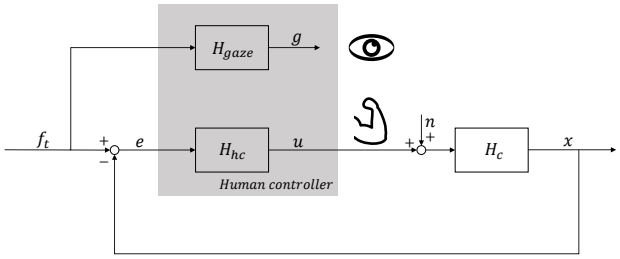

Fig. 2: Block diagram of eye-hand tracking task

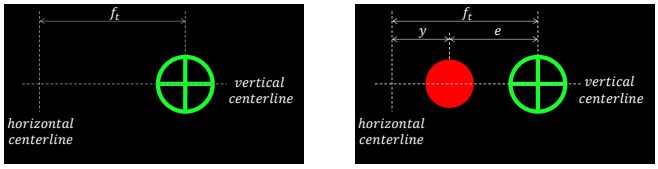

(a) (b)

Fig. 3: Eye-only and eye-hand display.

TABLE I: Forcing functions parameters

	Target forcing function f_t					
k (-)	n_{t_k} (-)	ω_{t_k} (rad/s)	$\phi_{t,2}$ (rad)	$\phi_{t,3}$ (rad)	$A_{t,2}$ (mm)	$A_{t,3}$ (mm)
1	4	0.614	0.6715	4.2134	60	60
2	7	1.074	3.8776	1.8319	60	60
3	11	1.994	3.5615	2.0325	60	60
4	17	2.915	1.6395	4.5036	6	60
5	23	4.449	0.0145	1.1575	6	6
6	29	5.676	1.8049	2.7667	6	6
7	37	6.596	5.1602	2.2903	6	6
8	53	8.130	5.6242	1.3415	6	6
9	79	12.118	6.2568	3.3524	6	6
10	109	16.720	0.0530	5.2293	6	6
11	157	24.084	4.6046	2.9707	6	6

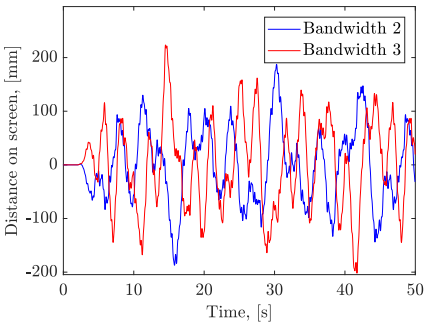

Fig. 4: Time traces of forcing functions used in tasks

The length of the forcing functions were taken to be $50s$ which was found to be an acceptable length in previous mentioned research [12], [13]. Run-in time was used to introduce the signal to the participants. The run-in time had a length of $9.04s$ and is described by (2). The remaining $40.96s$ were used for further analysis.

$$f_{run-in} = (\cos(f \cdot t + 0.5 \cdot \pi))^2) \tag{2}$$

In (1), the amplitude, frequency, and phase of the k^{th} sine in f_t are defined as A_{t_k}, ω_{t_k}, ϕ_{t_k}, respectively. The frequencies and phases of the target forcing function are listed in Table I. The signal was composed of sinusoids with a period that fit an integer number of times in the measurement window of $T_m = 50$ s to avoid spectral leakage: e.g., $\omega_{t_k} = 2\pi n_{t_k}/T_m$ with n_{t_k} an integer. Two different target functions were used in the tracking tasks, hence the two columns for both the phase shifts and the amplitudes. The phase shifts were determined such that the signal-to-noise ratio was neither too high nor too low. This was checked by calculating the Crest Factor (CF), which should have an average value, such that there were no large peaks in the signal but the signals also were not predictable.

The distribution of the amplitudes in both signals was determined using the same method as was used in [15], [19], that is, an augmented rectangular input spectrum with varying bandwidths. In preliminary research preceding this paper we performed experiments with four signals of increasing bandwidths using this same method [25]. To study the effect of bandwidths four signals of increasing bandwidth were used in tracking tasks where the gaze signal was analyzed. The amplitude levels were kept constant for all signals, which resulted in signals of different power. The amplitudes in the high-frequency range were a factor $\sqrt{10}$ lower than those for the low-frequency sinusoids as can also be seen in Table I. The higher the bandwidth and therefore the power of the signal, the more difficult the task was and this was apparent in the parameters of the gaze models. The research described in this paper will continue with two of those four signals (the middle two bandwidths will be referred to as '2' and '3' to keep it consistent with previous work [25]). The choice for these two specific amplitude profiles was based on a trade-off were a higher bandwidth would lead to a signal with too much power, resulting in a signal which would be impossible to track. The lowest bandwidth signal would result in only two low-frequency sinusoids with significant power. This results in the higher frequencies having a greater effect, making the signal again very difficult to track. Since it is important that all participants are able to succesfully complete the tasks, the two signals with medium bandwidth were chosen. This resulted in an easier and a more difficult task that were doable but still sufficiently challenging for the participants.

The resulting time traces of the forcing functions used in the tasks, are shown in Figure 4. It can be seen that the forcing function with the higher bandwidth has more power in the signal, which results in larger deflections on the screen and more oscillations.

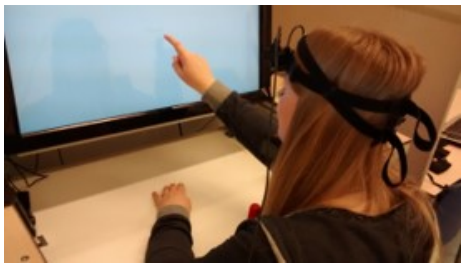

Fig. 5: Test setup when measuring eye-hand coordination

C. Apparatus

The test setup can be seen in Figure 5. There is a chinrest where the head can be placed on to limit head movements during the measurements and also to ensure that the head of all participants is in the same position during different trials. The distance from the head to the screen is $0.5m$.

The measuring of the gaze signals is done with an eye tracker (EyeSeeCam (ESC), München, Germany) as is shown in Figure 6a. This is an eye tracker that can be placed on the head with a non-invasive headband. There are infrared mirrors attached to the headband. These mirrors can reflect infrared light coming from LED's at the top of the ESC. This research used monocular eye movements analysis, so only the left eye of each participant was recorded and used for analysis. The recording of the left eye is done by a camera that is also attached to the headband and is directed towards the infrared mirrors. The recorded image of the eye is shown in Figure 6b. From the ESC, data can be extracted such as the visual angle, torsion and the pupil diameter. The data used for this research is the angle of the gaze. This is calculated by the software of the EyeSeeCam by making use of a pupil detection algorithm. The pupil is detected from the image of the recorded eye as can be seen in Figure 6b. The visual angle of the eye is then calculated, which can be converted to the position on the touchscreen with the distance to the touchscreen known. This signal can be used for the further analysis of the performance of the gaze.

The ESC can be seen placed on the head as in Figure 5. The touchscreen, also shown in this Figure is used to give inputs to the controlled element. In one of the lower corners of the screen (depending on which is the dominant hand) a blue bar is shown which can be used to give the inputs. This input signal can be used to analyse the hand dynamics.

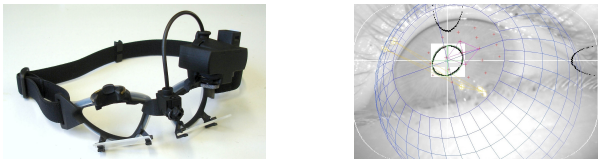

(a) (b)

Fig. 6: ESC and recorded image of the eye

TABLE II: Latin square design experiment

	Condition 1	Condition 2	Condition 3	Condition 4
Order 1	EH-3	EH-2	EO-3	EO-2
Order 2	EO-2	EO-3	EH-3	EH-2
Order 3	EH-2	EH-3	EO-2	EO-3
Order 4	EO-3	EO-2	EH-2	EH-3

D. Participants

In total 40 participants were recruited to participate in the experiment. Since the experiment was a between-subject experiment, each group consisted of 20 participants. The age of the younger group varied from 20 yrs old to 30 yrs old, where the age of the older group varied between 55 yrs old and 70 yrs old. This difference in age was expected to cause noticeable differences in the results based on previous research on the effect of ageing [26]. The age range of the older age group was taken between 55 yrs old and 70 yrs old, because it was expected that people above 70 yrs old would find the task too challenging and demanding such that no useful data could be collected. Additionally, the chosen age group of the older participants now coincided with the age group of patients participating in experiments at Erasmus Medical Center (EMC), making the results of this research useful as a normative database for future research.

E. Experiment procedure

For the experiment a Latin Square design was used to ensure there would be no learning or fatigue effects for certain conditions. The experiment consisted of four different conditions. These conditions were based on the two different types of tracking tasks (eye-only and eye-hand) and the two different forcing functions that were used. Each participant performed at each condition, however the order of appearance of each condition was changed according to the Latin Square design presented in Table II. In Table II 'EO' and 'EH' refer to the eye-only and eye-hand task, respectively. The numbers '2' and '3' refer to the bandwidth of the forcing function which was explained in Section II-B. Four condition orders were used such that every five participants of each age group performed the conditions in a different order. This was done to eliminate a learning effect between the conditions. Before the real measurements began, each participant practised the task at all conditions during the training phase. Training was continued until the participant showed a stable response and the participant felt familiar enough with the tasks. Stable performance refers to the tracking performance, for which the hand signal was used. For the gaze analysis, only gaze signals were used, this response however could not be calculated real-time. It was also expected that once the hand signal was stable enough, the gaze signal would be too.

Each condition was repeated eight times, which gave an overall stable average for that participant for that condition. In between conditions small breaks were taken by the participant and halfway the experiment a larger break was taken to minimize fatigue.

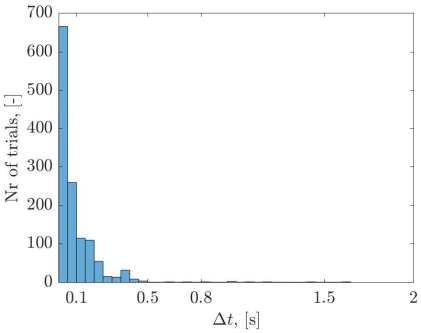

Fig. 7: Distribution of number trials for different Δ t

F. Data post-processing

Matlab was used to draw and recalculate the tasks on the touch screen and to save the data. The ESC was connected to a different computer. To be able to match the hand data saved by the Matlab computer to the eye data saved by the ESC computer, a trigger was sent from the Matlab computer to the ESC computer each time a trial started and ended. Due to memory build-ups in Matlab, the length of the trials deviated. This was either because the trigger was sent too late, or the time delay was gradually built up during the task. Therefore the data needed to be post-processed and a threshold needed to be set for an allowable software delay to determine whether a trial was valid or not. In order to do this a pre-analysis was done on the software delay that was present in the trials. Figure 7 shows the distribution of the Δt (software time delay) in all trials of all participants. As can be seen, most trials are within a 0.1s software time delay (73%). However, to determine whether this software time delay has a large influence on the final parameters of the models, further pre-analyses were done. The final parameters of the models were calculated using the method explained in Section II-G. Where models were created of the averages of the trials per condition for the final analysis ($40 \cdot 4 = 160$ trials), the models in this pre-analysis were created of all the trials ($40 \cdot 4 \cdot 8 = 1240$ trials). The parameters of these models were plotted against the software time delay such that insight could be gained whether certain parameters started to shift after a certain time delay. Each bar in Figure 8 shows the average of each trial that has a software time delay within the given limits of the bars, where every bar has a time span of $0.05s$. The first two bars therefore contain 73% of the data, since 73% of the trials had a software time delay below $0.1s$.

The gain in Figure 8a does not show different behavior with regard to the software time delay, however the other parameters do show an increase in case of the time constant and a decrease in case of the natural frequency and the damping coefficient. Together with the fact that most data stays within a $0.1s$ software time delay, it was decided that all trials within this limit were considered to be sufficiently accurate and reliable. Therefore $0.1s$ was taken as the threshold for the software time delay.

During the tracking tasks of $50s$ participants blinked, which resulted in data from the ESC containing errors and gaps. In

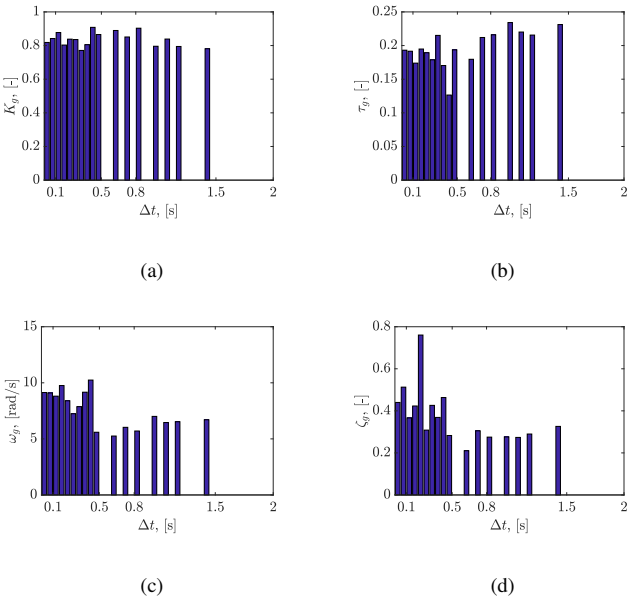

Fig. 8: Software time delay distribution of the model parameters of all trials.

order to continue the analysis of the gaze signal, the instances of these errors and gaps needed to be isolated and removed. This was done by taking every time interval where the pupil diameter gave disproportionate values. These cases occurred when the ESC could not register a pupil or registered the pupil at the wrong location. This resulted either in a very high pupil diameter or no diameter at all. This can be seen in Figure 9, where the top graph shows the pupil diameter. The time intervals of these occurences were determined and removed from the original gaze data of the trial. The resulting gaps were interpolated with a piecewise cubic spline algorithm. It is clearly visible that the trial in Figure 9 contained multiple blinks or errors because the pupil diameter spiked a few times which can be seen in the middle graph. The green graph represents the target signal, the blue graph the gaze signal and the red graph the hand signal. The bottom graph shows the same time trace, except that it is corrected for the blinks that were detected in the pupil diameter.

Trials with remaining errors that were not removed by the pupil diameter method, were not taken into account. These errors were caused by a participant showing abnormal behavior due to coughing, laughing, talking, looking away or blinking for a longer period of time. At these instances not enough data were recorded or the wrong kind of behavior was recorded. Since we are only interested in trials with correct tracking behavior, a more characteristic average was calculated without these faulty trials. In total 36 of 1240 trials were discarded this way.

G. System identification

A model was created on the average of the remaining trials of the participants per condition. The averaging of trials was

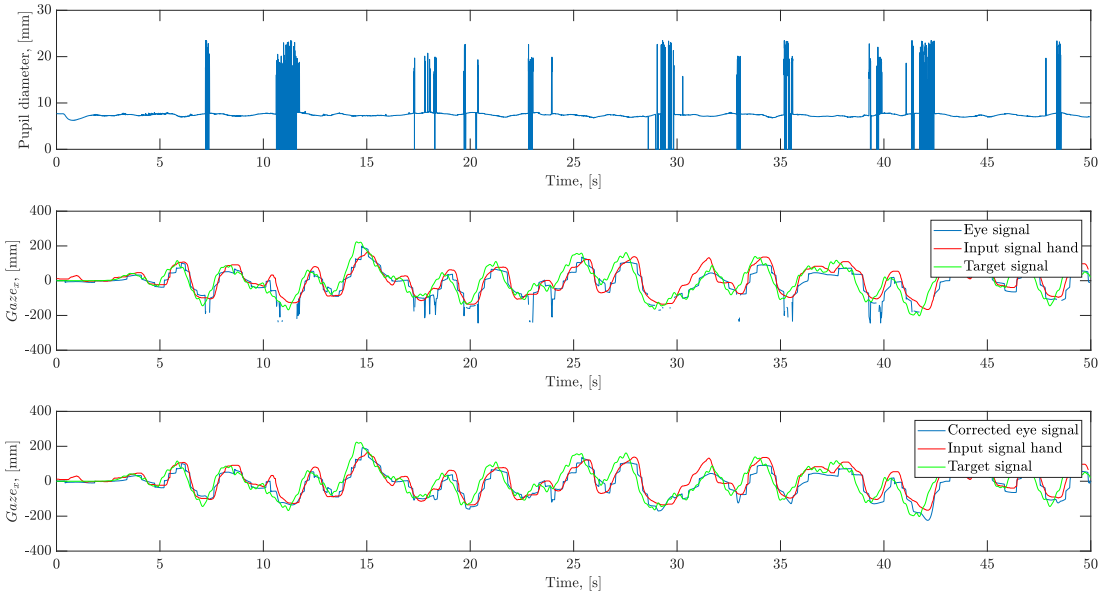

Fig. 9: Pupil diameter correction for blinks

done after the Fourier transform was completed, to give a characteristic model for the given participants at that specific condition. This meant 160 models in total were created for the gaze data. For the hand data only 80 models were created, since only the eye-hand condition involved hand input of the participants.

System identification was applied on these frequency traces in order to identify parameters that describe the gaze and hand behavior. The gaze block shown in Figures 1 and 2 can be calculated according to (3). The HC block shown in Figure 2 can be calculated according to (4). $G(j\omega_t)$ and $F_t(j\omega_t)$ are Fourier coefficients of the gaze (g) and target (f_t) signal. $U(j\omega_t)$ and $E(j\omega_t)$ are Fourier coefficients of the hand input signal (u) and the error signal used for tracking (e).

$$\hat{H}_g(j\omega_t) = \frac{G(j\omega_t)}{F_t(j\omega_t)} \tag{3}$$

$$\hat{H}_{hc}(j\omega_t) = \frac{U(j\omega_t)}{E(j\omega_t)} \tag{4}$$

$$H_g(j\omega_t) = K_g \cdot e^{-j\omega_t \tau_g} \cdot \frac{\omega_g^2}{(j\omega_t)^2 + 2\zeta_g\omega_g j\omega_t + \omega_g^2} \tag{5}$$

$$H_{hc}(j\omega_t) = K_{hc} \cdot \frac{1}{T_L(j\omega_t) + 1} \cdot e^{-j\omega_t \tau_{hc}} \cdot \frac{\omega_{hc}^2}{(j\omega_t)^2 + 2\zeta_{hc}\omega_{hc} j\omega_t + \omega_{hc}^2} \tag{6}$$

The FRF that was created from the measurements describing the gaze behavior is given in (5). The FRF of the hand signal is given in (6). In (6) an extra term is added because the systems dynamics of the to be controlled element is a gain. This has an influence on the behavior of the HC, resulting in an additional lag term for the FRF [14]. Where the terms involving these parameters (K_{hc}, τ_{hc}, ω_{hc}, ζ_{hc} and T_L) are commonly known for hand dynamics, prior to this research the optimal terms with parameters were not known for the gaze dynamics. Given the nature of the frequency response given in Figure 13, where a peak in the magnitude is visible and both the magnitude and phase start to decrease after a given frequency, a second order model with a delay term was thought to be sufficient to describe the behavior. In (5) K_g is the gain, τ_g the time constant, ω_g the natural frequency and ζ_g the damping ratio. To ensure that all frequency data points of the frequency response were weighted the same, a normalize cost function was used for both the gaze and the hand dynamics, described in (7). This ensured the first two input frequencies were not weighed less during the fitting.

$$\hat{\theta} = \arg\min_{\theta} \left[\sum_{k=1}^{N_t} \frac{\left| \hat{H}_g(j\omega_t[k]) - H_g(j\omega_t[k]\theta) \right|^2}{\left| \hat{H}_g(j\omega_t[k]) \right|^2} \right] \tag{7}$$

To quantify how well the model was fitted, the Variance Accounted For (VAF) can be calculated as is shown in Equation 8 [27]. Here $u[k]$ represents the actual signal and $u_{sim}[k]$ represents the simulated signal. A VAF of 100% means that the signal can be perfectly simulated by the model.

$$\text{VAF} = \left(1 - \frac{\sum_{k=1}^{\omega_t} \left| u[k] - u_{sim}[k] \right|^2}{\sum u[k]^2} \right) \times 100\% \tag{8}$$

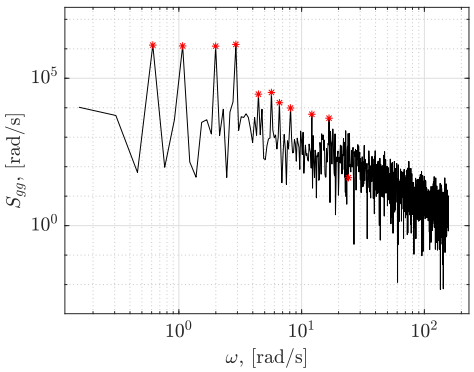

Fig. 10: Power Spectral Density of participant 1, group 2, condition 3-EH

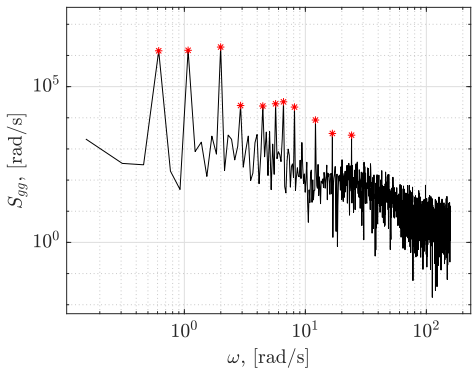

Fig. 11: Power Spectral Density of participant 1, group 2, condition 2-EO

H. Power Spectral Density

Visual inspection of the FRF resulted in a noticeable pattern where the last input frequency increased in magnitude when compared to the neighboring input frequency. There is no clear reason however, why the magnitude of the gaze dynamics would increase for high frequencies. Therefore the Power Spectral Density (PSD) was plotted for all trials, such that it could be seen whether there was excessive noise present. Figure 10 shows an example where the last input frequency hidden in noise and a clear peak is no longer noticeable. This shows that during the Fourier transform, actually primarily noise is analyzed which could prevent the model from accurately describing the actual response. Figure 11 shows an example where the peak at the last frequency is present, however the overall noise level rises for the highest frequency. The signal-to-noise ratio therefore decreases at this frequency, and this causes inaccuracies in the model as well. Overall 14.8% of all trials had a signal-to-noise ratio smaller than 1 at the last input frequency (noise level was higher than peak level) and in 26.6% of all trials, the noise level started to increases at the last input frequency. This was enough reason to give rise to uncertainties at this last input frequency and it was therefore not taken into account during the fitting of the models. Section II-I will focus on whether this decision actually resulted in a better fit for the models.

When analyzing the signal-to-noise ratio of the PSD and the linearity of the gaze, the relative remnant can be calculated [14]. The relative remnant can be calculated as is shown in (9), where $\tilde{S}_{gg.n}$ represents the level of noise and S_{gg} the level of the peak in the PSD. The relative remnant usually has a value between 0 and 1, however it is possible that it becomes negative when the noise level rises above the peak value of the input frequency in the PSD. When the relative remnant is close to 1, this indicates linear gaze. Often it is found that this value decreases for higher frequencies, indicating a lower signal-to-noise ratio. A lower signal-to-noise ratio means that particular input frequency is found less pronounced in the response which could be because it was more difficult to track for example.

$$\rho_g^2(j\omega_t) = 1 - \frac{\tilde{S}_{gg,n}(j\omega_t)}{S_{gg}(j\omega_t)} \tag{9}$$

I. Data analysis

All data were gathered such that time traces could be made as is shown in Figure 12. The run-in time is not shown in Figure 12, that is why the data start at $9.06s$. Using the method described in Section II, models were created for the participants for every condition. An example of the same trial as was used in Figure 12, can be seen in Figure 13. It is clearly visibile here that the last input frequency is not taken into account during the fitting.

As was explained in Section II-H, the last input frequency was not taken into account during the fitting. This was done by giving this frequency a weight of zero. During the initial fitting of the models, it was noticed that the model often would lie above the magnitude of the first two input frequencies. Since the magnitude of the first two input frequencies influences the gain parameter directly, this would cause an unfair comparison of that parameter, since it does not represent the data. Therefore the first two input frequencies were weighted more than the others. This ensured that the models would always go through the first two data points and therefore the gain parameter could be compared for groups and conditions in a useful way.

To analyze whether the weightings on the first two input frequencies and no weight on the last input frequency actually resulted in better models, the VAF scores were compared. The 95% confidence intervals of the VAF scores are presented in Figure 14. All conditions are shown, with 'EO' referring to the eye-only task, 'EH' to the eye-hand task, and '2' and '3' to the different bandwidth forcing functions again. The blue graph shows the VAF scores of the model when no weightings were applied. The red graph shows the VAF scores when the last input frequency was given a weight of zero (case I). The green graph shows the VAF scores when the first two input frequencies are given a higher weight (case II) and lastly the black graph shows the VAF scores when both the last input frequency is given a weight of zero and

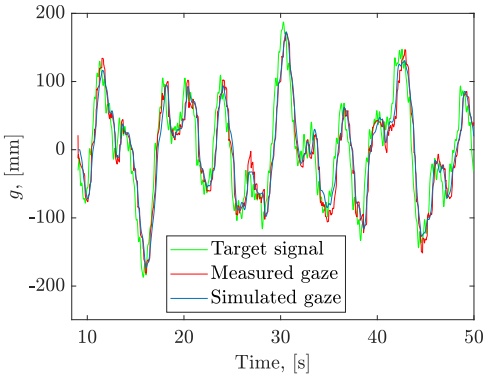

Fig. 12: Time traces of target, measured and modelled gaze of subject 14 in condition 2-EO

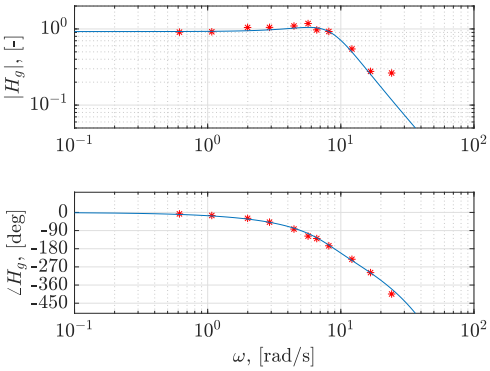

Fig. 13: Fitted model FRF of subject 14 in condition 2-EO

the first two input frequencies are given a higher weight. As can be seen, the VAF scores improve in both case I and case II but the largest improvement is seen when both cases are applied.

An example of a model transformed back to the time domain is shown in Figure 12. As can be seen, the two time traces are almost identical, resulting in a very high VAF of 97.6%. It can be seen that the higher frequencies are less present in the modelled time trace, however these frequencies clearly do not have enough effect on the VAF.

A metric used to compare the performance of the two groups, the gaze performance is calculated. The gaze performance is represented by the variance of the error divided by the variance of the target signal, $\sigma_e^2/\sigma_{f_t}^2$. This performance is normally used for tracking data to describe whether the tracking error was reduced by the input given (≤ 1), or if this was actually increased (≥ 1). For gaze data, there is no element influenced by the gaze input, so the performance just gives a measure how well the target was followed by the eyes compared for the two groups.

J. Post-analysis

To extend the results from our particpant groups to the entire population, statistical methods are used. There are many statistical tests that can be used, but since we used a between-

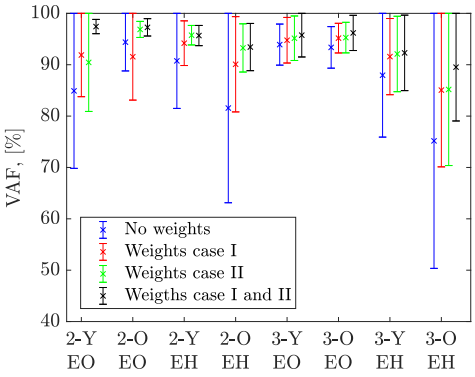

Fig. 14: VAF of different fitting attempts. 'Y' denoting the younger and 'O' the older participant group

subject design for the experiment with multiple conditions, a mixed ANOVA test would be suitable. The mixed ANOVA test can evaluate the main effects between the groups, the main effects of the conditions and also the interaction effects between these factors [28].

The mixed ANOVA test however assumes that the data are normally distributed. This can be tested with the Kolmogorov-Smirnov test. When the data are not normally distributed, there are non-parametric alternatives. To test the effect between the two groups, the Kruskal-Wallis test is used. To test the effects between the conditions, the Friedman test is used. This test will give a significant result when an effect between two or more conditions is present. It cannot evaluate however which two conditions show the significant effect. To evaluate this, the Wilcoxon test can be used which also involves a Bonferroni correction to adjust the significance levels since the effects are now split over the different conditions [28].

The disadvantage of the non-parametric tests is that they cannot evaluate the interaction effects between the groups and conditions. However, it could be that the outcome of the Friedmand and the Wilcoxon test show different significant effects for one group than for the other. This could then still give different results for the two groups, which is what we are interested in.

K. Hypotheses

Three hypotheses were proposed for this research.

H.I: The gaze performance of the older participants is expected to be lower.

The reaction time of the older group will likely be higher, influencing the time delay. A lower performance is expected to be apparent in a lower gain K_g and a larger time constant τ_g for the older group [14]. Additionally, the relative remnant is expected to be lower for the older group, since this would also suggest they are less capable of tracking the higher frequencies and therefore more noise is expected in that frequency range.

H.II: The natural frequency ω_g is expected to be lower and the damping ratio ζ_g is expected to be higher for the older group.

Due to ageing affecting the slowness of motion and muscles,

the stiffness of the eyes is likely different for the older group.
H.III: The performance of the hand dynamics of the older group is expected to be lower and the second order model parameters show similar differences between the groups to the gaze dynamics.
The lower performance for the older group is to be seen in a lower gain parameter K_{hc}, higher lag term time constant T_L and a higher time constant τ_{hc}. Also the second order model parameters are expected to show similar differences as for the gaze dynamics, resulting in a lower natural frequency ω_{hc} and a higher damping ratio ζ_{hc} for the older group.

III. Results

A. Gaze performance

As a measure to determine how well the participants followed the target with their eyes, the gaze performance can be calculated as was explained in Section II-I. The data presented in Figure 15 was not normally distributed according to the Kolmogorov-Smirnov test, therefore non-parametric tests were done to check for significant effects within and between the groups. The box plots show the medians and quartiles and the black asterixes show the means of the data. There was found to be a significant effect between the conditions for the older group according to Friedman's test ($\chi^2(3) = 22.5, p < 0.05$). The results of Wilcoxon's post hoc test are shown in Table III for the older group only (denoted by 'O'), since the younger group did not show significant results. The older people showed a significantly different performance for 2-EO - 3-EH and 3-EO - 3-EH. The performance increases for 3-EH compared to 2-EO and 3-EO, showing that the 3-EH tracking condition in general is more difficult than the eye-only condition for older people only. The results of the Kruskal-Wallis test are also shown in Table III. As can be seen there is a significant difference between the groups for condition 2-EH. The performance of the older group increases compared to the younger and therefore is worse. This pattern is noticeable too for condition 3-EH, however this is not significant.

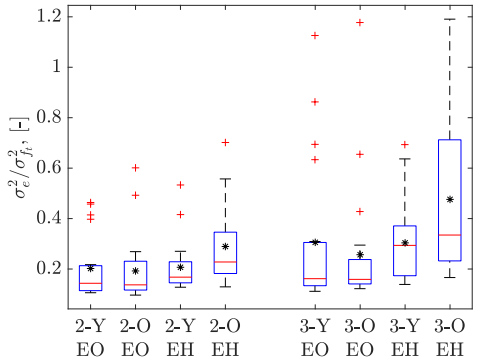

Fig. 15: Gaze performance

TABLE III: Results of Kruskal-Wallis and Friedman test, where ** is highly significant ($p < 0.01$), * is significant ($0.01 \leq p \leq 0,05$), and - is not significant ($p \geq 0,05$)

	Wilcoxon		Dependent measures $\sigma_e^2/\sigma_{f_t}^2$	
	Factor	df	W	Sig.
O	2-EO - 3-EO	3.0	-0.250	-
	2-EO - 2-EH	3.0	-1.000	-
	2-EO - 3-EH	3.0	-1.750	*
	3-EO - 2-EH	3.0	-0.750	-
	3-EO - 3-EH	3.0	-1.500	*
	2-EH - 3-EH	3.0	-0.750	-

Kruskal-Wallis		Dependent measures $\sigma_e^2/\sigma_{f_t}^2$	
Factor	df	H	Sig.
2-EO	1.0	0.007	-
3-EO	1.0	0.000	-
2-EH	1.0	4.683	*
3-EH	1.0	2.997	-

B. Parameters

The parameters that were estimated to fit the gaze models are presented in Figure 16. They show the parameters of all models including all conditions and both groups. The differences can therefore be interpreted in different ways and will be discussed one by one. The most important results are those that describe differences between the two age groups. The parameters of the young age group are indicated in the Figure by 'Y' where the older age group is denoted by 'O'. As was explained in Section II two different tasks were designed, one where only following the target with the eyes was sufficient and one where a target had to be tracked by hand. The eye-only and the eye-hand condition are once again denoted by the 'EO' and 'EH' respectively. Lastly, it was explained in Section II-B that two different forcing functions were used, which resulted in four conditions. The two different forcing functions are denoted again by '2' for the lower bandwidth and '3' for the higher bandwidth. The box plots in Figure 16 show the quartiles and the black asterixes represent the means of the data.

The following Section will explain the differences between the parameters and will use the statistical tests described in Section II-J to give the conclusions more weight. The mixed ANOVA test was used for the gain K_g, since the Kolmogorov-Smirnov test gave non-signifcant results. As can be seen already from the box plots in Figure 16 the other parameters have a large spread for some conditions causing the data to not be normally distributed. Therefore the non-parametric tests of Kruskal-Wallis, Friedman and Wilcoxon were performed for the time constant τ_g, the natural frequency ω_g and the damping ratio ζ_g, to test for within and between group effects. The Friedman test showed significant results for τ_g in the older group ($\chi^2(3) = 16.02, p < 0.05$), for ω_g in the younger group, ($\chi^2(3) = 10.26, p < 0.05$), and for ζ_g for both groups, (young: $\chi^2(3) = 49.67, p < 0.05$, old: $\chi^2(3) = 46.62, p < 0.05$). The results of the mixed ANOVA test, the Kruskal-Wallis and the Wilcoxon test are presented in

Table IV.There are some outliers present which have an effect on the group distribution, however they are deliberately left in the data to prevent influencing the outcome and reducing the subject size. This would otherwise make the results less trustworthy.

1) Age: None of the parameters shows a significant main effect for the groups as can be seen in Table IV. This is also confirmed in Figure 16. Therefore age does not affect the parameters as a variable alone. There do appear to be some changes between the older and younger group during the eye-hand tracking condition. In both bandwidth forcing functions, the gain K_g is lower for older people in the tracking condition. Also the time constant τ_g shows some different values for the two groups. Again this is primarily noticeable when comparing the eye-only and the eye-hand tracking condition. In the eye-hand tracking condition the older age group has higher time constants. The parameters that describe the second order model in the FRF are more difficult to compare, since the spread of the older group is large, especially in the eye-hand tracking condition. This shows there is more variability inside the older group. The differences of the gain K_g, the time constant τ_g and the natural frequency ω_g might be attributed to the interaction effects that will be discussed in Section III-B4.

2) Bandwidth: The influence of adding more power to the forcing function can be seen by comparing the parameters of the different bandwidths. This effect is significant for the gain K_g according to the Mixed ANOVA results. Also the time constant τ_g, the natural frequency ω_g and the damping ratio ζ_g show significant differences between the two forcing function, altough this effect is primarily noticeable for 2-EO - 3-EH. This indicates that the combined effect of changing task and forcing function gives significantly different results.

3) Task: The differences in parameters for the two tasks appear to be largest. The effect of task condition is highly significant for the gain K_g. The gain K_g is lower for both the younger and the older group for both forcing functions in the eye-hand tracking condition. The time constant τ_g is significantly higher for 3-EH and both eye-only tracking conditions. Also the damping ratio ζ_g is significantly different for the two tasks for both groups according to the Wilcoxon test in Table IV. This is confirmed in the boxplots in Figure 16 where the ζ_g increases for the eye-hand tracking condition.

4) Interaction effects: Lastly, the results of the Mixed ANOVA test showed a significant effect of the interaction between the task condition and groups. This causes the main differences between the groups that are visible in the gain K_g. This effect means that the difference in task condition is larger for the older group than it is for the younger group. In Figure 16 it can be seen that the gain is lower in the eye-hand tracking condition compared to the eye-only tracking condition and this effect is less distinct for the younger group.

Even though the non-parametric tests cannot evaluate interaction effects, the outcome of the Kruskal-Wallis and the Wilcoxon test can give different results for both groups. This is the case for the time constant τ_g, where a significant effect was found for the older group and not the younger group. The older group shows a significantly higher τ_g for 3-EH than for the eye-only conditions, indicating that this group shows worse behavior for the eye-hand tracking condition. For the natural frequency ω_g the Wilcoxon test shows a significantly higher natural frequency for 3-EH when compared to 2-EO for the younger group and not the older group, indicating another difference between the groups. The Wilcoxon test showed similar results for the damping ratio for both groups, therefore no group effect can be descibed for the damping ratio ζ_g.

C. Hand dynamics

Figure 17 shows the parameters of the hand dynamics including a sixth plot with the parameters K_{hc}/T_L. This is done because the gain K_{hc} influences the starting point of the magnitude of the FRF and T_L influences when the lag term starts to have effect, decreasing the magnitude of the FRF. Therefore the two parameters could cancel each other's effect, resulting in the same gain in the integrator part of the model. The parameters estimated for the hand dynamics were all normally distributed, therefore only the Mixed ANOVA test was performed, of which the results are shown in Table V. Significant differences were found for the influence of the bandwidth of the forcing functions for the gain K_{hc}, the natural frequency ω_{hc}, the damping ratio ζ_{hc} and the lag time constant T_L.

There was also a main group effect for the gain K_{hc} and the lag time constant T_L. However no significant effect was found for the combined factor K_{hc}/T_L, therefore indeed the two parameters seem to cancel out each other's effects and the gain in the integrator part of the model is similar for both groups.

No interaction effects were found to be significant.

D. Relative remnant

The relative remnant is shown in Figure 18. The median is taken for the data points and the interval patches show the first and third quartiles of the distribution. The median is taken because the mean was in some cases influenced severely by a few large deviating values. This caused the data to not be normally distributed and the mean would therefore not represent the data well. These deviations are visible in the quartiles and are present in all cases for the higher frequency range. This shows that more noise is present in the higher frequency range but there is also variability within the groups. For the eye-only tracking condition the graphs are very similar for both groups. The eye-hand tracking conditions show more differences however, indicating more noise is present in the eye-hand condition. There is also a difference noticeable between the group for the eye-hand condition. The older group stays below the younger group consistently. This indicates that more noise is especially present for the older group.

IV. Discussion

This research aimed at quantifying the ageing effect on gaze dynamics by comparing the results of two groups, being a group with older participants and a group with younger participants. With the ageing effect known, it is worthwhile extending this research to quantify the gaze dynamics of

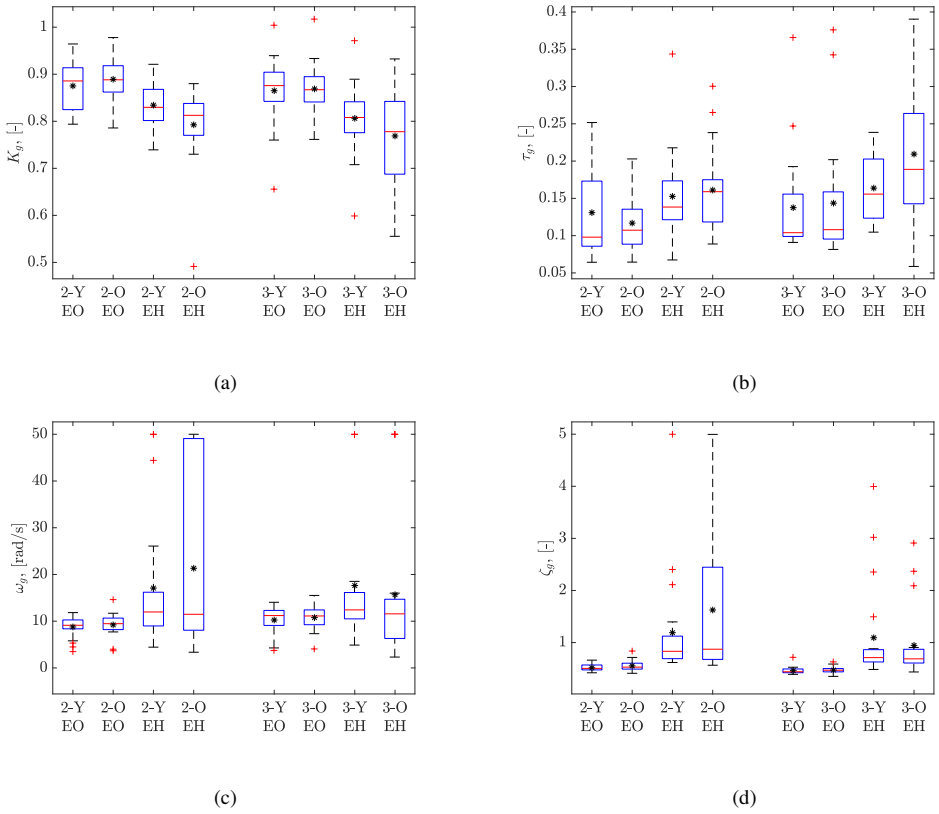

Fig. 16: Parameters of fitted models of the gaze dynamics.

TABLE IV: Results of Mixed ANOVA, Kruskal-Wallis and Friedman test, where ** is highly significant ($p < 0.01$), * is significant ($0.01 \leq p \leq 0,05$), and - is not significant ($p \geq 0,05$)

Mixed ANOVA		Dependent measures	
		K_g	
Factor	df	F	Sig.
Task	1.0	48.1	**
BW	1.0	8.9	*
G	1.0	0.8	-
Task × BW	1.0	2.6	-
Task × G	1.0	6.7	*
BW × G	1.0	0.9	-
Task × BW × G	1.0	0.9	-

	Wilcoxon		Dependent measures					
			τ_g		ω_g		ζ_g	
	Factor	df	W	Sig.	W	Sig.	W	Sig.
Y	2-EO - 3-EO	3.0	n/a	n/a	-0.45	-	0.775	-
	2-EO - 2-EH	3.0	n/a	n/a	-0.90	-	-2.075	*
	2-EO - 3-EH	3.0	n/a	n/a	-1.20	*	-2.550	*
	3-EO - 2-EH	3.0	n/a	n/a	-0.50	-	-1.300	*
	3-EO - 3-EH	3.0	n/a	n/a	-0.75	-	-1.775	*
	2-EH - 3-EH	3.0	n/a	n/a	-0.25	-	0.475	-
O	2-EO - 3-EO	3.0	-0.30	-	n/a	n/a	0.850	-
	2-EO - 2-EH	3.0	-1.05	-	n/a	n/a	-2.050	*
	2-EO - 3-EH	3.0	-1.45	**	n/a	n/a	-2.500	*
	3-EO - 2-EH	3.0	-0.75	-	n/a	n/a	-1.200	*
	3-EO - 3-EH	3.0	-1.15	*	n/a	n/a	-1.650	*
	2-EH - 3-EH	3.0	-0.40	-	n/a	n/a	0.450	-

Kruskal-Wallis		Dependent measures					
		τ_g		ω_g		ζ_g	
Factor	df	H	Sig.	H	Sig.	H	Sig.
2-EO	1.0	0.003	-	0.036	-	1.171	-
3-EO	1.0	0.018	-	0.001	-	1.353	-
2-EH	1.0	0.176	-	0.000	-	0.105	-
3-EH	1.0	2.997	-	1.113	-	0.165	-

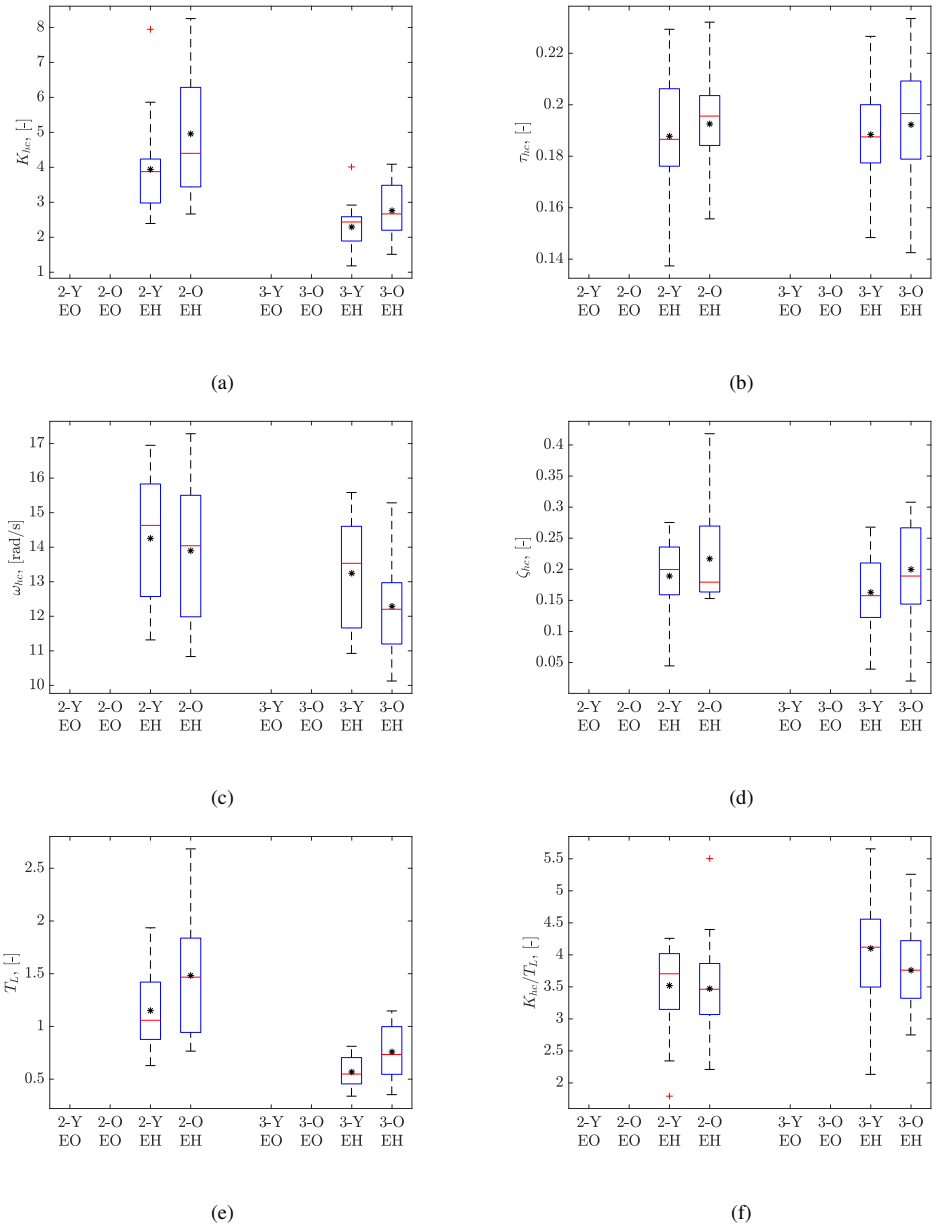

Fig. 17: Parameters of fitted models of the hand dynamics.

TABLE V: Results of Mixed ANOVA, where ** is highly significant ($p < 0.01$), * is significant ($0.01 \leq p \leq 0,05$), and - is not significant ($p \geq 0,05$)

Mixed ANOVA		Dependent measures											
		K_{hc}		τ_{hc}		ω_{hc}		ζ_{hc}		T_L		K/T_L	
Factor	df	F	Sig.	F	Sig.	F	Sig.	F	Sig.	F	Sig.	F	Sig.
BW	1.0	118.7	**	0.005	-	22.2	**	5.1	*	109.1	**	29.3	-
G	1.0	5.1	*	0.453	-	2.1	-	2.8	-	7.1	*	0.8	-
BW $\times$ G	1.0	2.4	-	0.035	-	1.2	-	0.2	-	1.3	-	3.3	-

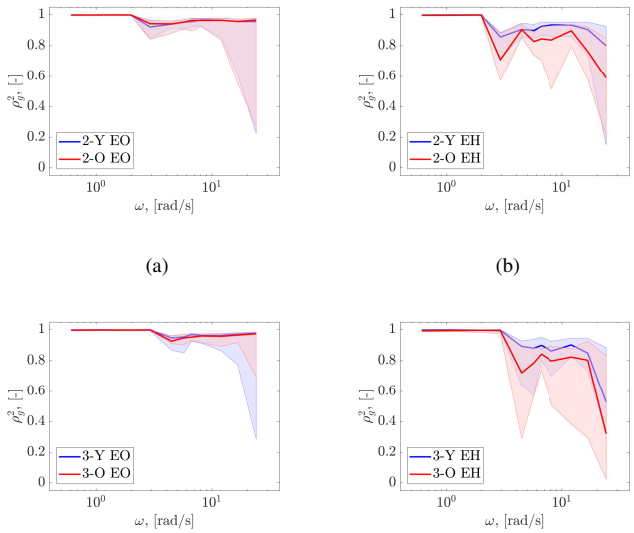

(a) (b) (c) (d)

Fig. 18: Relative remnant

people with neurodegenerative diseases, such that diseases could potentially be differentiated at an earlier stage of the disease than is currently possible. This could be used additionally to the hand dynamics, of which the results were also shown.

Hypothesis I expected older people to have a lower gaze performance than younger people. According to the Figures presented in Section III-A this was true for the 2-EH condition. On average the gaze performance increased with 35% for the older group which means they performed worse. This shows that the eye-hand tracking condition was more demanding for the older group than it was for the younger group. This is also confirmed because there was a significant effect for 2-EO - 3-EH and 3-EO - 3-EH for the older group. The main group effect was not visible for the 3-EH condition where this would be expected. This could be because the 3-EH condition was hardest for all participants and therefore the younger group did not outperform the older group significantly. The box plots also indicate this because the performance increases slightly for the 3-EH condition compared to the 2-EH condition of the younger group, although not significantly.

Related to the performance, it was expected that there would be an effect of ageing on the model parameters, however there were no main effects for the groups. There was an interaction effect however which causes the gain K_g to be decreasing for a higher bandwidth for the older group more than for the younger group. A lower gain means the participants were not able to reach the full amplitude of the signal they were trying to follow with their eyes. This is also confirmed by the higher time constant τ_g for the eye-hand tracking condition. It could be that the older participants were not fast enough to reach the outer ends of the screen with their eyes. This suggests that the gaze of older people is not fast enough to reach the outer ends when the task gets more demanding.

The performance is also influenced by the signal-to-noise ratio and it was expected that older people would have a lower signal-to-noise ratio, thus also a lower relative remnant (a relative remnant of 1 would indicate perfect linear gaze and a negative remnant would indicate a signal-to-noise ratio smaller than 1). The relative remnant should be lower for the older group since more noise is expected in the high frequency range for older people, thus a lower relative remnant. This was not confirmed for the eye-only condition as can be seen in the graphs shown in Figure 18, however there were clear differences visible for the eye-hand tracking condition. The relative remnant of the older people is lower for this condition, showing that the signal-to-noise ratio is indeed lower for older people in this condition. This suggests that older people are less able to show linear gaze.

Overall it does confirm that the gaze performance of the older participants in the tracking condition is lower.

Hypothesis II expected differences in the second order term of the model when comparing the two groups. The results did not confirm this, since the Kruskal-Wallis gave no significant results. Also the Wilcoxon test showed similar results for both groups for the damping ratio ζ_g. For both groups, the damping ratio increased for a higher bandwidth and for the eye-hand tracking condition. This suggests less overshoots happen for the eye-hand tracking condition with a higher bandwidth signal, which would be confirmed by the effect in the gain and time delay described above. This was not a differentiating factor between the groups however.

The natural frequency did show a significant effect for 2-EO - 3-EH for the younger group which was not present for the older group. The reason this effect is not visible for the older group is because the natural frequency decreases for the 3-EH condition compared to the 3-EH condition of the younger group, making the difference with the 2-EO condition not large enough. Apparently the older group can follow up to less high frequencies in the 3-EH condition, which is in line with the other parameter changes discussed above.

In general the natural frequency increases slightly for the eye-hand task compared to the eye-only task. This effect combined with the damping ratio changes would indicate that higher frequencies can be followed while having more damping when manual tracking is involved. This could be because the eyes are used as a means to steer the hands. The enhancing effect of manual tracking is also found in previous research [22]. The results were not significant however and this can therefore not be said with certainty. Even though a higher natural frequency is an improvement, the performance during the eye-hand task is still worse than for the eye-only task. Apparently the gained performance in the high frequency range, is not enough to improve the overall performance.

As can be seen in Figure 16, there is a large spread for the second-order model parameters in the older group. The VAF scores presented in Figure 14 indicate that the models describe the behavior well, so there are no outliers caused by fitting issues. This does not mean however that the difference is not caused by identification problems. It could be that the

dynamics described by the outlying parameters (very high natural frequency and damping ratio) do not describe the actual behavior. This is possible if the dynamics is not captured within the input frequency range. If a peak is present outside this frequency range, this would affect the damping ratio severely. These identification issues do result in unrealistic systems. The damping ratios are extremely high and these cases are accompanied by extremely high natural frequencies. Since the damping ratios are larger than 1, this means the identified systems are overdamped. This causes the bode plots not even to show the entire dynamics of the second order system, since there are two corner frequencies. The frequency at which the 'second integrator' part starts to have effect is outside the identified frequency range. The dynamics therefore say something about which we cannot say anything. It seems that the dynamics used for quantifying the gaze dynamics are unsuitable for these cases and therefore cannot say something about the actual gaze dynamics. Additionaly, the natural frequencies which are higher than 24 rad/s are per definition questionable, since these frequencies are higher than the highest input frequency and are therefore not excited during the tracking task.

Another reason for a large spread for the natural frequency and damping ratio could be the noise present in the gaze signal. The relative remnant shown in Figure 18 shows that more noise is present in the eye-hand tracking condition, especially in the older group. This indicates that the signal-to-noise ratio is lower for this condition and group, influencing the FRF. The model fitted to the corresponding magnitude and phase describes behavior that is therefore not representing the actual behavior completely accurate.

Lastly, hypothesis III expected that the parameters describing the hand dynamics would show similar effects to the gaze dynamics. The gain parameter K_{hc} showed contradictory results, because the older people had a significantly higher gain. This could be explained however because the lag term constant T_L also was significantly higher for the older group. These two parameters combined did not show a significant difference between the two groups, however Figure 17f indicates a lower K_{hc}/T_L for the older group. This would suggest that the older group would still be outperformed by the younger group, since the gain in the integrator part is lower. It does suggest that the older group waits longer until responding to the error between the target and element that is building up during the tracking. This is already visible in the lower frequency range. They seem to compensate for this with a higher gain, resulting in overshoots in the hand signal.

The time constant τ_{hc} was not significantly higher for the older group, however Figure 17b does indicate a slight increase for the older group.

The second order model parameters did not show significant results. It does confirm that the higher bandwidth forcing function is more difficult since the natural frequency decreases and the damping ratio increases. An increasing damping ratio was also found in previous research involving Parkinson's patients [12], indicating that ageing effects are to some extent similar to effects of neurodegeneration. To be certain of this however, more research would have to be done with patients.

It was shown in Section II-H that the response at the highest input frequency showed unexpected behavior in many cases. This caused issues in the fitting process and it was therefore decided that it was better to not take this input frequency into account during the fitting of the models. This improved the quality of the models since the VAF scores increased. For the comparison of the parameters of the model used now, this was found to be acceptable. It could be however that there is another reason why this high input frequency caused deviating results. It could be that a second peak is characteristic for gaze dynamics and that it was not possible to capture this with the used frequency range and model. A solution might be to change the target forcing function, such that even higher frequencies are excited and estimated in the FRF. For this research this was not possible however, since the rectangular amplitude profile caused the target forcing function to be already challenging enough for the participants. Using a target forcing function with even higher frequencies, the amplitudes need to be distributed such that the task is still possible to track for the participants. The forcing functions used in this research would become too difficult if a higher frequency was added without changing the shape of the amplitude spectrum.

As was explained in Section II-F there were software time delays built up during the experiments, which caused some trials to not represent valid data. In order to obtain data of better quality, the time delays need to be eliminated in future experiments. As such, more data will be available to obtain an average of high certainty for the different participants.

The ESC only recorded monocularly resulting in only the left eye of the participants being measured. In doing this, it was not taken into account that participants could have a dominant eye that was not the left one. This could have an influence on the gaze data and future research could test if this is indeed true.

Despite the limitations of this research, there were differences found between the groups in the gaze dynamics. First of all, the technique of tracking tasks is thus very suitable to quantify gaze dynamics, and secondly it allows differences between two age groups to be quantified. With the ageing effect on the gaze dynamics known, experiments can be conducted with patients of different neurodegenerative diseases in the future to test the technique as classification tool. Differences between the two groups were most apparent in the eye-hand condition. More research will have to be done to determine which conditions are best suited for experiments with patients. The results of this research indicate that a higher bandwidth forcing function results in a more difficult task. A higher bandwidth signal can therefore be used to challenge the patient up to their own limits. The results of the gaze and hand dynamics show similar results, which makes it difficult to conclude whether using one is better than the other. Identifying the gaze dynamics could therefore be an addition to identifying the hand dynamics, since it gives more comparable results. This could be useful for different neurodegenerative diseases since different affected brain regions could result in different symptoms.

V. Conclusions

This research investigated whether a difference in gaze dynamics could be identified between older and younger people. Experiments were conducted with 20 older and 20 younger participants who had to perform two types of tracking tasks with two forcing functions of increasing bandwidth. One was an eye-only task where the target only needed to be followed with the eyes and the other an eye-hand tracking task where manual tracking of a target was asked. The gaze was recorded and using system identification techniques, models were created for the participants for all conditions. These models were described by four parameters (K_g, τ_g, ω_g and ζ_g). The gaze performance was significantly worse for the older people when tracking a lower bandwidth signal in the eye-hand condition. Also only the older group showed a significantly worse performance for the eye-hand task compared to the eye-only task for the higher bandwidth signal. Furthermore, K_g was significantly lower for older people between the two different tasks. τ_g was significantly higher in the eye-hand tracking condition for older people only. The second order model parameters did not show significant results between the two groups. Similar results were found for the hand dynamics described by five parameters (K_{hc}, τ_{hc}, ω_{hc}, ζ_{hc} and T_L), however less apparent. Although K_{hc} and T_L showed significant differences for the two groups, the combined parameter K_{hc}/T_L was not significantly worse for the older group. The other parameters did not change significantly for the two groups.

In conclusion, it is possible to identify changes in gaze dynamics between younger and older people. The best condition to identify changes, is the eye-hand tracking condition, especially when using the higher bandwidth forcing function. It is therefore encouraged that research should continue to identify changes in gaze dynamics for people with neurodegenerative diseases. The normative database set up in this research can be used as a comparison with healthy control subjects when extending to patients. Since the spread in the second order model parameters of the gaze was very large for the older group, this shows that ageing has different effects on different people. In future research, the gaze dynamics could be used as an addition to investigating differences of hand dynamics which has shown promising results in previous research [12], [13].

References

[1] D. Purves, *Neuroscience, 3rd Edition*. Sinauer Associates, 2004.

[2] M. R. MacAskill and T. J. Anderson, "Eye movements in neurodegenerative diseases," *Current Opinion in Neurology*, vol. 29, no. 1, pp. 61–68, 2016.

[3] M. M. Hoehn and M. D. Yahr, "Parkinsonism: onset, progression, and mortality. 1967." *Neurology*, vol. 50, no. 2, p. 318 and 16 pages following, feb 1998.

[4] C. G. Goetz, S. Fahn, P. Martinez-Martin, W. Poewe, C. Sampaio, G. T. Stebbins, M. B. Stern, B. C. Tilley, R. Dodel, B. Dubois, R. Holloway, J. Jankovic, J. Kulisevsky, A. E. Lang, A. Lees, S. Leurgans, P. A. LeWitt, D. Nyenhuis, C. W. Olanow, O. Rascol, A. Schrag, J. A. Teresi, J. J. Van Hilten, and N. LaPelle, "Movement Disorder Society-sponsored revision of the Unified Parkinson's Disease Rating Scale (MDS-UPDRS): Process, format, and clinimetric testing plan," *Movement Disorders*, vol. 22, no. 1, pp. 41–47, jan 2007.

[5] M. F. Folstein, S. E. Folstein, and P. R. McHugh, "Mini-mental state. A practical method for grading the cognitive state of patients for the clinician." *Journal of psychiatric research*, vol. 12, no. 3, pp. 189–98, nov 1975.

[6] B. Dubois, A. Slachevsky, I. Litvan, and B. Pillon, "The FAB: a Frontal Assessment Battery at bedside." *Neurology*, vol. 55, no. 11, pp. 1621–6, dec 2000.

[7] Fahn S. and Elton R., "Unified Parkinson's Disease Rating Scale," *Recent Developments in Parkinson;s Disease*, vol. 2, pp. 153–163, 1987.

[8] R. Peters, "Ageing and the brain," *Postgrad Med J*, vol. 82, pp. 84–88, 2006.

[9] J. N. Trollor and M. J. Valenzuela, "Brain ageing in the new millennium," *Australian and New Zealand Journal of Psychiatry*, vol. 35, pp. 788–805, 2001.

[10] S. Dowiasch, S. Marx, W. Einhäuser, F. Bremmer, J. J. Foxe, A. Einstein, M. Escudero, S. Mccormick, and N. Carvalho, "Effects of aging on eye movements in the real world," *Frontiers in Neuroscience*, 2015.

[11] R. D. Seidler, J. A. Bernard, T. B. Burutolu, B. W. Fling, M. T. Gordon, J. T. Gwin, Y. Kwak, and D. B. Lipps, "Motor Control and Aging: Links to Age-Related Brain Structural, Functional, and Biochemical Effects," *Neurosci Biobehav Rev*, vol. 34, no. 5, pp. 721–733, 2010.

[12] R. de Vries, "A tracking task for quantifying loss of motor skills due to parkins's disease," Unpublished M.Sc. Thesis, Faculty of Aerospace Engineering, Delft University of Technology, 2015.

[13] Y. Haartsen, "Quantifying loss of motor skills after cerebellar stroke," Unpublished preliminary M.Sc. Thesis, Faculty of Aerospace Engineering, Delft University of Technology, 2017.

[14] D. McRuer, D. Graham, E. Krendel, and W. Reisener, "Human Pilot Dynamics in Compensatory Systems, Theory Models and Experiments with Controlled Element and Forcing Function Variations," The Franklin Insitute, Tech. Rep., 1965.

[15] Duane T. McRuer and Henry R. Jex, "A Review of Quasi-Linear Pilot Models," *IEEE Transactions on Human Factors in Electronics*, vol. HFE-8 No 3, 1967.

[16] Ezra S. Krendel and Duane T. McRuer, "A Servomechanisms Approach to Skill Development," *J. Franklin Inst.*, 1960.

[17] Duane T. McRuer and Ezra S. Krendel, "Mathematical models of human pilot behavior," *AGARDograph AGARD-AG-188*, 1974.

[18] Duane T. McRuer and D. H. Weir, "Mathematical models of human pilot behavior," *IEEE Trans. Man-Mach. Syst.*, vol. 10, no. 4, pp. 257–291, 1969.

[19] R. J. Wasicko, D. T. McRuer, and R. E. Magdaleno, "Human Pilot Dynamic Response in Single-Loop Systems with Compensatory and Pursuit Displays," Systems Technology, Inc, Tech. Rep., 1966.

[20] Kasper van der El, Daan M. Pool, Herman J. Damveld, Marinus M. van Paassen, and Max Mulder, "An Empirical Human Controller Model for Preview Tracking Tasks," *IEEE Transactons on Cybernetics*, vol. 46, no. 11, 2016.

[21] P. W. Koken and C. J. Erkelens, "Influences of hand movements on eye movements in tracking tasks in man," *Experimental Brain Research*, pp. 657–664, 1991.

[22] D. C. Niehorster and W. W. F. Siu, "Manual tracking enhances smooth pursuit eye movements," *Journal of Vision*, vol. 15, no. 2015, pp. 1–14, 2015.

[23] R. Xia and G. Barnes, "Oculomanual coordination in tracking of pseudorandom target motion stimuli," *Journal of Motor Behavior*, vol. 31, pp. 21–38, 1991.

[24] K. A. Flowers, "Visual 'closed-loop' and 'open-loop' characteristics of voluntary movement in patients with parkinsonism and intention tremor," *Brain*, vol. 99, no. 2, pp. 269–310, 1976.

[25] J. Büskens, "Quantifying gaze dynamics," Unpublished preliminary M.Sc. Thesis, Faculty of Aerospace Engineering, Delft University of Technology, 2018.

[26] J. L. Fozard, M. Vercruyssen, S. L. Reynolds, P. A. Hancock, and R. E. Quilter, "Age Differences and Changes in Reaction Time: The Baltimore Longitudinal Study of Aging," *Journal of Gerontology*, vol. 49, no. 4, pp. P179–P189, 1994.

[27] F. M. Nieuwenhuizen, P. M. T. Zaal, M. Mulder, M. M. Van Paassen, and J. A. Mulder, "Modeling Human Multichannel Perception and Control Using Linear Time-Invariant Models," *Journal of Guidance, Control and Dynamics*, 2008.

[28] A. Field, *Discovering Statistics Using SPSS*. Sage Publications, 2005.

Part II

Preliminary Report

Chapter 2

Preliminary Research Questions

Since analyzing the eye movements during tracking tasks is different from analyzing the tracking performance, it is not given that the same bandwidth of the forcing is best used. A goal of the preliminary researcg is therefore to find out what the influence is of the bandwidth of the forcing function on the eye movements. Literature showed that there might be an influence of manual tracking, however there are opposing views on this subject. Therefore a second goal of this phase is to find out whether there is an effect of mannual tracking during the tracking task on the eye movements.

Based on the motivation, goals and objectives stated above, a research question is drafted which is given below.

How can the gaze dynamics be identified using a cybernetic approach and how can this approach identify differences between age categories?

This research question can be answered by answering the following sub-questions.

1. What is the optimal bandwidth to identify gaze dynamics?
2. What is the influence of manual tracking?
3. What is the relation between aging effect and neurodegenerative diseases?

The remainder of this report will be structured as follows. Chapter 3 will give information about different neurodegenerative diseases, what eye movements exist, what eye symptoms come with those diseases and why the ageing effect is a comparable case to investigate. Chapter 4 will explain the concept of tracking tasks and will continue how these tasks can be used to identify the gaze dynamics. To answer the subquestions preliminary experiments were conducted which will be explained in Chapter 5. Finally, Chapter 6 will give the proposal of the final experiment.

Chapter 3

Oculomotor system and the impact of neurodegenerative diseases on eye movements

The relevance of this research is to identify gaze dynamics for people with neurodegenerative diseases, it is therefore important to know first what different neurodenegerative diseases exist. This Chapter will therefore describe some well-known neurodegenerative diseases in Section 3-1 and will elaborate on the different symptoms that can be involved in parts of the brain. Before this Chapter will go into detail of some diseases, first some general information will be given on neurodegeneration.

Furthermore, Section 3-2 will go in more detail about the different eye movements and which eye symptoms exist in some neurodegenerative diseases. Section 3-3 will discuss some eye symptoms that can exist in certain well-known neurodegenerative diseases.

Lastly, this Chapter will describe the effect of aging, since one of the experiments will compare the results of young people with old people. Section 3-4 will therefore explain why this scenario may be a comparable situation to the neurodegenerative diseases scenario.

3-1 Neurodegeneration

Neurodegeneration starts with the damaging or death of pathways of the neurons or of the neurons itself. Neurons are the cells that receive, process and transmit information by making use of electrical or chemical signals. When neurons are damaged or have died, they cannot be replaced by the body. Diseases involving neurodegeneration therefore are incurable. Since neurons are the building blocks of the brain and spinal cord, it is apparent that the brain will

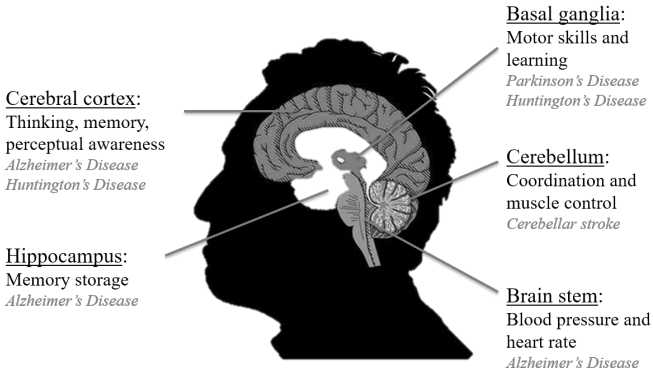

Figure 3-1: Neurodegenerative diseases influences different brain regions

lose some functionality when neurons are damaged. This is what happens in neurodegenrative diseases. Through some reason, neurons or pathways of neurons get damaged or die in a location of the brain. The location where the damage occurs, influences the different symptoms that come with the disease. Some well known neurodegenerative diseases are listed below.

- Parkinson's disease
- Alzheimer's disease
- Huntington's disease

Different parts of the brain influence different eye movements because the different regions control other functions. Because neurodegenerative diseases can cause for neuronal loss in different parts of the brain, the disease could influence different eye movements. An example of this is shown in Figure 3-1.

The oculomotor system is the part of the Central Nervous System (CNS) that maintains visual stability and also controlls the eye movements (Hejtmancik and Nickerson (2017)). It is made out of many brain regions that cooperate in order to be able to see a stable image (Squire (2009)). How this works in the eye is explained in Section 3-2. It can be seen in Figure 3-1 that different functions of the oculomotor system involve multiple brain regions. So regardless of whether the disease has a focal or widespread effect, symptoms to the oculomotor system are possible.

3-2 Eye movements

Without probably realizing it, people make a lot of different eye movements. The reason for eye movements is because the human eye can only perceive detail in a small subset of the gaze. This field of view where the acuity is highest is called the foveal view. The part of vision outside this foveal view is called the peripheral view (Ludwig, Davies, Eckstein, and Wurtz (2014)). Where foveal view can be used to obtain high quality details, peripheral view is limited by sparse and irregular photoreceptors resulting in the weak distinguishing of detail, color and shape. Eye movements are therefore necessary to overcome these limitations and obtain as much information as possible.

There are different eye movements, each having different functions and they are also controlled by different regions of the brain. This Section will elaborate on the differences of these eye movements obtained from literature and researches. The different functions will be explained, and it will be concluded which eye movements are most interesting for the remainder of this research.

3-2-1 Saccades

One type of eye movements is a very fast shift of the eyes. When something draws your attention, the foveal view is shifted towards the object/event such that it can be perceived in more detail. The fast shift that changes the view to approximately the point of interest is called a saccade. Saccades are characterized by their rapid and ballistic nature (Purves (2004)). It is a ballistic movement because the movement cannot be adjusted once it has started. When the target for which the saccade was started, moved during the movement, the eye would not be able to stop the saccade. A second saccade would have to be made to correct the error. This happens when an undershoot or overshoot occurs.

Saccades can be made voluntarily but also involuntarily and the movements can range from very small movements to larger ones. Saccades used to scan the room can be large movements, but the eye movements made while reading a book are also saccades and are obviously smaller movements. Moving the eyes to a new target in space involves two aspects: controlling the *amplitude* and the *direction* of the eye movements.

The amplitude of the saccadic eye movements is related to the duration of neuronal activity in the oculomotor nuclei (Purves (2004)). This nucleus is located in the midbrain and consists of several subnuclei. Each subnucleus controls a particular muscle of the eye (Remington (2012)). These muscles also determine the direction the eye moves. There are six muscles that control the eye, which can be seen in Figure 3-2 (Remington (2012)). The six muscles control different rotations, which can be seen in Figure 3-3. The rectus muscles control upward, downward, outward and inward movements called elevation, depression, abduction and adduction respectively. The two other muscles insert the eye at oblique angles and influence the torsion of the eye called intorsion (towards the nose) and extorsion (away from the nose) (Swenson, Cohen, Fadul, Jenkyn, and Ward (2008)). Separately adjusting each

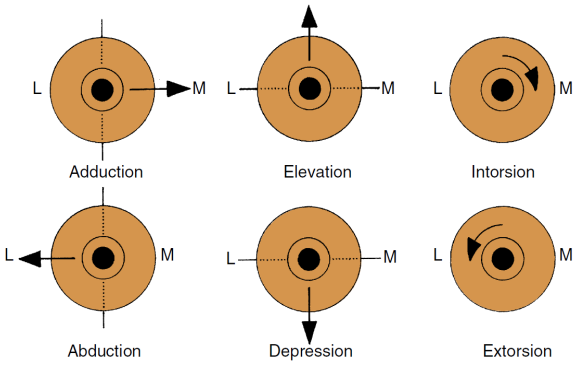

Figure 3-3: Muscles controlling the eye Remington (2012)

muscle could specify the direction of movements of the eye. This would be overwhelming however, therefore the direction of the eye movement is determined by circuit neurons in two gaze centers resonsible for two different axes (Purves (2004)). This causes eye movements to be classified as horizontal or vertical eye movements. Activation of both gaze centers results in oblique movements.

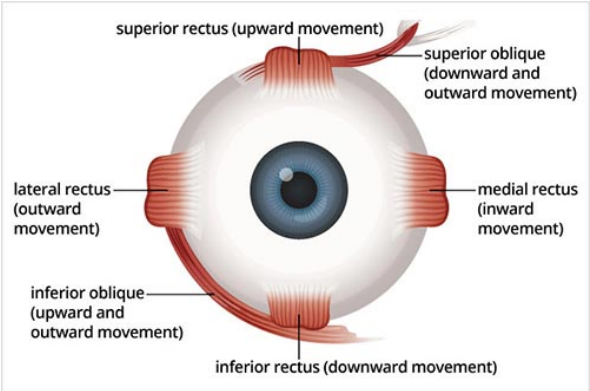

Figure 3-2: Muscles controlling the eye Khodadadian (2017)

It was stated already that often saccades are made when changing the foveal view quickly towards something (although it is possible to make saccades in the dark as well). For the former case, sensory information is needed to initiate the movement. This sensory information thus needs to be transformed from the location of the target to horizontal and vertical eye movements. There are two structures responsible for this: the superior colliculus of the midbrain and the frontal eye field, a region of the frontal lobe (Purves (2004)), both of which are illustrated in Figure 3-4. The frontal eye field projects to the superior colliculus which contains a map representing the visual field and in turn it projects the location to the gaze centers (Paramedian Pontine Reticular Formation (PPRF) meaning horizontal gaze center in Figure 3-4). Saccadic commands are generated in the premotor brainstem regions which cause the muscles to act accordingly (Hanes and Wurtz (2000)).

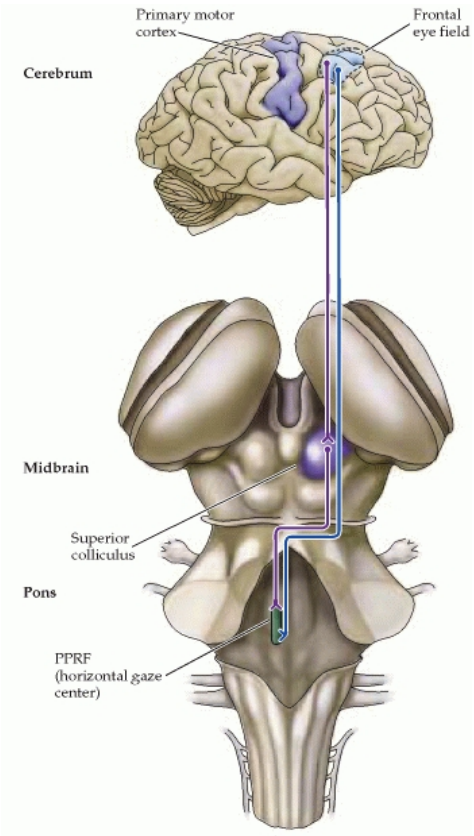

Figure 3-4: Mid brain with superior colliculus and frontal lobe Purves (2004)

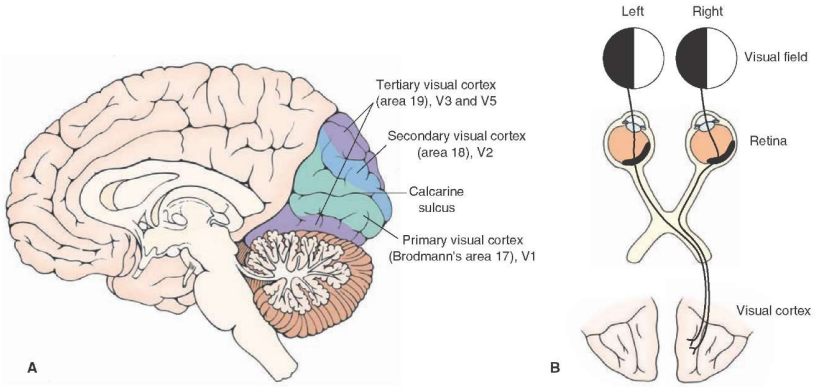

Figure 3-5: Visual System The Crankshaft Publishing (2017)

3-2-2 Smooth pursuit movements

Another eye movement is the smooth pursuit. This kind of eye movement is used to track or follow a moving target. The movement is a much slower one than the saccade and is only made voluntarily. Also it is impossible for most people to make a smooth pursuit eye movement when there is no target. When moving the eye without following a moving target, actually a lot of saccades are made. This also happens when moving the eyes to an imaginary target in the dark.

Since the pursuit movement is used to follow a moving target, information is needed about the speed of the moving target. When this is derived, eye movements can be made with approximately the same speed (Sparks (2002)). Not only the speed is used, but also the acceleration of the target and its position relative to the fovea. In a way, a smooth pursuit movement can be seen as a closed-loop system that tries to stabilize the target on the fovea. It does that by constantly translating signals and converting errors from the ideal path into compensatory eye movements (Thier and Ilg (2005)). In that sense, the velocity, acceleration and location are used as error signals. Furthermore, predictability is very important for this movement, since the lag between the eye and the target can be reduced or even be turned into a lead if the target can be anticipated. The onset of the pursuit movements is an open-loop however, because visual signals have not yet had time to correct the pursuit velocity or direction.

Since constant visual feedback is needed, signals will ascend from the retina to activate neurons in the primary visual cortex shown in Figure 3-5. From there the signal is sent to the middle temporal visual cortex where it is processed to produce a motion signal (Remington (2012)). Krauzlis (2003) found that the superior colliculus is involved in the initiation of the smooth pursuit movement. The cerebellum as seen in Figure 3-6 is involved in the processing of visual signals as well. This is needed for the coordination of vestibular reflexes and also for the adjustment during the open-loop smooth pursuit (Thier and Ilg (2005)).

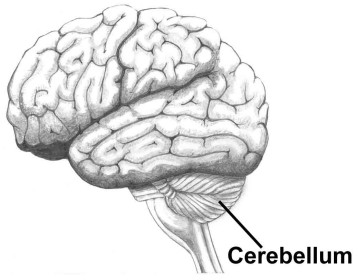

Figure 3-6: Muscles controlling the eye Myers (2006)

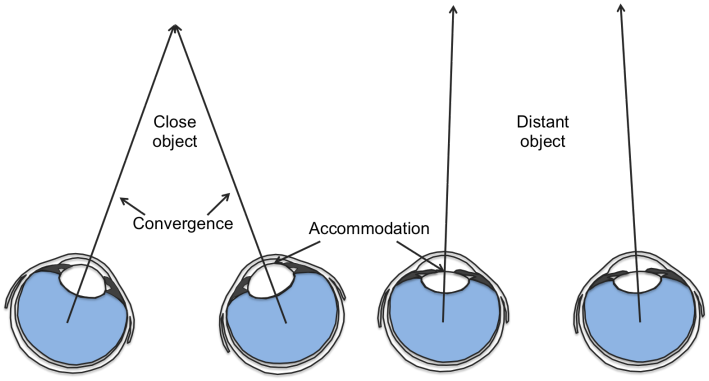

Figure 3-7: Vergence eye movements Wang (2017)

3-2-3 Vergence

Vergence movements are used to be able to have objects into foveal view which are located at different distances from the eye. When an object where the eyes are fixated on, moves closer towards the eyes, the eyes will rotate towards each other in order to get the object into foveal view of both eyes again (Sparks (2002)). This is shown in Figure 3-7. The medial rectus muscles will bring the eyes towards the nose and the lateral rectus muscles will bring the eyes away from the nose. Whereas the smooth pursuit eye movements and the saccades involved movement where both eyes move in the same direction (conjugate), vergence movements involve disconjugate movements.

Mays (1984) found that conjugate and vergence signals are generated independently. These signals are then combined at the extraocular motoneurons and eye movements are made. The amount of vergence needed for the two eyes is in almost all cases different. This is because it would only be the same if the object of interest was located on a plane equally between the eyes. This means that the amplitude of the vergence movements is different for the two eyes.

It was stated that the reason for vergence is to align the object of interest into foveal view again, this sensory stimulus is called binocular disparity. Binocular disparity refers to the fact that the left and right eye observe an object differently because of the horizontal separation between the eyes. The brain uses this disparity to extract information about the depth of

the object and thus stereopsis is developed (depth perception, the ability to see the object by both eyes as one image (Ang (2010))). There is however another sensorty stimulus that can activate vergence movements, and that is visual blur. Visual blur can occur because of a lack of focus and is resolved by making acommodative vergence eye movements (Waitzman (2017)).

3-2-4 Vestibulo-ocular reflex

The Vestibulo-ocular Reflex (VOR) is a reflex that causes eye movements when the vestibular system is activated. This reflex can be noticed when moving the head but fixating on an object. The eyes are able to keep the object stable into foveal view even though the head moves. The reflex thus counteracts the head movements by making the eye move in the opposite direction. It can be easily demonstrated when you focus on an object and move your head. The vestibular system detects the change in position of the head and thus produces fast corrective eye movements. The slower corrective movements are produced when the visual system detects a change in position since the vestibular system is relatively insensitive to slower movements. In this last case the smooth pursuit system is actually activated which relies on visual cues.

Since the vestibular system initiates the VOR, the 3-neuron arc that consists of the vestibular ganglion, vestibular nuclei and the oculomotor nuclei is involved (Amin (2016)). The vestibular nuclei are located in the brainstem. The VOR however does not depend on visual information. The movements involved can be both rotational as well as translational. So the reflex is activated when someone walks or turns around towards an object.

3-2-5 Optokinetic reflex

The reflex that is interacting with the VOR when the head is rotating in stationary visual environment is the Optokinetic Response (OKR) (Kreutzer, DeLuca, and Caplan (2011)).This reflex is important for stabilizing the image of visual input on the retina. The reflex occurs when someone is following a moving target, but the target moves out of the visual field. The reflex makes sure the eyes return again to the position where they could see the object originally. The movement can be experienced when driving a car. Surrounding objects on the road move very fast in the periphery of the driver. The primary fixation need to be maintained on the road, however rapid ocular responses are necessary to perceive the fast moving objects. The OKR makes sure the eye moves quickly from the fast moving objects that move out of view to the road.

3-2-6 Relevant eye movements

The above sections described the different eye movements the human eye makes in everyday life. Some data is given of the eye movements, concerning reactions times and velocities in Table 3-1.

Table 3-1: Oculomotor subsystems Sparks (2002)

Subsystem	Computation	Reaction time [ms]	Velocity [deg/s]
Gaze shifting			
Saccadic	Distance of target image from fovea	200	400-800
Pursuit	Target velocity	125	0-30*
Vergence	Location of target in depth	160	30-150**
Gaze holding			
Vestibular	Rotation or translation of head or body	15	Follows head up to 800 deg/s
Optokinetic	Speed and direction of full-field image motion	60	Supplements VOR in low-frequency range

*If target motion is unpredictable. ** Faster if it occurs in conjunction with a saccade. VOR, vestibulo-ocular reflex.

As can be seen, the reflexes have the shortest reaction time and the saccadic movement is very fast. For the following research however, not all eye movements are relevant to take into account.

Since a tracking task will be performed on a screen that is placed at fixed distance from the subject's heads, vergence movements are not likely to be made. Also, vergence movements could only be measured if the eyes were tracked binocularly. However, the test setup allows for monocular measurements. Vergence movements will therefore not be taken into account.

In the test setup a chin rest is placed, to make sure head movements of the subjects are limited. In this way, the VOR is tried to be limited as well and therefore this reflex is also not taken into account.

It is the purpose of the tracking task that subjects will be able to track a moving object. However, this moving object stay within the visual field of the subjects and therefore the OKR will not be activated.

The remaining eye movements that will be investigated in this research are there the saccades and the smooth pursuit movements. Since subjects will be following a moving target with their eyes, subject will make primarily smooth pursuit eye movements. Saccades are likely to be made when the subject were to lose the moving target and needed to 'catch-up'.

3-3 Oculomotor system in neurodegenerative diseases

As stated before, the oculomotor system is part of the CNS and helps maintain visual stability and also controlls eye movements. Now the different eye movements are known and it has been explained which movements are relevant for this research, this section will give some examples of oculomotor symptoms in neurodegenerative diseases. Also this Section will explain the influence of manual tracking.

3-3-1 Oculomotor symptoms in neurodegenerative diseases

Parkinson's disease
Parkinson's disease involves neurodegeneration because the neuronal loss is located at the

substantia nigra, a part of the brain responsible for the production of dopamine and the transmittance of dopamine to the basal ganglia. People with Parkinson's disease therefore have a shortage of dopamine. This dopaminergic dysfunction causes the motor impairment primarily but has an influence on the visual system as well. For instance, reductions of dopamine levels in the basal ganglia and frontal cortex can also reduce the levels in the superior colliculus. This could be a factor that causes defective saccades (Armstrong (2011)). In approximately 75% of Parkinson's patients abnormal saccadic and smooth pursuit movements are found (Shibasaki, Tsuji, and Kuroiwa (1979)). The reaction time and the maximum saccadic velocity of horizontal gaze are slower. Also smooth pursuit movements can be interrupted by saccades. This means that during the tracking task more catch-up saccades are to be expected.

Alzheimer's disease
The neuronal loss that is involved with Alzheimer's disease is primarily located in the cerebral cortex. The cerebral cortex consists out of four different lobes, each controlling other functions. These lobes are listed in Table 3-2.

Table 3-2: Lobes of the cerebral cortex (Stanley and Swierzewski (2015))

Lobes	Function
Frontal lobe	Voluntary movements Planning Memory Emotion
Parietal lobe	Interprets pain, pressure and temperature etc.
Temporal lobe	Understanding sounds, emotion and memory
Occipital lobe	Understanding visual images

In Alzheimer's disease all lobes are affected, making it difficult to know what causes eye symptoms. For instance, frontal, parietal and temporal pathology may all contribute to impaired eye movements (Molitor, Ko, and Ally (2015)). Alzheimer patients show abnormal saccades, which can be caused by impaired attention. The impairment in the saccades is similar to the impairment of the smooth pursuit, which is primarily an increased latency to the initiation of the movement. No brain region has been identified yet that contributes to the impairment of the smooth pursuit movement (Stanley and Swierzewski (2015)).

3-3-2 Influence manual tracking

Research has been done to investigate the effect of manual tracking.With manual tracking the action refers to the tracking of a an object with the person's hand. The question these researches concerned themselves with was whether this action would influence the

eye movements. Koken and Erkelens (1991) found that this effect was present, but only when the target moved with a predictable signal, being a single sinusoid for example. When a random appearing signal was used, the effect of manual tracking was unnoticeable. They tested this by comparing an experiment where the participants had to follow a signal with their eyes with a similar experiment where they also had to track the signal manually.

Niehorster and Siu (2015) disagreed with this outcome since the two test cases in the experiment did not give similar information to the participant. This is because when the participants tracked the signal manually, they saw more information than when only the eyes had to follow the signal. The information where the hand was, was not shown when the participants only had to look at the signal. Therefore (Niehorster and Siu (2015)) conducted new experiments where the participants first tracked the signal manually and the position of the hand was recorded. After that the participants had to follow the signal with their eyes only while the hand signal of the previous experiment was replayed. In this way the two experiments presented exactly the same information. The result they found confirmed an effect of manual tracking on the eye movements. They found that the overall smooth pursuit gain was higher and also there were made less catch-up saccades. Thus they claim that the enhancement of the eye movements with concurrent manual tracking was not reliable on the predictability of the signal.

When searching for literature on the neural mechanisms underlying eye-hand coordination, there is not one theory why it would or would not make sense that manual tracking influences eye movements. Engel, Anderson, and Soechting (2000) proposed the idea that eye and motor systems are driven by the same neural signals and in that way the two are coupled. Scarchilli and Vercher (1999) writes that eye-hand coordination is enabled by an exchange between the eye and motor systems of efferent and afferent neurons. Afferent neurons being the neurons that send sensory information to the CNS and efferent neurons the ones that send information away from the CNS.

Although there is a debate whether the effect of manual tracking on eye movements is really noticeable when using pseudo-random signals, this research is interested whether the two scenarios (with or without manual tracking) show different results when comparing patients with controls. It could be that patients show a different effect of manual tracking when comparing the eye movements with and without concurrent manual tracking. Therefore the two scenarios are both used in the experiments. The two scenarios are hereafter referred to as the 'eye following' and 'tracking' scenario.

3-4 Effect of aging

It was stated in the introduction that this research will conduct an experiment involving young and old people to proof the concept of identifying and comparing gaze dynamics. This is done because it is within control of this research to find enough subjects for this experiment for significant results and it is very difficult finding enough patients to participate. Since aging has an effect on the brain as well, it could well be that older people show the same

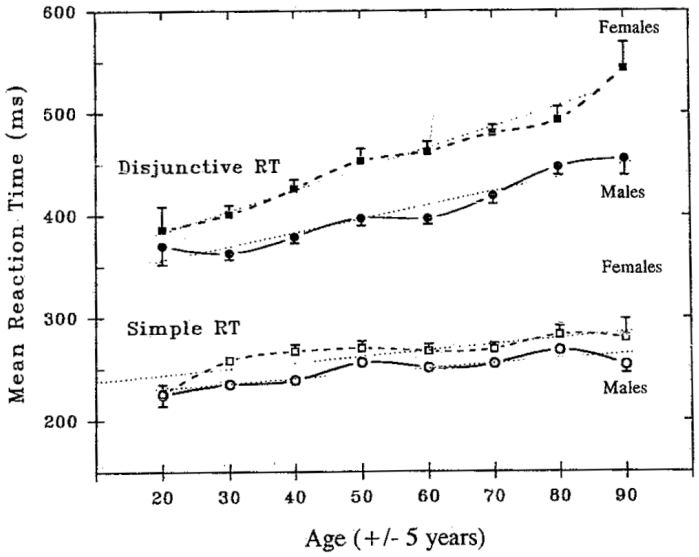

Figure 3-8: Reaction time given for males and females as a function of age (Fozard et al. (1994))

results to some extent as the patients would. This is further elaborated in the coming Section.

It has been found that the volume and/or weight of the brain decreases with age. This rate is around 5% per decade after the age of 40, (Peters (2006)). This decrease is reported to be caused by neuronal loss (Raz (2004)), but whether this is in fact the only cause, is not clear (Trollor and Valenzuela (2001)). The prefrontal cortex (part of the frontal lobe) was found to be most affected as is stated in Trollor and Valenzuela (2001). This research also found that the occipital cortex was affected least. This would be in line with the cognitive changes, eg. memory. The memory can be divided into four sections: episodic memory, semantic memory, procedural memory and working memory. Aging affects only two of those sections: the episodic memory (where when and how the information was learned) and the semantic memory (memory for meanings/facts). In Alzheimer patients the episodic memory is also affected (Peters (2006)).

Other symptoms involved in aging are slower reaction times, lower attentional levels, slower processing times and impairment in sensory and perceptual functions (Peters (2006)). These factors might also contribute to a lower performance during tracking tasks. The effects of aging on eye movements could include increased saccadic latencies and a decreased smooth pursuit gain (Dowiasch et al. (2015)). They also found that the saccade frequency, amplitude, peak velocity and mean velocity are reduced with age.

In Section 3-3-1 the importance of dopamine was already explained. With aging the dopaminergic system also degenerated with a result that the dopamine levels decrease (Seidler et al. (2010)). This may contribute to a decline in the gross and fine motor skills.

In Figure 3-8 it can be seen that the reaction time increases with increasing age, with

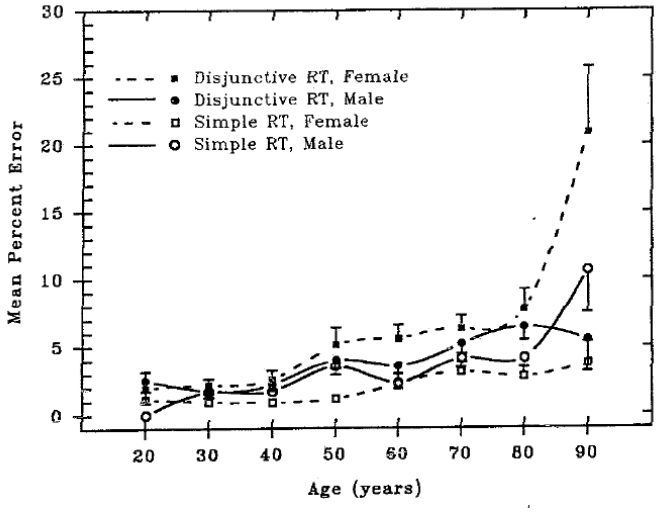

Figure 3-9: Mean percent error given for males and females as a function of age (Fozard et al. (1994))

Simple Reaction Time (SRT) and Disjunction Reaction Time (DRT), (DRT is also known as 'go-no-go' reaction time). In the experiment by Fozard et al. (1994) participants were asked to respond to a tone. In the SRT condition participants had to respons to two tones, one high and the other a low tone. In the DRT condition participants only had to respond to the high tones. For both conditions the reaction time increased with increasing age. Also, with increasing age the error increases, so the accuracy decreases, as can be seen in Figure 3-9.

Chapter 4

Identifying system dynamics

A tracking task is a manual control task where the HC controls a system, while that system is being perturbed by a target signal. The goal during the tracking task is to minimize the error between the system to be controlled and the target. Controlling a system and minimizing the error can be a very common task such as controlling a bicycle or a car, but also an aircraft with gusts of wind. A tracking task can also be as simple as following a moving circle presented on a touchscreen with your finger.

When performing such a task, the HC uses information obtained via sensory systems. This information is processed in the brain and commands are given to the muscles to give an input to the system dynamics. It was exptected that a difference would exist between people with a neurodegenerative disease and healthy people, as was confirmed in de Vries (2015) and Haartsen (2017). Since visual information is very important when performing a tracking task it makes sense that a difference could also be expected in the gaze signal between these two groups. By identifying the gaze dynamics, more insight will be given on eye movements during tracking tasks. Since this is still rather unknown, identifying the gaze dynamics of healthy subjects is the first step.

This section describes the technique used to identify HC dynamics by making use of tracking tasks.

4-1 SOP

Krendel and McRuer (1960) proposed a human manual control hierarchy called the Succesive Organization of Perception (SOP). The SOP is a framework that describes three different stages of control behavior: compensatory, pursuit and precognitive control. The HC could show different strategies depending on the features of the control task.

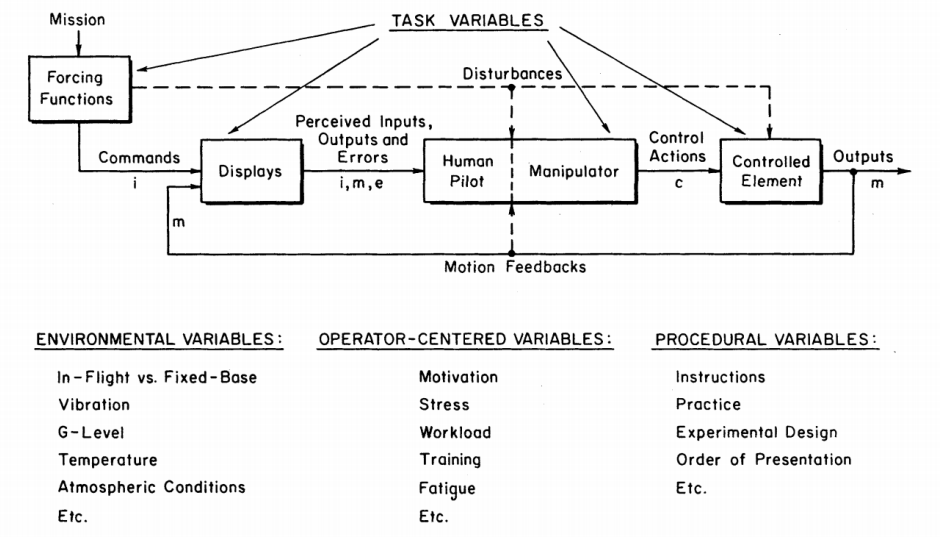

Figure 4-1: Variables affecting the manual tracking task system D. T. McRuer and Jex (1967)

In the compensatory stage the HC only uses the error to act on. In the pursuit stage the HC acts on either two of the following parameters: error, target and the system output. Lastly, in the precognitive stage the HC generates perfect target tracking and does not act on any specific feedback.

The experiment conducted for this research consisted of the two conditions: the tracking and eye following condition. The tracking condition is a pursuit task, but the unpredictable target signal used induces compensatory behavior as will be explained in Section 4-2-4. The eye following condition only shows the target since there is no controlled element. Both tasks are therefore assumed to induce compensatory behavior.

4-2 Tracking tasks

As was briefly stated in the introduction of this section, a tracking task is a task were the HC tries to control a system by minimizing the error between the target and the system. It can therefore be used to induce certain behavior of the HC. This behavior can however be different for different tasks. That is because the HC is a multimode, adaptive, learning controller, capable of exhibiting an enormous variey of behavior (D. T. McRuer and Jex (1967)). For that reason, the design of the task is very important. The controller's characteristics depend on four kinds of variables which are described below and presented in Figure 4-1, (D. T. McRuer and Jex (1967)).

Environmental variables
This variable describes the environment surounding the controller. The temperature for instance can have an effect on the performance of the controller. The examples shown in Figure 4-1 are taken from an aerospace application, but some are still relevant in the application for this research.

Operator-centered variables
Examples of an operator-centered variable are motivation, training and fatigue. These can naturally have a large effect on the performance of the controller.

Procedural variables
This variable describes how the experiment was conducted, for instance the instructions and the order of presentation.

Task variables
There are four task variables that determine the characteristics of the task and thus have a large influence on the HC behavior. These are the forcing function, display, manipulator dynamics and the controlled element dynamics.

The display is the means used to show the input to the HC. Examples of different display that are often used are the compensatory display, the pusuit display and the preview display. Each display shows the same task but contains other inputs for the HC.

The manipulator dynamics takes into account, any dynamics that might be present in the hardware used to give inputs by the HC. These could include the dynamcis of the joystick or touchscreen.

The dynamics of the controlled element can directly infuence how the HC reacts and therefore is an important factor.

Lastly, the forcing function describes the path of the target in case of a target function and is the most important task variable. It can also describe a disturbance function, thus describing the path of the disturbance. The target function and the disturbance function can also be used at the same time.

4-2-1 Displays

As was briefly mentioned in Section 4-2 there are several displays that can be used in a manual tracking task. The compensatory display is shown in Figure 4-2a and shows only the error between the target and the controlled element. The HC is therefore not able to see what the controlled element is doing, only whether the error increases or decreases. The corresponding block diagram is shown in Figure 4-3a

With a pursuit display the output of the system and the target signal are also presented as can be seen in Figure 4-2b and Figure 4-3b. Therefore the error can be derived and used since $e(t) = f(t) - x(t)$. With this display, more information is shown and thus can be used to the advantage of the HC. For instance, it is easier for the HC to get used to the dynamics because the controlled element is shown separately. Also, mistakes can be detected earlier

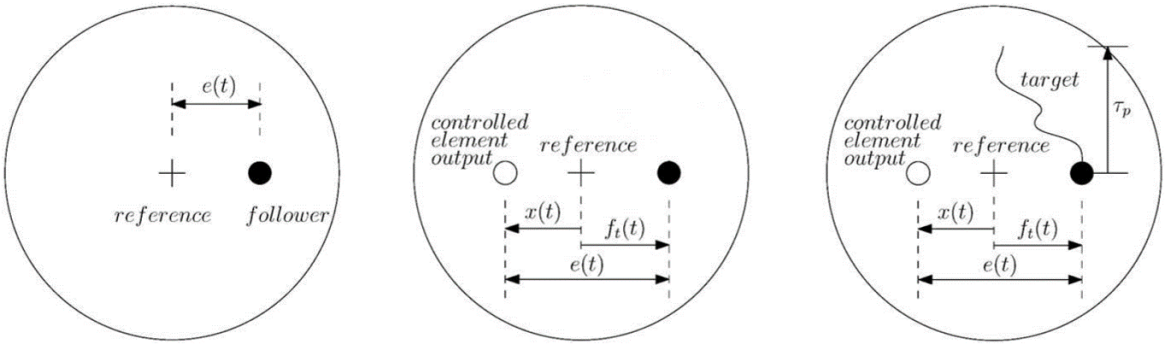

(a) Compensatory display **(b)** Pursuit display **(c)** Preview display

Figure 4-2: Displays for manual tracking tasks van der El et al. (2016)

and corrected. However, it does not necessarily mean that a pursuit display induces pursuit behavior, since the HC can still choose to only act on the error and thus show compensatory behavior.

A preview display shows a part of the future path of the target together with a pursuit display as is shown in Figure 4-2c and Figure 4-3c. This means the HC is able to know where the target is going and decrease the delay. The length of the preview time influences whether the HC uses the preview for higher or lower frequencies (van der El et al. (2016)). The HC can choose to use the preview or choose not to use it. Therefore again it does not mean that a preview automatically induces different behavior, especially for unexperienced subjects.

Flowers (1976) found that a pursuit display for people with Parkinson's Disease is suitable. Also de Vries (2015) used this display and thus using a same display makes for a comparable situation.

The block diagrams shown in Figure 4-3 only show the control loop of the tracking task with the HC shown as one or multiple blocks with the control command as output. Since the research objective of this report focusses on the gaze dynamics, the block diagram will have to be shown a bit differently. This can be seen in Figure 4-4 with the gaze signal given as g.

4-2-2 Manipulator dynamics

The manipulator dynamics are often combined with the neuromuscular system (NMS) dynamics and are represented as a single, lumped, low-order model (second or third order low-pass transfer function) (Mulder et al. (2017)).

4-2-3 Controlled element dynamics

The dynamics of the controlled element are often chosen to be a gain, single integrator or a double integrator. This has a direct influence on the HC since according to the crossover

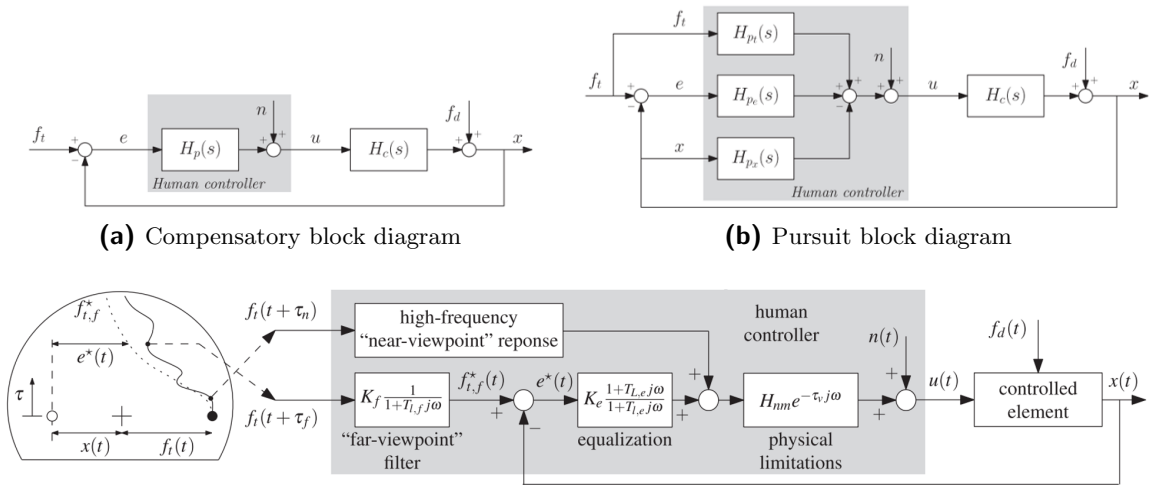

(a) Compensatory block diagram

(b) Pursuit block diagram

(c) Preview block diagram

Figure 4-3: Block diagrams for manual tracking tasks van der El et al. (2016), Mulder et al. (2017)

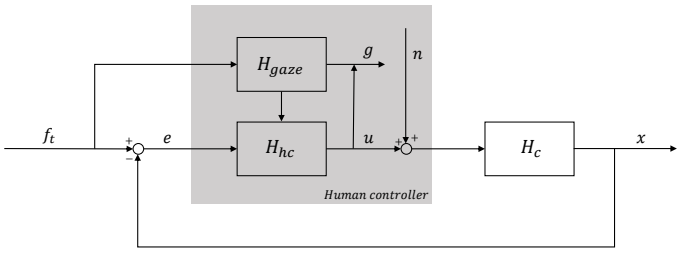

Figure 4-4: Pursuit block diagram with gaze dynamics included

model the combined system represents a single integrator (D. T. McRuer and Jex (1967)). Controlling a gain system is easiest since the HC is influencing the position of the controlled element. With a single integrator the velocity is controlled and with a double integrator the acceleration, thus making the task very difficult. A more difficult task can challenge the HC to show more distinct dynamics which can be desirable. However, Haartsen (2017) found that single integrator dynamics was already very difficult for patients to perform and therefore a gain dynamics was more suitable. Since this research also involves experiments with patients, a gain dynamics is used.

4-2-4 Forcing functions

As stated, the forcing functions are very important to induce the correct HC behavior. It is of importance that the forcing functions appear random because then the HC cannot anticipate the target signal and the crossover model is valid for compensatory behavior (Mulder et al. (2017)). This is typically done by using quasi-random multi-sine signals, consisting out of multiple sine signals chosen in the frequency range where the dynamics of interest is visible.

$$f(t) = \sum_{k=1}^{N_f} A_f(k) \sin(\omega_f(k)t + \phi_f(k)) \tag{4-1}$$

Equation (4-1) describes the target function. Four parameters are used to describe the multi-sine function. N_f represents the total number of sinusiods that are summed. de Vries (2015) used 11 sinusoids and was able to capture the entire frequency spectrum showing the dynamics of interest. ω_f are the frequencies of the individual sinusoids. The dynamics defined in de Vries (2015), was the tracking behavior but it is not expected that the gaze dynamics will appear at a very different frequency spectrum. That is why the same frequencies and the same number of sinusoids will be used in this research as a baseline. The frequencies each are an integer multiple of the natural frequency, often used are prime number to avoid harmonic sinusoids. Lastly ϕ_f are the phase shifts and A_f the amplitudes of the sinusoids. For $\phi_f$the same values are taken as in previous mentioned research. The amplitudes, A_f influence the bandwidth of the multi-sine and since it is not known yet at what bandwidth the dynamics are best defined, this will be varied as a preliminary experiment, which will be explained more in Section 4-2-5.

The length of the signals was taken at $50s$ which is the same length as was used by de Vries (2015) for patients. The first $9.04s$ was used as run-in time. This run-in time was created with the signal staying zero for four seconds followed by a cosine function shown in Equation (4-2).

$$f_{run-in} = (\cos(f \cdot t + 0.5 \cdot \pi))^2 \tag{4-2}$$

As stated before, a disturbance can be also be added and can be described in the same way. To have both a target and a disturbance signal means there are more data points to calculate the frequency response function. It also means the task itself will be more challenging for the

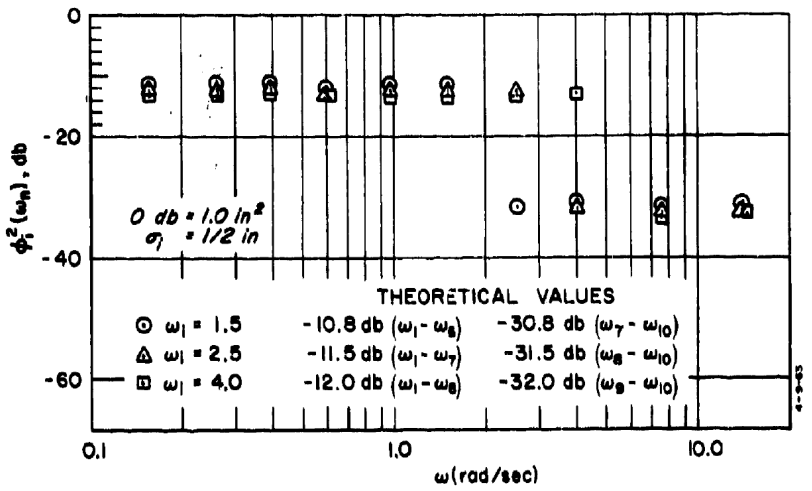

Figure 4-5: Measured input power spectra magnitudes D. McRuer et al. (1965)

subjects. de Vries (2015) found that for patients the task was demanding enough when only a target function was used. Therefore this research will also only consider a target function.

4-2-5 Bandwidths

The bandwidth of a signal is defined as the frequency until where the signal has significant power. A higher bandwidth means the signal will be more difficult. Since it is not known at which bandwidth the gaze dynamics will be best visible, multiple bandwdiths will be tested in preliminary experiments. D. McRuer et al. (1965) also experimented with tracking tasks with varying bandwidths. These signals are shown in Figure 4-5.

Figure 4-5 shows three signals consisting out of 10 sinusoids with varying bandwidths, which can be seen from the amplitude that drops down for the seventh, eighth or ninth amplitude (so at 1.5, 2.5 or 4 rad/s). The ratio between the high and low amplitude levels is always 10. What can also be seen in this Figure is that the amplitude levels for the different bandwidths drop down for the higher bandwidths. This is because the total amount of power in the signal has to stay constant. That means that if the amplitude of a higher frequency has more power, the entire amplitude profile has to drop down to result in the same total power.

This causes a dilemma because either the amplitudes of the different signals are changing, or the power of the signals are changing. Both scenarios are given in Figure 4-6.

D. McRuer et al. (1965) chose to keep the power constant. This research will keep the amplitudes constant (Figure 4-6a), since comparing bandwidths with the same amplitude levels will be easier.

4-3 System identification

With system identification techniques the dynamics of the gaze can be identified. The gaze block of interest is shown in Figure 4-7. A method that is often used to identify dynamics is

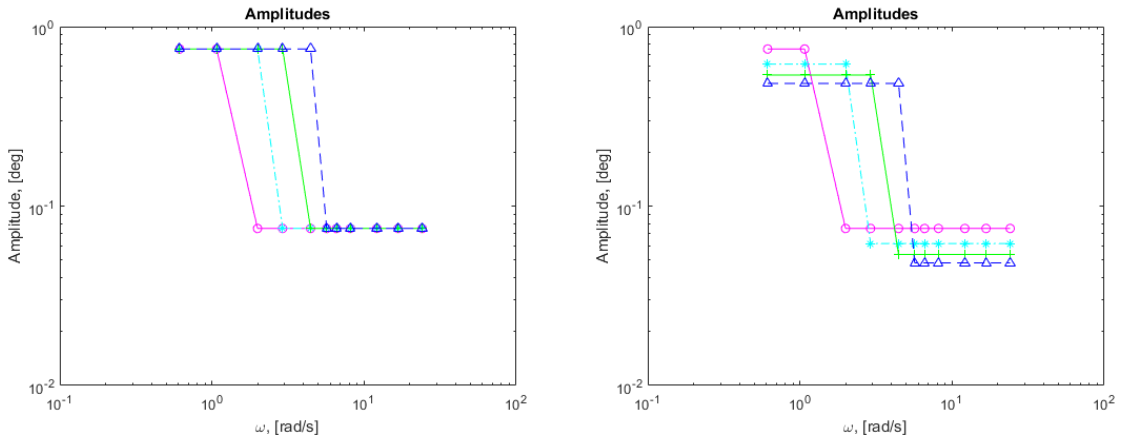

(a) Constant amplitudes **(b)** Constant power

Figure 4-6: Amplitude spectrum varying bandwidth

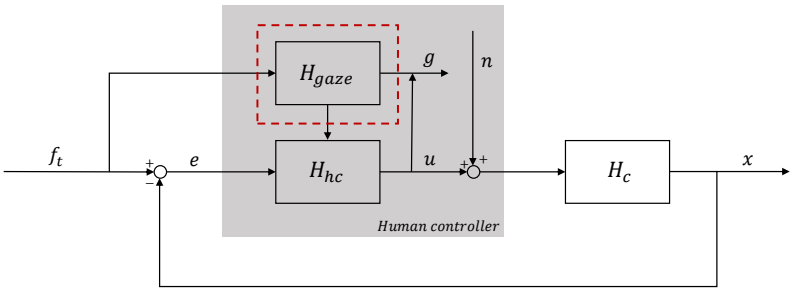

Figure 4-7: Gaze dynamics inside multi-loop block diagram

the Fourier Coefficient Method (FCM). This is a black-box identification tool in the frequency domain. That means that no assumptions are made on the dynamics to be identified. Since the dynamics of the gaze signal has not yet before been identified, a black-box is necessary since no assumptions can be made on the model. This method models the HC as a quasi-linear system, consisting of a linear response to the perveiced variables and a remnant signal that accounts for the non-linearities (D. McRuer et al. (1965)).

When the signal-to-noise ratio at the frequencies where the multi-sine signal has power is very high, the remnant can be dropped and the gaze block can be defined as the Frequency Response Function (FRF) given in Equation (4-3).

$$\hat{H}_{gaze}(j\omega_t) = \frac{G(j\omega_t)}{F_t(j\omega_t)} \tag{4-3}$$

$G(j\omega_t)$ and $F_t(j\omega_t)$ are Fourier coefficients of the gaze (g) and target signal (f_t). From this FRF the frequency response can be calculated and the magnitude and the phase can be plotted. The next step is to estimate the model for the gaze dynamics. The model of D. T. McRuer and Jex (1967) investigated HC dynamics for compensatory displays and

developed the crossover model. For pursuit displays the extended crossover model was developed. The model also included dynamics for the neuromuscular system which is often represented as a second-order low-pass filter given in Equation (4-4).

$$H_{nms}(j\omega) = \frac{\omega_{nms}^2}{(j\omega)^2 + 2\zeta_{nms}\omega_{nms}j\omega + \omega_{nms}^2} \tag{4-4}$$

The parameters used in this model are the neuromuscular natural frequency (ω_{nms}) and the damping ratio (ζ_{nms}). It is not known yet whether this same low-pass filter will fit the gaze dynamics, but it is likely since the eyes also contain muscles that limit the bandwidth of the dynamics. It is also highly probable that there will be a delay ($e^{-j\omega\tau_e}$) and a gain (K_e). The parameters to be identified for the gaze dynamics are therefore K_g, τ_g, ω_g, ζ_g.

After a model is selected, the involved parameters can be estimated. This is done by using a cost function to optimize for the best solution. An example of the cost function is given in Equation 4-5. When more emphasis is needed on the higher frequencies, the function can be normalized which gives the result as is given in Equation 4-6.

$$\hat{\theta} = \arg\min_{\theta} \left[\sum_{k=1}^{N_t} \left| \hat{H}_{gaze}(j\omega_t[k]) - H_{gaze}(j\omega_t[k]\theta) \right|^2 \right] \tag{4-5}$$

$$\hat{\theta} = \arg\min_{\theta} \left[\sum_{k=1}^{N_t} \frac{\left| \hat{H}_{gaze}(j\omega_t[k]) - H_{gaze}(j\omega_t[k]\theta) \right|^2}{\left| \hat{H}_{gaze} \right|} \right] \tag{4-6}$$

The cost function is used to minimize the difference between $\hat{H}_{gaze}$ and H_{gaze}. This is done by calculating the cost by taking an initial solution, repeating this multiple times (50-100) and selecting the optimum solution.

To quantify how well the model is fitted, the Variance Accounted For (VAF) can be calculated as is given in Equation 4-7 (Nieuwenhuizen, Zaal, Mulder, Van Paassen, and Mulder (2008)). Here u represents the actual signal and u_{sim} represents the simulated signal. A VAF of 100% means that the sinal can be perfectly simulated by the model.

$$\text{VAF} = \left(1 - \frac{\sum |u - u_{sim}|^2}{\sum u^2} \right) \times 100\% \tag{4-7}$$

Chapter 5

Preliminary experiment

Before the final exeriment can be conducted a few decisions have to made first concerning the design of the experiment. Some of these questions were shortly addressed in Chapter 3 and concerned the bandwidth and the influence of manual tracking. To be able to make these decisions preliminary experiments were conducted which will be described in this chapter. One experiment was conducted to test address both questions.

5-1 Experiment Setup

This section will explain the experiments that were conducted. First it will discuss the signals that were used in Secion 5-1-1. After that Section 5-1-2 will continue with explaining how the gaze signals were measured. Section 5-1-3 gives the details of the experiments.

5-1-1 Signals defined

As was explained in Chapter 4, the optimal bandwidth to determine the gaze dynamics is not known. Therefore four signals have been tested in the preliminary experiment. The bandwidth was changed by changing the amplitude of the different frequencies of the multi-sine signal. The target signal was based on the signal used in de Vries (2015) in choosing the frequencies and phase shifts. The amplitudes however are chosen differently and are determined with a method also used by D. T. McRuer and Jex (1967). This method has been explained in Section 4-2 and the determined amplitudes are shown in 4-6a. The variables that make up the different signals are given in Table 5-1. The numbers given to the different amplitudes will be used to distinguish between them in this report. Amplitude 1 corresponds to the signal with the lowest bandwidth and amplitude 4 corresponds to the signal with the highest bandwidth.

The result of the different signals are shown in Figure 5-1. Postive values of the signals are the deflection to the right on the touchscreen, negative values are the left deflections. The effect

Table 5-1: Variables of the multi-sine signals

Target, f_t						
n_t	$\omega_t, rad/s$	ϕ_t, rad	$A_{t,1}, deg$	$A_{t,2}, deg$	$A_{t,3}, deg$	$A_{t,4}, deg$
4	0.614	7.239	0.75	0.75	0.75	0.75
7	1.074	0.506	0.75	0.75	0.75	0.75
11	1.994	7.860	0.075	0.75	0.75	0.75
17	2.915	8.1847	0.075	0.075	0.75	0.75
23	4.449	9.012	0.075	0.075	0.075	0.75
29	5.676	6.141	0.075	0.075	0.075	0.075
37	6.596	6.776	0.075	0.075	0.075	0.075
53	8.130	6.265	0.075	0.075	0.075	0.075
79	12.118	4.432	0.075	0.075	0.075	0.075
109	16.720	2.672	0.075	0.075	0.075	0.075
157	24.084	8.009	0.075	0.075	0.075	0.075

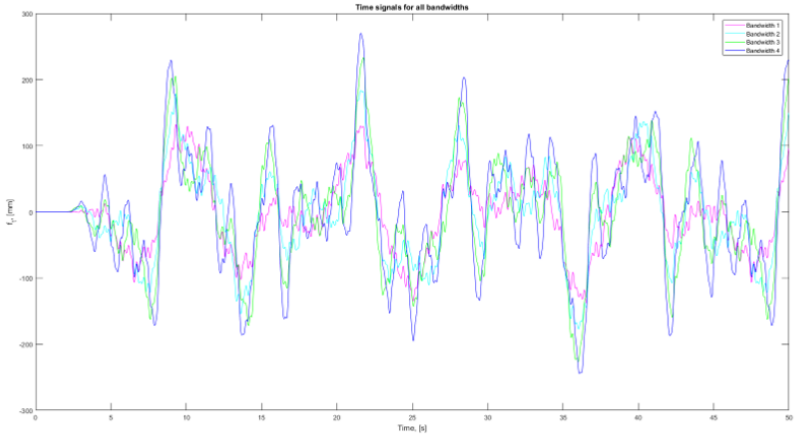

Figure 5-1: Time reponse of the four different signals

of the different total amount of power in the signals can be seen, since the total deflection of the signals is very different. Also there is a difference in the oscillations visible in the signals. This is because the signals where relatively few frequencies have significant power, there are too few slow oscillations. This results in the higher frequencies having more effect. The signal where there are more frequencies with significant power the higher frequencies have relatively little effect since the intermediate frequencies are present with power.

5-1-2 EyeSeeCam

The measuring of the gaze signals is done with an eye tracker called the EyeSeeCam (ESC) as is shown in Figure 5-2a. This is an eye tracker that can be placed on the head with a non-invasive headband. There are infrared mirrors attached to the headband . These mirrors can reflect infrared light coming from infrared LED's. The recording of the eye is done by a camera (or multiple cameras) that is also attached to the headband and is directed towards

(a) ESC with one camera

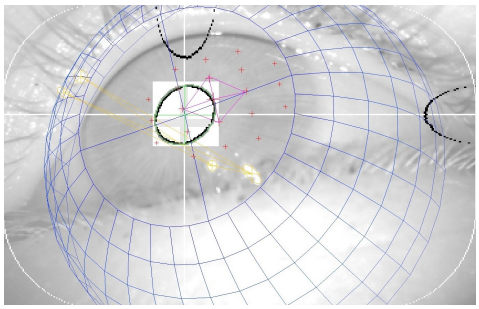

(b) Recorded image of eye

Figure 5-2: Measuring gaze signal

Table 5-2: Experiment design

Experiment	Bandwidths	Trials	Subjects	Total
Tracking	4	5	10	200
Eye folowing	4	3	10	120
Total				320

the infrared mirrors. The recorded image of the eye is shown in Figure 5-2b.

From the ESC a lot of data can be extracted. The data used for this research is the angle of the gaze. This is calculated by the software of the ESC by making use of a pupil detection algorithm. The pupil is detected from the image of the recorded eye as can be seen in Figure 5-2b. The visual angle of the eye is then calculated, which can be converted to the position on the touchscreen with the distance to the touchscreen known. This signal can be used for the further analysis of the performance of the gaze.

5-1-3 Experiment design

The design of the experiment is given in Table 5-2. As can be seen there were 10 subjects that participated in the experiments. These were students in the age group 22-27 years from both Erasmus University and Delft University of Technology. Each trial had a duration of $50s$. This length was determined in de Vries (2015) and was based on what was still possible for patients to do, since the normal length of around $90s$ was considered too long and invasive for the patients.

The test setup can be seen in Figure 5-3. There is a chinrest where the head can be placed on to limit head movements during the measurements and also to ensure that the head is in the same position during different trials. The distance from the head to the screen is $0.5m$. The ESC can be seen placed on the head and also the touchscreen is visible. The touchscreen is used to give inputs to the controlled element. In one of the lower corners of the screen (depending on which is the dominant hand) a blue bar is shown which can be used to give the inputs.

The displays showing the two different conditions are shown in Figure 5-4. The blue circle with the cross represents the target signal. The red filled circle in Figure 5-4b represents the

Figure 5-3: Test setup when measuring eye-hand coordination

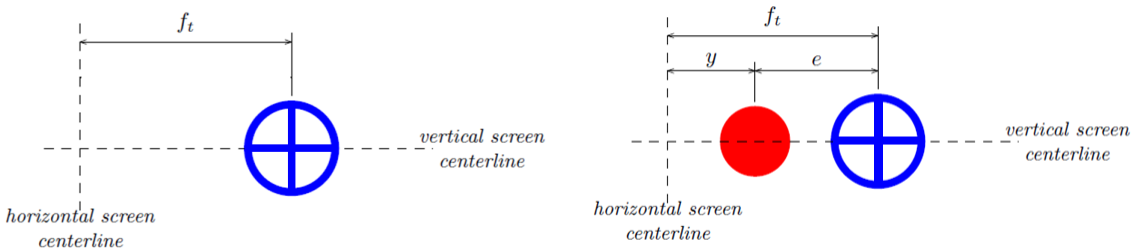

(a) ye following condition **(b)** Tracking condition

Figure 5-4: Display of two conditions

to be controlled element. It is the goal of the subjects to steer the red filled circle into the blue circle for the tracking condition. In the eye following condition where no controlled element is present, the goal is to follow the blue circle as accurately as possible. The cross is added to the blue circle to make sure the subjects have a precise point to look at, and this is kept the same in the tracking condition. In the tracking condition the bar is shown for the inputs. The eye following condition does not need a bar, since no element needs to be controlled and the subjects only need to follow the target with their eyes.

To prevent any learning effects that can cause anticipation between the different bandwidths, the order of the appearance of the different signals was changed for each person. The starting signal as well as the order was different for everyone. Therefore the subject was not able to know whether the next signal would be a higher or lower bandwidth. Also the order between the two conditions was changed. Because fatigue could happen after intensively tracking fast signals, there could be a difference between the first and second conditions with relation to how tired the subjects were. Therefore half of the group first started with the eye following task and continued with the tracking task and the other half of the group this was switched around.

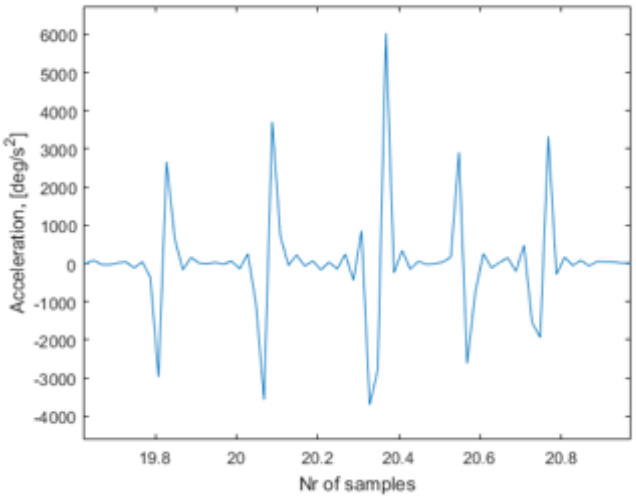

Figure 5-5: Characteristic acceleration profile of saccades movements

5-2 Results

This section will show and discuss the results of the experiments, after which Section 5-3 will continue with the discussion of the results and the conclusion.

5-2-1 Errors and blinks

The gaze signals that are obtained from the ESC still contain gaps and errors. This is partly because people blink. When a subject blinks, the ESC cannot find the pupil so there will be missing data in the signal. Also since the ESC makes use of infrared light, the pupil detection works on finding the darkest spot in the recorded image. This can cause an error when for instance an eyelash is seen as the darkest spot. These errors can be detected because they appear as a large peak in the signal. These error are removed and the gaps because of the blinks are interpolated before continuing with the analysis.

5-2-2 Saccade detection

As was explained in Section 3-2 saccades are very fast eye movements where the eye quickly changes foveal view. They eye therefore moves from one location to another in a very short time. This move is therefore easy to detect because it has such a distinct characteristic. When the position would appear in a quick change, the velocity of the eye will be large peak since the velocity is very high. The acceleration therfore would be two large peaks in opposite directions, because the velocity of the eye quickly increases at first and soon after quickly decreases again. An example of how this would look is given in Figure 5-5.

The time when these saccades happened can be derived from Figure 5-5 and the saccades can be detected in the original signal. This can be seen in Figure 5-6. The Figure shows saccades

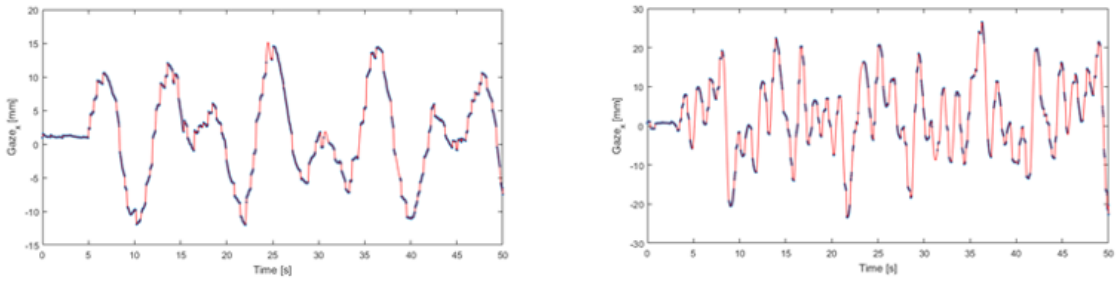

(a) Bandwidth 1 **(b)** Bandwidth 4

Figure 5-6: Saccade detection in position signal

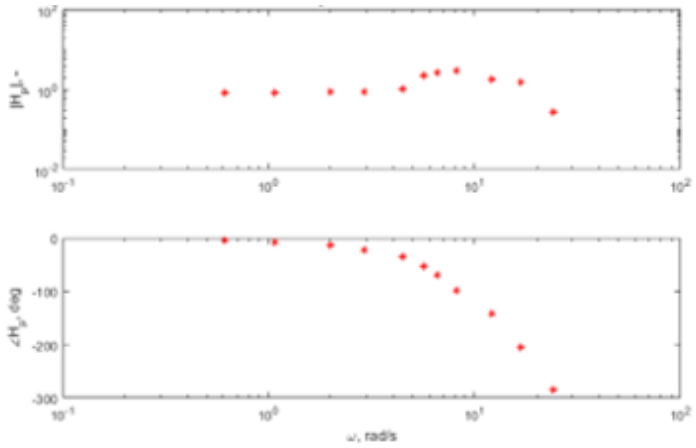

Figure 5-7: Bode plot for eye following condition, bandwidth 4

detected in the signals with lowest and highest bandwidths (1 and 4 respectively). It can be seen that there are differences between the saccades detected. For instance, in the signal with the higher bandwith, a larger part of the signal is defined as saccade. When the saccades are removed however, the accumulated distance travelled by the eye is also larger for the higher bandwidth signal. This is also because that signal moves more and at greater distances. This difference can be used to distinguish between controls and subjects in the final experiment. For the remainder of this report, the entire signals are used however and no saccades were removed during analysis yet.

5-2-3 Results

When all the subjects had finished the experiments, the trials were averaged such that each subject had one result for every bandwidth for both conditions. For each of these cases, a model was fitted. This resulted in eight models for every subject (four bandwidths, two conditions), so 80 models in total. Before the model was fitted, from the Bode plots the type of model had to be estimated. An example of a Bode plot is given in Figure 5-7.

It can be seen from Figure 5-7 that the signal is followed well for lower frequencies, since

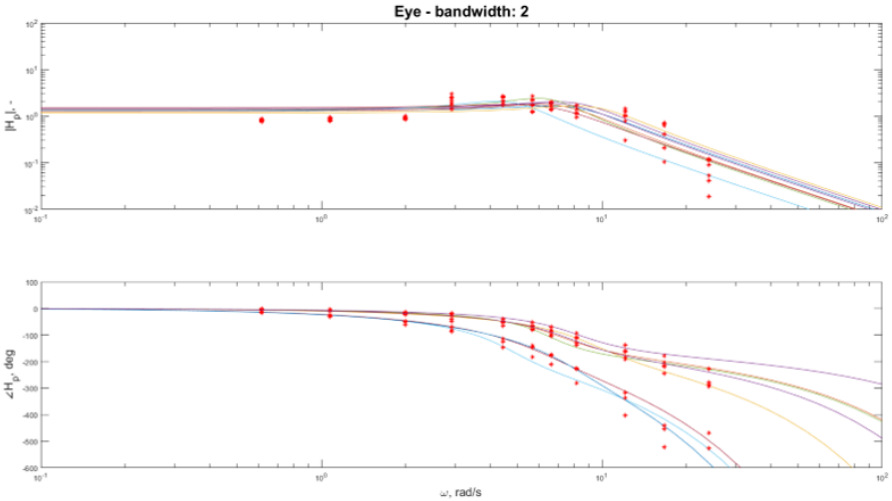

Figure 5-8: Fitted models for eye following condition, bandwidth 2

the data points lie around value 1. For the higher frequencies the lag increases which can be seen in the phase plot, meaning that there is a delay present. Als it can be seen that there is a peak present in the magnitude plot. This suggests that a second-order FRF would be suitable. The model that was used to indentify the gaze dynamics is given in Equation 5-1. The parameters to be identified were the gain (K_e), the time delay constant (τ_e), the natural frequency of the gaze (ω_g) and the damping ratio of the gaze (ζ_g). These parameters represent the agresiveness of the gaze signal, the reaction time, the frequency at which the gaze system oscillates on its own and whether the system is overdamped or underdamped respectively.

$$H_g(j\omega) = K_e \cdot e^{-j\omega\tau_e} \cdot \frac{\omega_g^2}{(j\omega)^2 + 2\zeta_g\omega_g j\omega + \omega_g^2} \tag{5-1}$$

The fitting was done using the cost function described in Chapter 4. An example of one condition with one bandwidth with the resulting models is given in Figure 5-8.

To be able to compare the identified parameters, they have been plotted together in Figure 5-9. This Figure shows a subfigure for every identified parameter (K_e, τ_e, ω_g and ζ_g). Every subfigure shows eight box plots, grouped per two for the two conditions (E for eye following and T for tracking). The bandwidth increases from left to right, so the two most left box plots belong to the two conditions of bandwidth 1, then bandwidth 2 and so on.

5-2-4 Missing data

The tracking tasks is running on Matlab R2010. The computer running Matlab is connected to a trigger which is also connected to the ESC. This trigger send a command to the ESC indicating the start and end of each trial. In that way the tracking task shown on the touchsceen and the gaze signal can be matched in time. Unfortunately due to memory problems in either Matlab or the touchscreen (or both) there were induced delays in

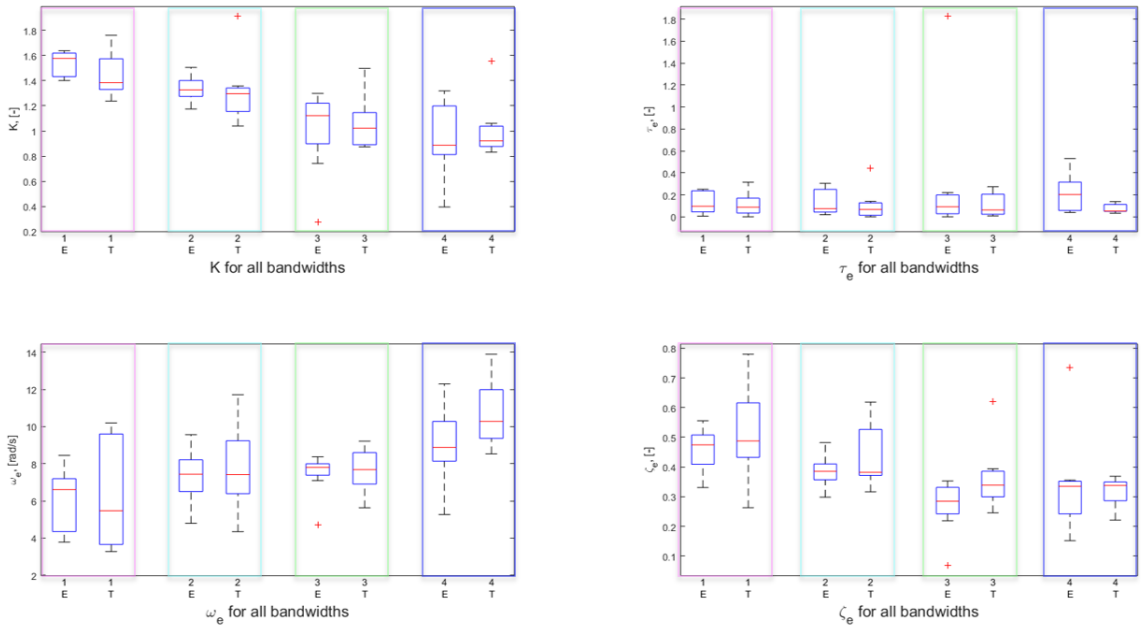

Figure 5-9: Box plots for identified parameters

Table 5-3: Percentage change parameters with increasing bandwidth

	K_e	τ_e	ω_g	ζ_g
Eye following	64%	-	46%	34%
Tracking	42%	-	73%	66%

the task and/or the display. This caused the trigger to send the command to the ESC either too late or too soon (depending on the delay coming from Matlab or the touch-screen). This resulted in timing issues when trying to match the gaze signal to the true signal.

A threshold of $0.2s$ was taken as maximum difference between the gaze signal and the true tracking signal. When this difference was larger than the threshold, the data was not taken into account. This caused for only 60% to be useful data.

5-3 Discussion

What can be seen from Figure 5-9 is that with increasing bandwidth the gain decreases. The time delay constant stays around the same value. The natural frequency of the gaze increases. Lastly, the damping ratio of the gaze decreases. The precentual increases or decreases are shown in Table 5-3.

These changes suggest that with increasing bandwidth, the stiffness of the system that is identified increases, since the natural frequency increases and the damping ratio decreases.

Table 5-4: ANOVA results for tracking condition to test bandwidth effect

	K_e	τ_e	ω_g	ζ_g
p	< 0.05	≥ 0.05	< 0.05	≥ 0.05

The reason why this experiment was conducted, was to try to find out if there was an optimal bandwidth at which the gaze dynamics would be possible to identify. With the results obtained, certain selection criteria were identified. These will be discussed one by one.

Largest difference between conditions
It is the purpose of the final experiment to find a difference between patients and controls. Since no experiment was yet conducted in the preliminary phase with patients, it is difficult to predict for what condition this difference would be largest. However, when there would be no difference between the two conditions in the preliminary experiments of controls, there would be no immediate reason to conduct both conditions again on patients and controls. Therefore the largest difference between the two conditions in the preliminary phase would be desirable, since even if the difference between patients and controls would not appear in the final experiment, at least the difference between the two conditions would still be present to analyse.

This was tested with a paired t-test to find significance between the two conditions. Unfortunately due to the missing data explained in Section 5-2-4, not every subject had data for every model. There was only one case that showed significant results, for ω_f with bandwidth 4. The other cases showed no significant results.

Largest difference between bandwidths
The same reasoning applies to the difference between bandwidths as for the above mentioned conditions. When there would be no difference between the conditions, it would be possible to test two bandwidths in the final experiments, such that more results can be obtained. This would however cause this research to deviate from the initial plan to select a bandwidth that was most suitable.

To test for significance between bandwidths, an anova test was performed. Again because of the missing data there was not enough data to use for the eye following condition. This is because for the four different bandwidths, different subjects have data. The left-over subjects that have data for all bandwidths is not enough for that condition. It was possible however to perform an anova test for the tracking condition. The result showed a significant effect in the bandwidths for K_e and ω_g as can be seen from the p-values in Table 5-4. τ_e was not significant as was expected, but ζ_g also showed no significant result although the results seemed to indicate this.

Smallest spread of the parameters
When the spread of the parameters would be smallest, the model is defined with the highest certainty. This would mean less deviations are expected which would be good when

comparing the parameters.

The difference in spread is not consistent for the bandwidths and different parameters, therefore this criterium cannot be used to decide on one bandwidth.

Best fit for the model
The VAF can be calculated to compare the models. The model where the VAF is highest, is the model which can predict the gaze response best. Since ultimately the gaze dynamics need to be compared, a high VAF, therefore a good estimate is very important.

Predictability of the signal
Even though the signals used are all quasi-random signals, subjects might still experience them to be predictable. A predictable signal induces a non-linear response, in which case the analysis is not valid. Therefore any predictable signal cannot be used for the final experiment. This was the case for bandwidth 4 and therefore this bandwidth will not be used.

What is doable for patients
The last criterium is the intensiveness of the signals and is actually a very important one. This is because if there is a signal which is very difficult or intensive to follow or track the patients will not be giving any useable results. Since the patients are in general older and also are in less physical health, the signal cannot be too invasive for them. The experience of the signals for the subjects was that the signal with bandwidth 4 was too fast and therefore this one is expected to be too difficult for the patients. Also bandwidth 1 is not suitable, because of the lack of slow oscillations, the signal appeared shakey and therefore this bandwidth will also not be used in the final experiment.

5-4 Conclusion

From the results it can be concluded that it is possible to identify the gaze dynamics for all the four bandwidths that were tested. It it also clear that the dynamics identified is different for the different bandwidths.

Based on the criteria above, there are two bandwidths left to select: bandwidth 2 and 3. The signal with bandwidth 3 is more difficult and therefore more challenging. This could be a good thing, since this could show more distinct dynamics (a higher bandwidth shows a more distinct peak in the magnitude plot). When the dynamics is pushed to the limits in that way it could result in a larger difference between patients and controls which would be desirable. However, a higher bandwidth also means a more intensive signal which could be too intensive for the patients.

Since the proof of concept of the final experiment will be conducted with healty controls of a young age group and an older age group, this older age group can be used to test the signal

with bandwidth 3. It is expected that if these subjects do not experience troubles tracking this signal, then it would be possible for patients too. If not, signals with bandwidth 2 will be used in the experiments.

Chapter 6

Proposal final experiment

Based on the conclusions given in Chapter 5 this Chapter will give a proposal for the final experiment.

6-1 Subjects

As mentioned in Chapter 3 a proof of concept will be done by comparing experiment results from younger subjects with older subjects. The results will thus proof whether this way of analyzing gaze data can give new insights but it will also show the effect of aging on gaze performance. Eventually, experiments will be conducted with patients when they come in at the Erasmus Medical Center (EMC). These appointments are part of a larger research held at the EMC. It is still unknown how many patients are likely to come in during the time of this research. To compare the results of the patients experiments will be conducted with age-matched controls.

For the proof of concept experiment it will be aimed to have subject groups of 20 older people and 20 younger people. Since it is a between-subject experiment, more subject are needed and these numbers are expected to be enough to give significant results. The age of the younger participants will be around 22-27 again. The age of the older participants will be in the same age-group as the patients such that these results can be used as controls in the final experiment with patients. If the effect between the older and younger group is not quantifyable, older people will be selected to participate.

6-2 Control task

The same as in the preliminary experiments, there will be two conditions: the eye following task and the actual tracking task.

The final experiment will be a horizontal-axis target-tracking pursuit tracking task again, where the display will be the same as the one used in the preliminary experiments. The task will be shown again on a touchscreen so the subject will have to give their control input with a touchscreen again. This is thought to be intuitively easier for most people.

The target will move with a forcing function consisting of eleven sinusoids at the same frequencies as the preliminary forcing function. The bandwidth, so the amplitude distribution of the sinusoids will be bandwidth 3 as was explained in Chapter 5. The phase shift has not been changed yet from what was used in de Vries (2015) but could be altered by looking into the crest factor.

The dynamics of the controlled element in the tracking task will be a gain again, since the patients will be more likely to complete the task succesfully.

6-3 Apparatus

The same test setup will be used as was shown in Chapter 5. That means a touchscreen will be used to display the tasks and to give control inputs. A chinrest that can be adjusted to the correct height will be there to limit head movements. The ESC will be used to measure the eye movements.

6-4 Experiment design

The length of the trials will be kept the same, so $50s$ of which the last $40.96s$ will be used for analysis since there is a run-in time of $9.04s$. For the final experiments, more trials will be done than in the preliminary experiments. It is expected that eight trials will be sufficient to give enough results and also still doable for the patients. During the experiment the subject will be given sufficient breaks and they can stop if they would like to.

The subjects will perform eight trials for both conditions. Their goal is to minimize the error between the red filled circle (controlled element) and the blue circle (target) for the tracking condition. The goal for the eye following condition is to look as accurately as possible to the target.

A training phase is done at the start of the experiment such that the subjects can familiarize themselves with the tracking task. To motivate the subjects, their performance score will be shown at the end of each run. This is only possible for the tracking case, since the score is the performance of the tracking which will not be done in the eye following condition.

Part III

Paper Appendices

Appendix A

Experiment Consent Form

Experiment Consent Form

Aging effect in quantifying gaze dynamics

I hereby confirm that:

1. I volunteer to participate in the experiment conducted by the researcher (**Jasmijn Büskens**) under Supervision of **dr.ir. Daan Pool** from the Faculty of Aerospace Engineering of TU Delft and **dr.ir. Johan Pel** from the Erasmus Medical Center. I understand that my participation in this experiment is voluntary and that I may withdraw and discontinue participation at any time, for any reason.
2. I have read the experiment briefing. Also, I affirm that I understand the experiment instructions and have had all remaining questions answered to my satisfaction.
3. I understand that my participation involves performing a simple manual control task on a touch screen where eye movements are recorded with an eye tracker.
4. I confirm that the researcher has provided me with detailed safety and operational instructions for the hardware (touch screen and eye tracker) used in the experiment.
5. I understand that the researcher will not identify me by name in any reports or publications that will result from this experiment, and that my confidentiality as a participant in this study will remain secure.
6. I understand that this research study has been reviewed and approved by the TU Delft Human Research Ethics Committee (HREC) and the Erasmus University. To report any problems regarding my participation in the experiment, I know I can contact the researchers using the contact information below or, if necessary, the TU Delft HREC (hrec@tudelft.nl).
7. I have been given a copy of this consent form.

My Signature	Date
My Printed Name	Signature of researcher

Contact information researcher:	Contact information research supervisor
Jasmijn Büskens	dr. ir. Daan Pool
j.buskens-1@student.tudelft.nl	d.m.pool@tudelft.nl
+31 6 50445685	+31 15 2789611

Appendix B

Experiment Briefing

EXPERIMENT BRIEFING

QUANTIFICATION OF GAZE DYNAMICS IN A PURSUIT TRACKING TASK BY MEASURING EYE MOVEMENTS

Thank you for your contribution to this experiment! You will be participating in a tracking experiment in the Vestibular Ocular Laboratory at the Neuroscience Departments of the Erasmus University. During this experiment, the eye movements will be measured such that the dynamics of the gaze can be identified. The gaze dynamics can be used to investigate aging effect and the effect of neurodegeneration. This briefing will introduce you to the experiment and what is expected of you as a participant.

GOAL OF THE EXPERIMENT

The goal of this experiment is to investigate the difference in gaze dynamics between young adults (20-30 yrs) and older adults (55-75 yrs). If this difference is quantifiable with system identification techniques, the same tool can be used to investigate differences between healthy control subjects and people with neurodegenerative diseases. In this way diagnosis of these diseases can be faster and more accurate.

PURSUIT TASKS

The tasks you will carry out are a pursuit following task and a pursuit tracking task. In one task it is your goal to follow the target (blue circle with cross) as precise as possible with your eyes only (Figure 1). In the other task, it is your goal to minimize the error between the target and the controlled element (red circle) (Figure 2). The corresponding displays are shown below. The target will be moving horizontally only and it will be unpredictable.

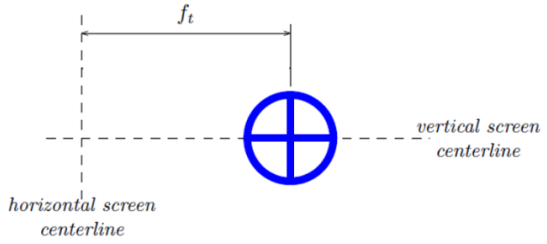

FIGURE 1: DISPLAY OF EYE FOLLOWING CONDITION

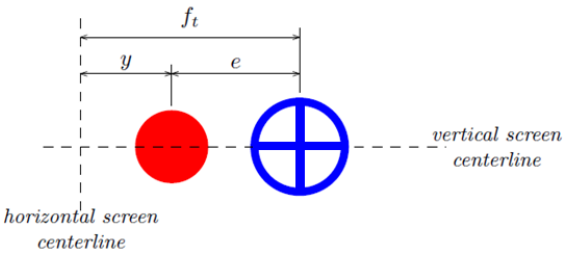

FIGURE 2: DISPLAY OF TRACKING CONDITION

During the pursuit tracking task, inputs to the system can be given via a touch screen. The eye movements are measured by an eye tracker which can be positioned on the head with a headband (Figure 3). A chinrest is provided to keep the head still and gloves can be used as is desired when using the touch screen.

FIGURE 3: EYE TRACKER USED FOR EYE MEASUREMENTS

PROCEDURE

Four conditions will be tested in total. The pursuit following and the pursuit tracking display will both be used to present two different signal with which the target will move. The difference between these signals is the bandwidth. Each condition will consist out of 8 trials, resulting in 32 trials in total, each lasting for 50 s.

Training	Trial 1	Trial 2	Trial 3	Trial 4	Optional	Optional	Optional	Optional
Condition 1	Run 1	Run 2	Run 3	Run 4	Run 5	Run 6	Run 7	Run 8
Condition 2	Run 1	Run 2	Run 3	Run 4	Run 5	Run 6	Run 7	Run 8
Break								
Condition 3	Run 1	Run 2	Run 3	Run 4	Run 5	Run 6	Run 7	Run 8
Condition 4	Run 1	Run 2	Run 3	Run 4	Run 5	Run 6	Run 7	Run 8

FIGURE 4. EXPERIMENT PLAN

The first session will start with a training set of 4 runs (or more if needed) to let you get familiar with the system and the tasks. Between the different conditions there will be a break. Additional breaks can always be taken when the participant feels any fatigue.

Appendix C

FRF models

C-1 Younger participants

C-1-1 Models Participant 1

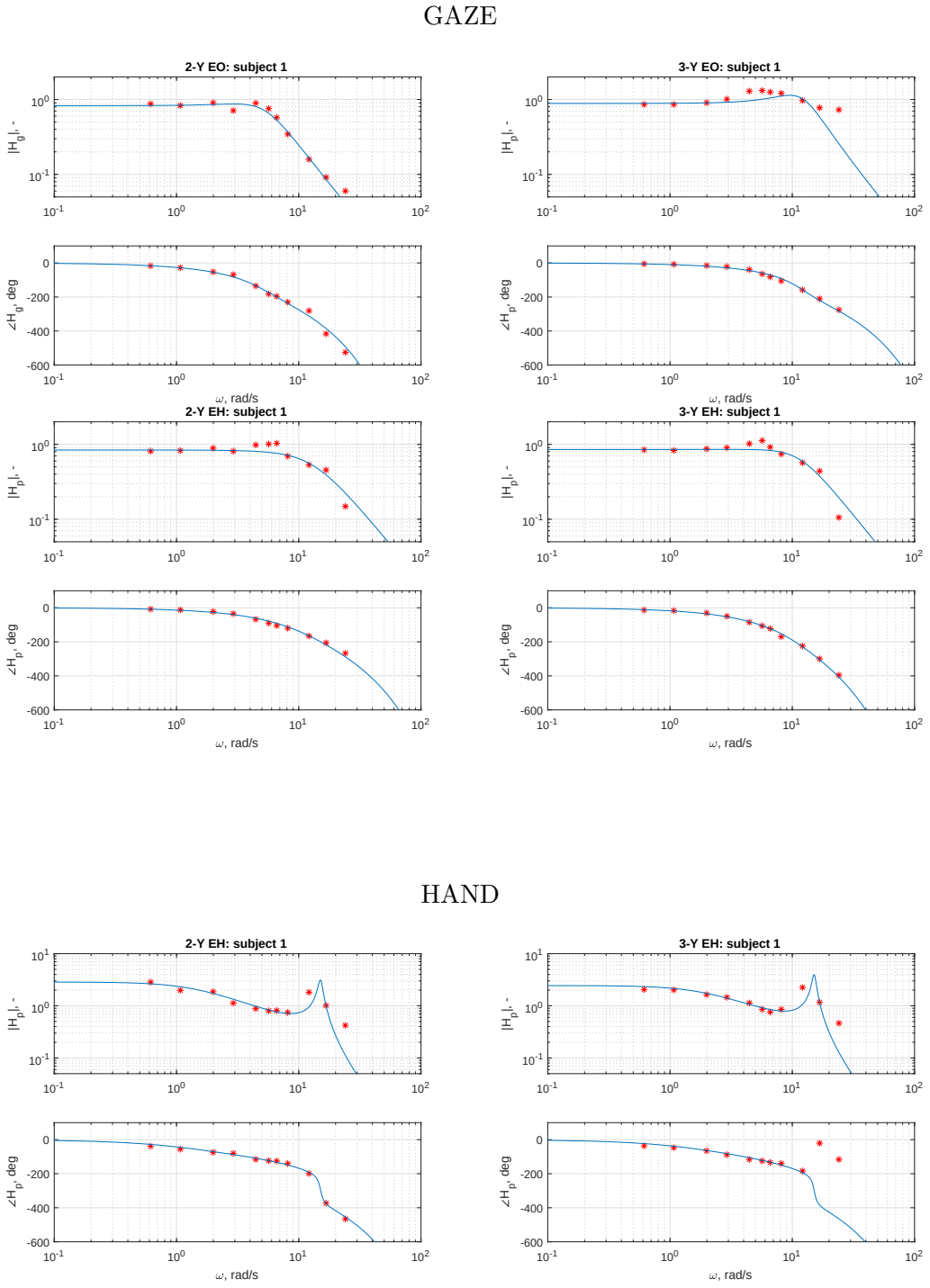

Figure C-1: FRF with fitted models for the gaze dynamics and the hand dynamics of subject 1.

C-1-2 Models Participant 2

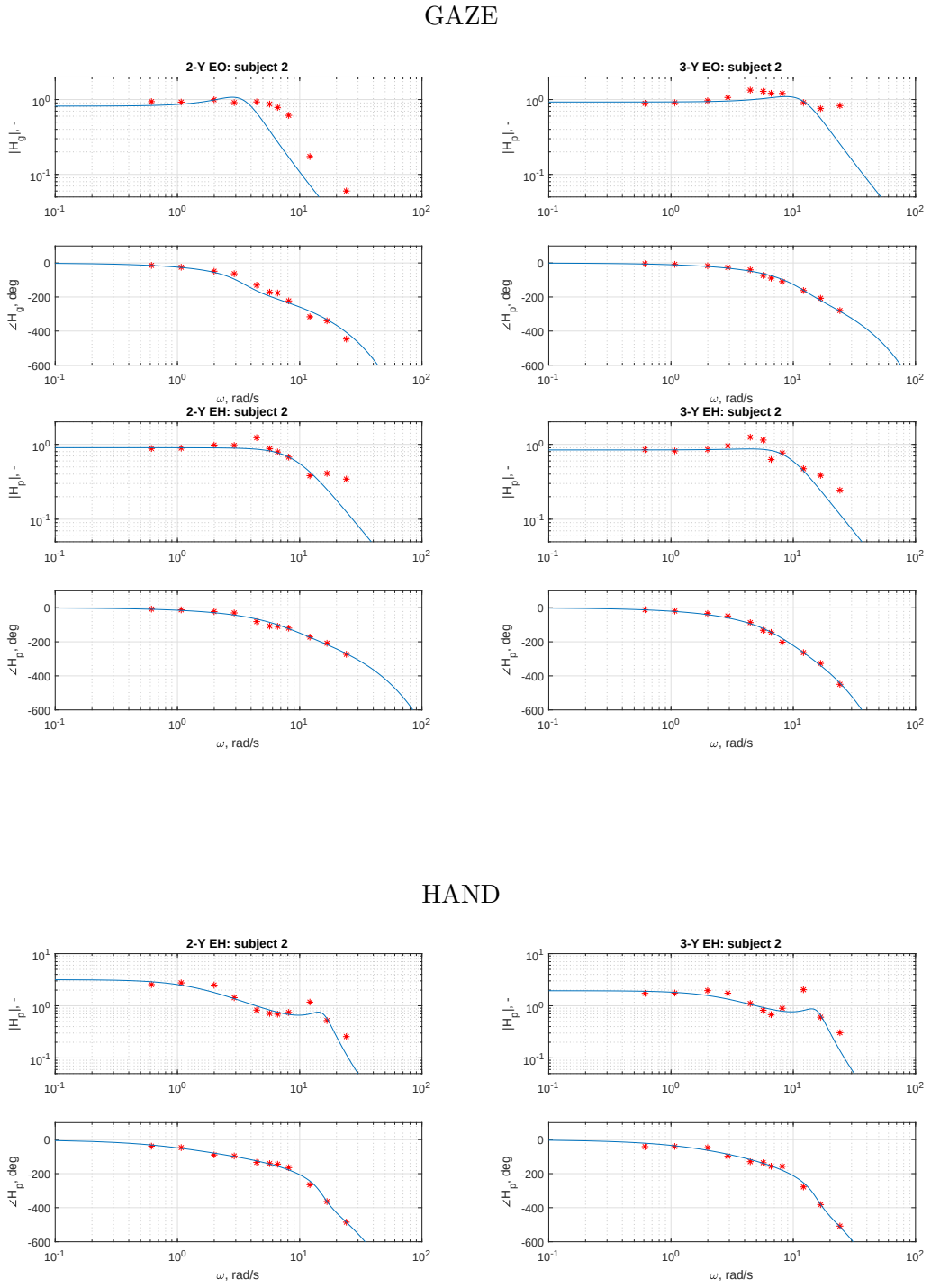

Figure C-2: FRF with fitted models for the gaze dynamics and the hand dynamics of subject 2.

C-1-3 Models Participant 3

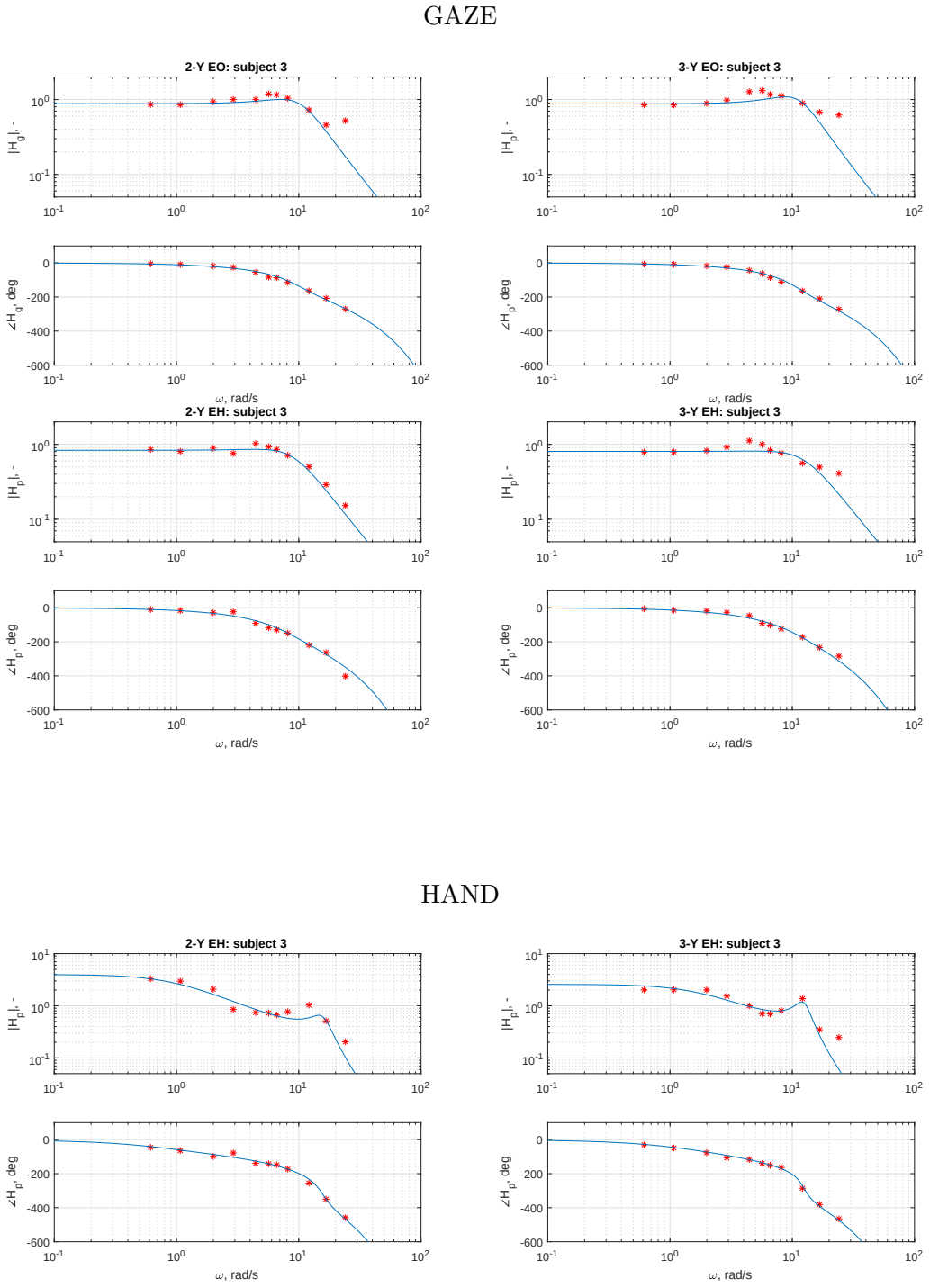

Figure C-3: FRF with fitted models for the gaze dynamics and the hand dynamics of subject 3.

C-1-4 Models Participant 4

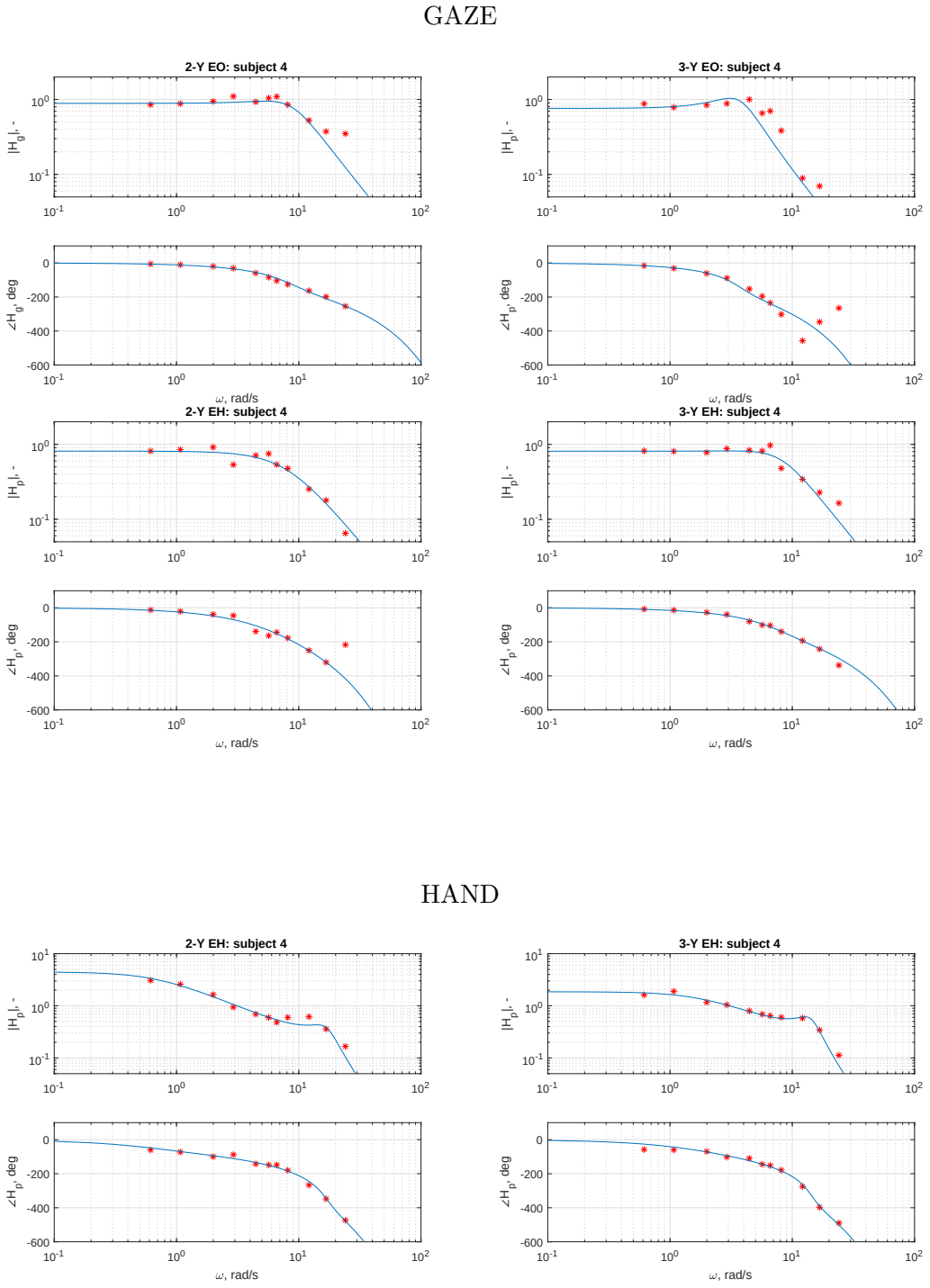

Figure C-4: FRF with fitted models for the gaze dynamics and the hand dynamics of subject 4.

C-1-5 Models Participant 5

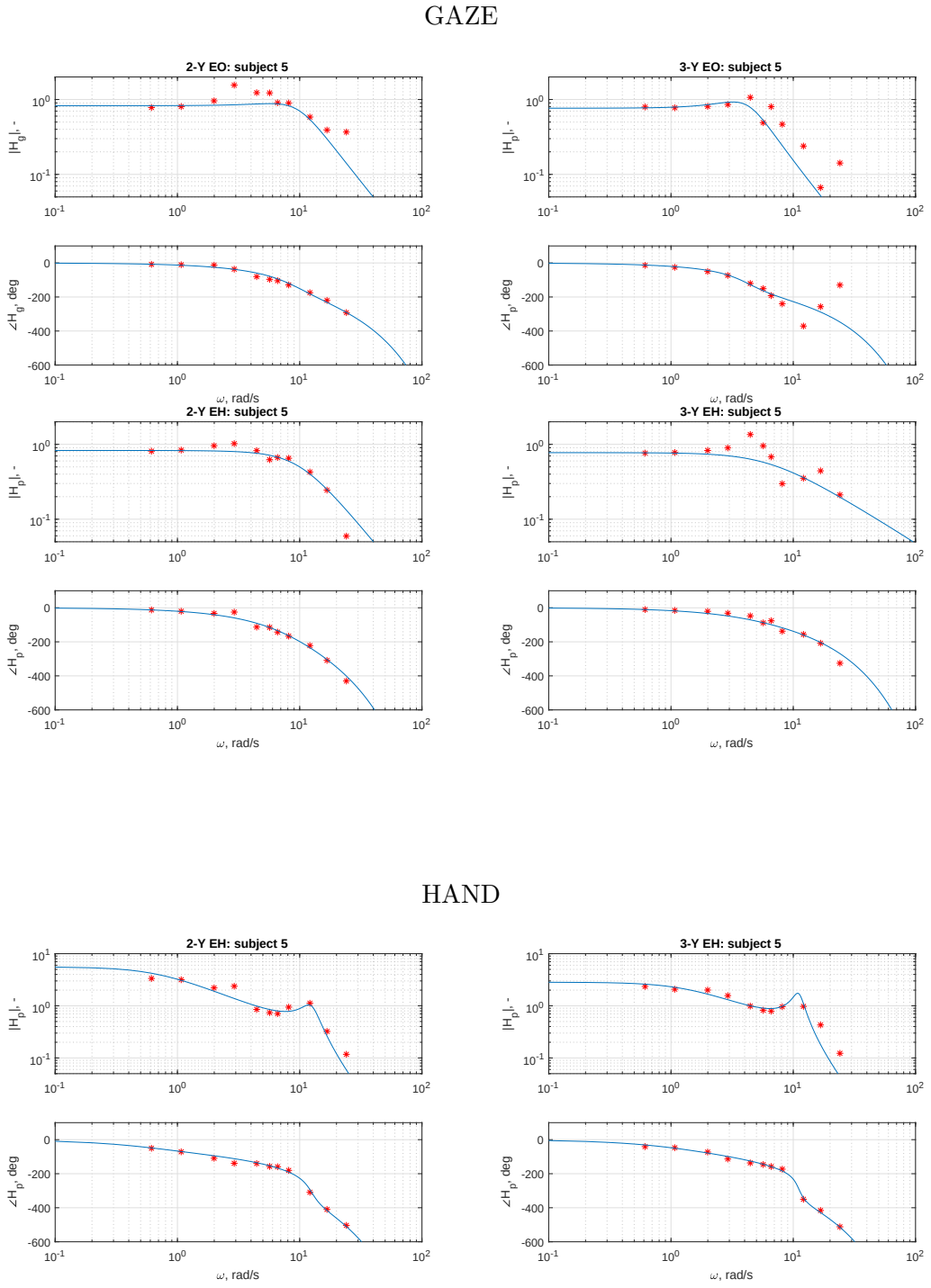

Figure C-5: FRF with fitted models for the gaze dynamics and the hand dynamics of subject 5.

C-1-6 Models Participant 6

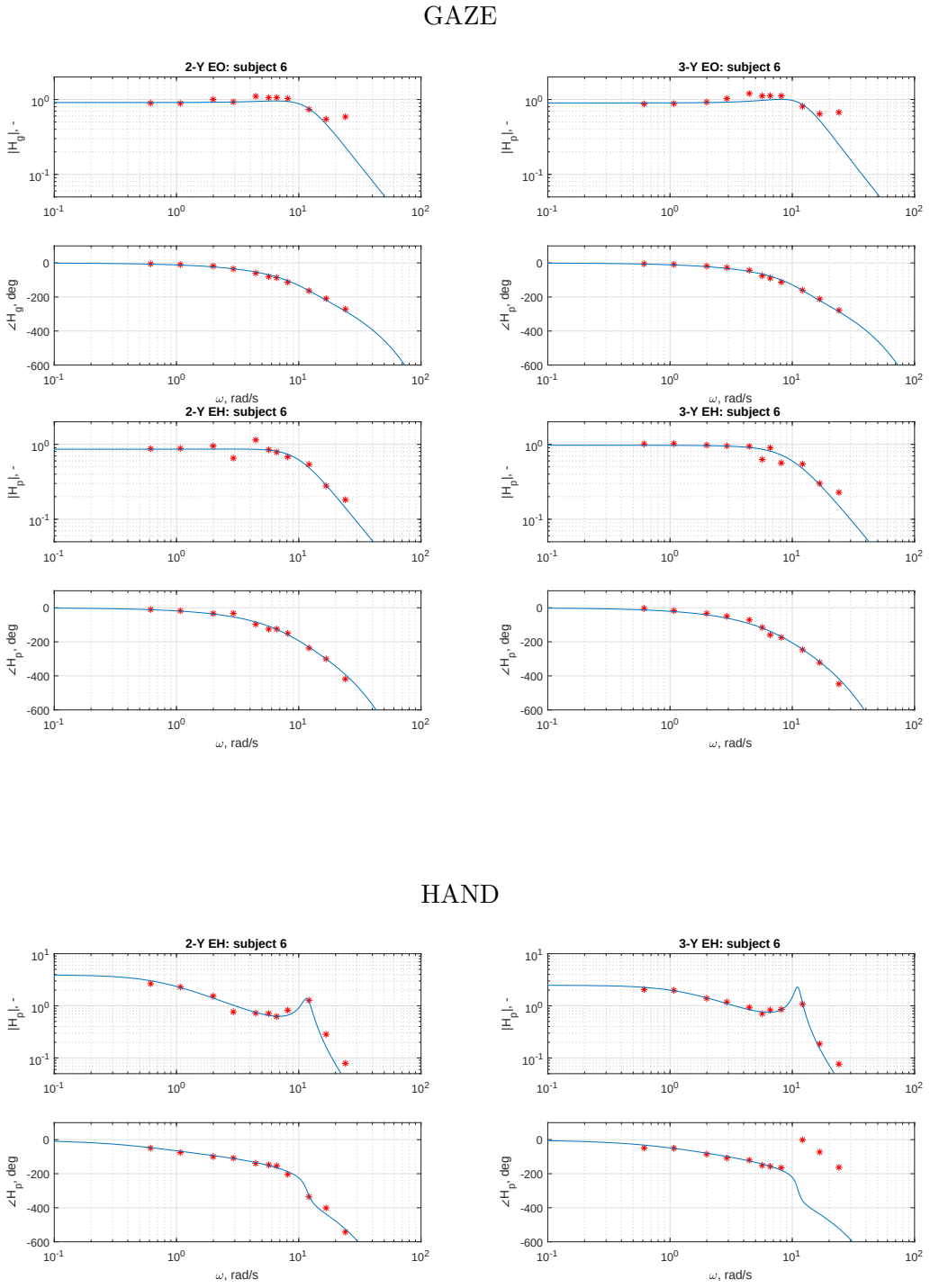

Figure C-6: FRF with fitted models for the gaze dynamics and the hand dynamics of subject 6.

C-1-7 Models Participant 7

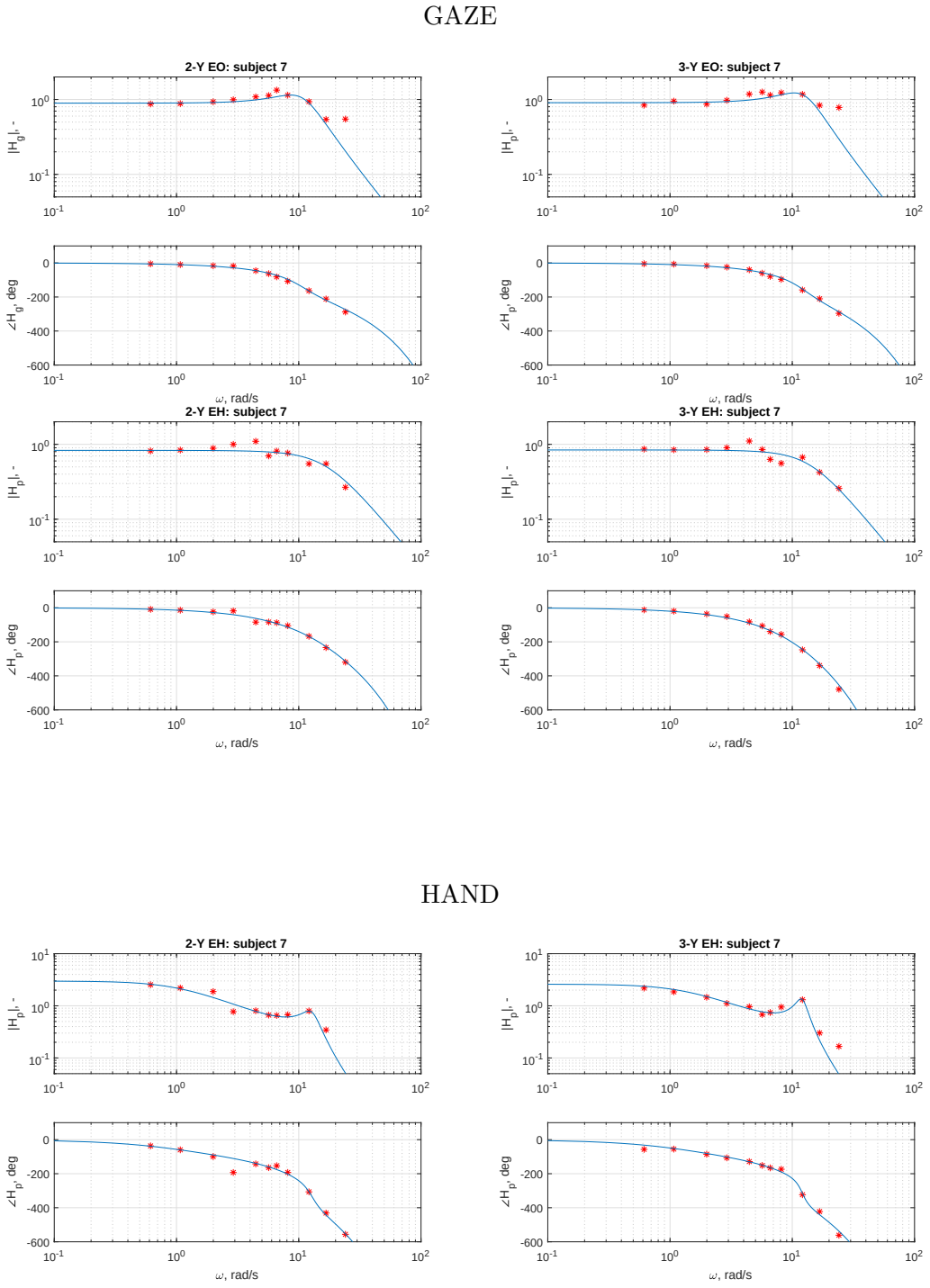

Figure C-7: FRF with fitted models for the gaze dynamics and the hand dynamics of subject 7.

C-1-8 Models Participant 8

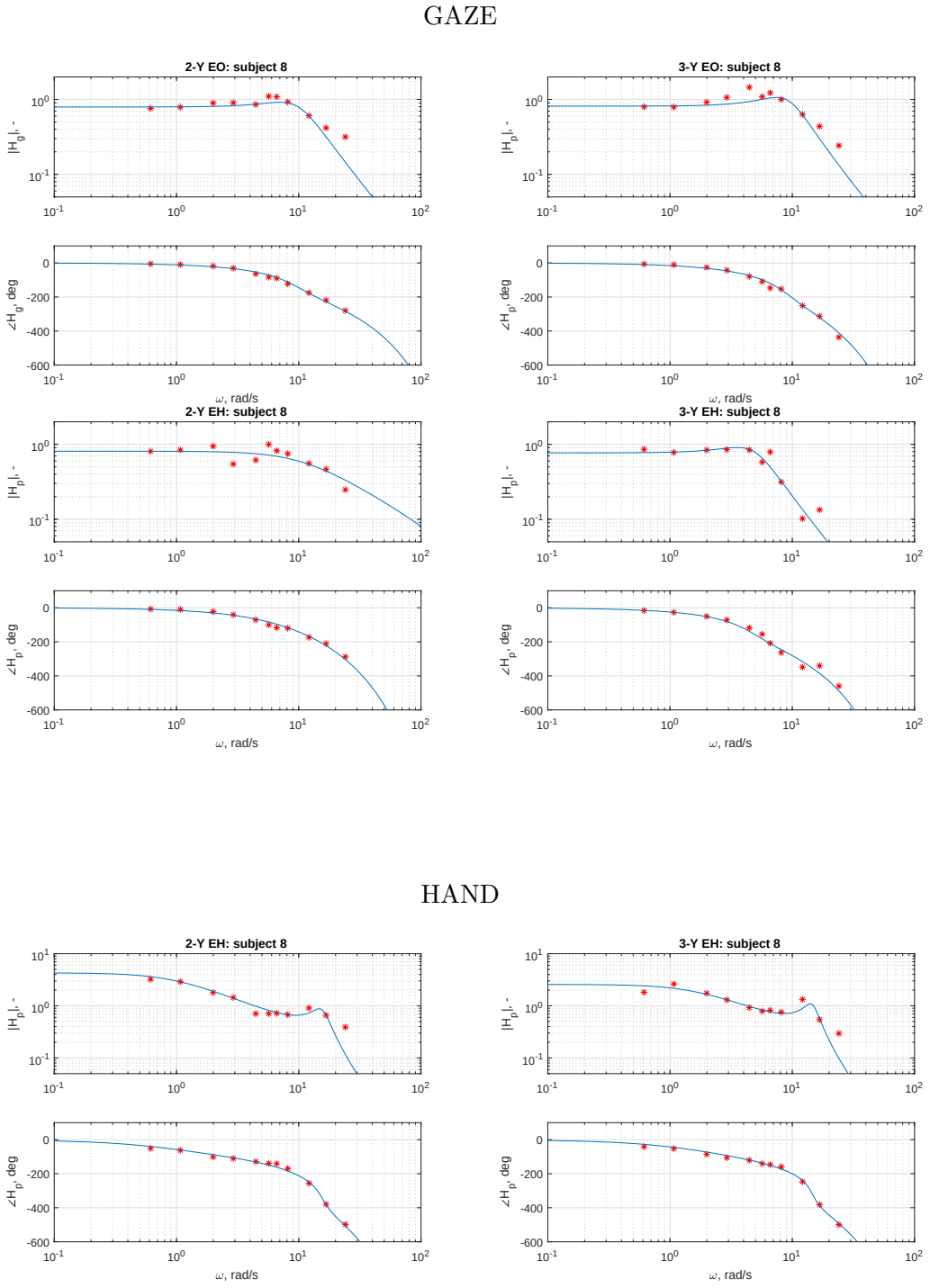

Figure C-8: FRF with fitted models for the gaze dynamics and the hand dynamics of subject 8.

C-1-9 Models Participant 9

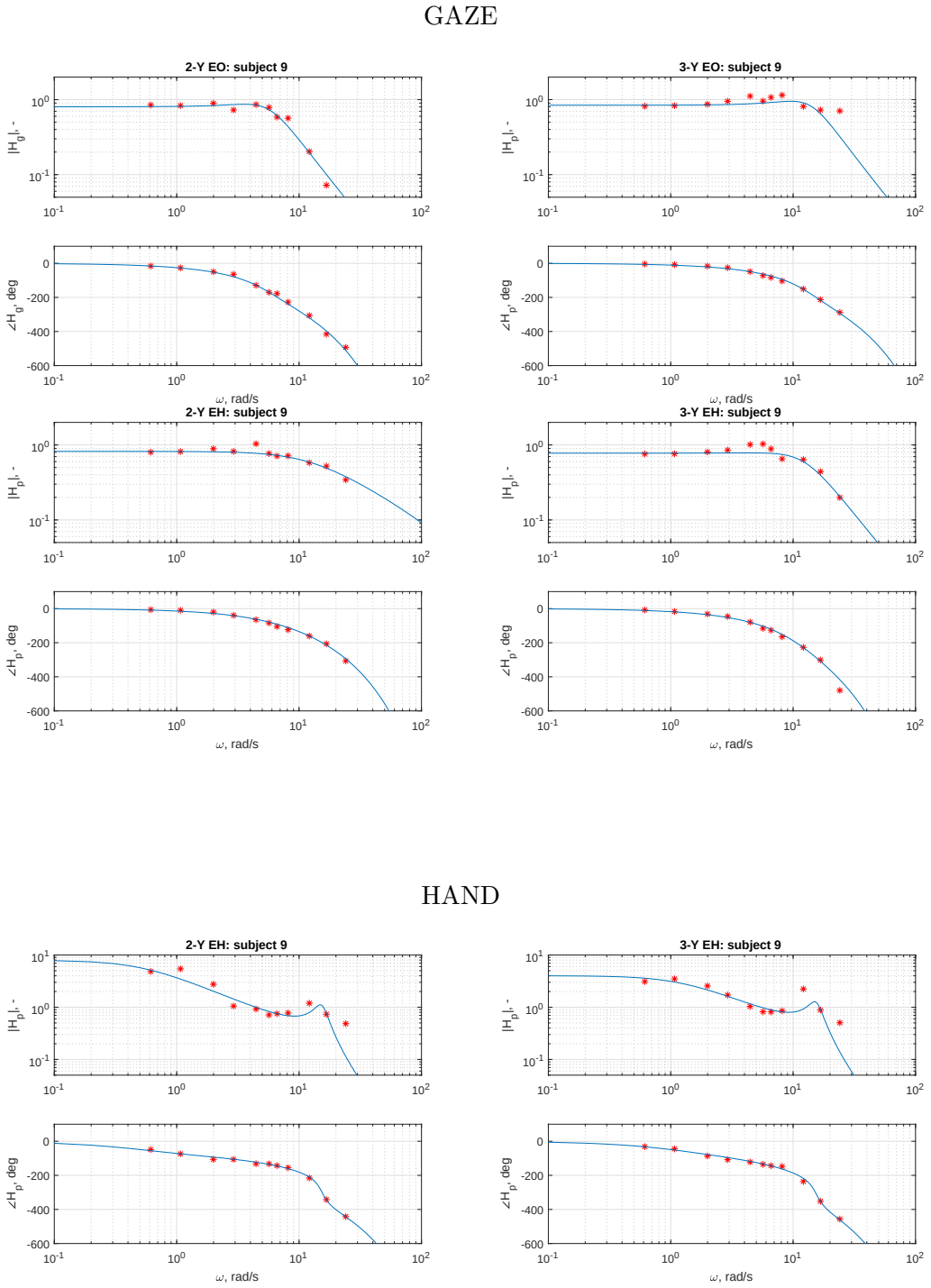

Figure C-9: FRF with fitted models for the gaze dynamics and the hand dynamics of subject 9.

C-1-10 Models Participant 10

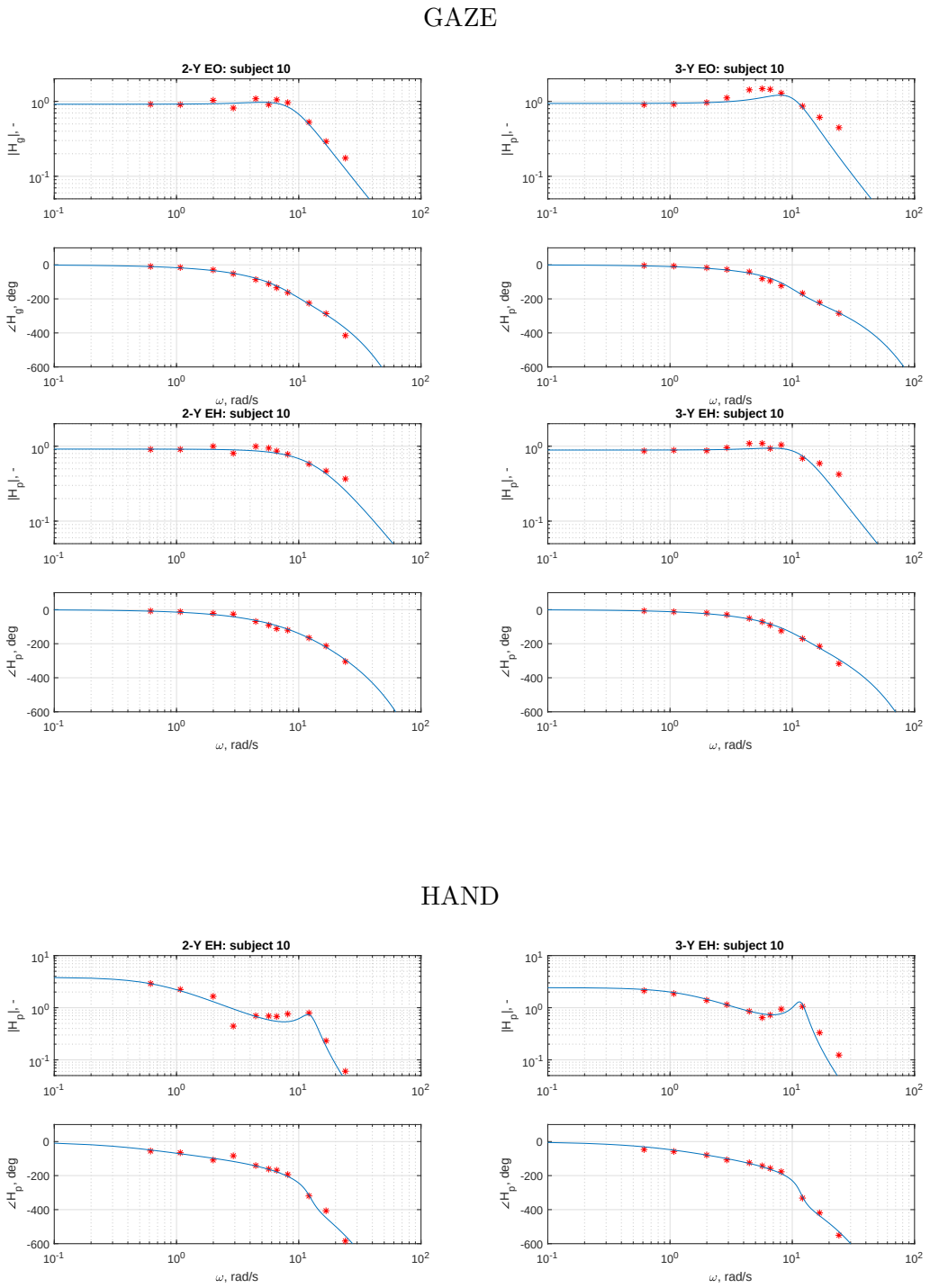

Figure C-10: FRF with fitted models for the gaze dynamics and the hand dynamics of subject 10.

C-1-11 Models Participant 11

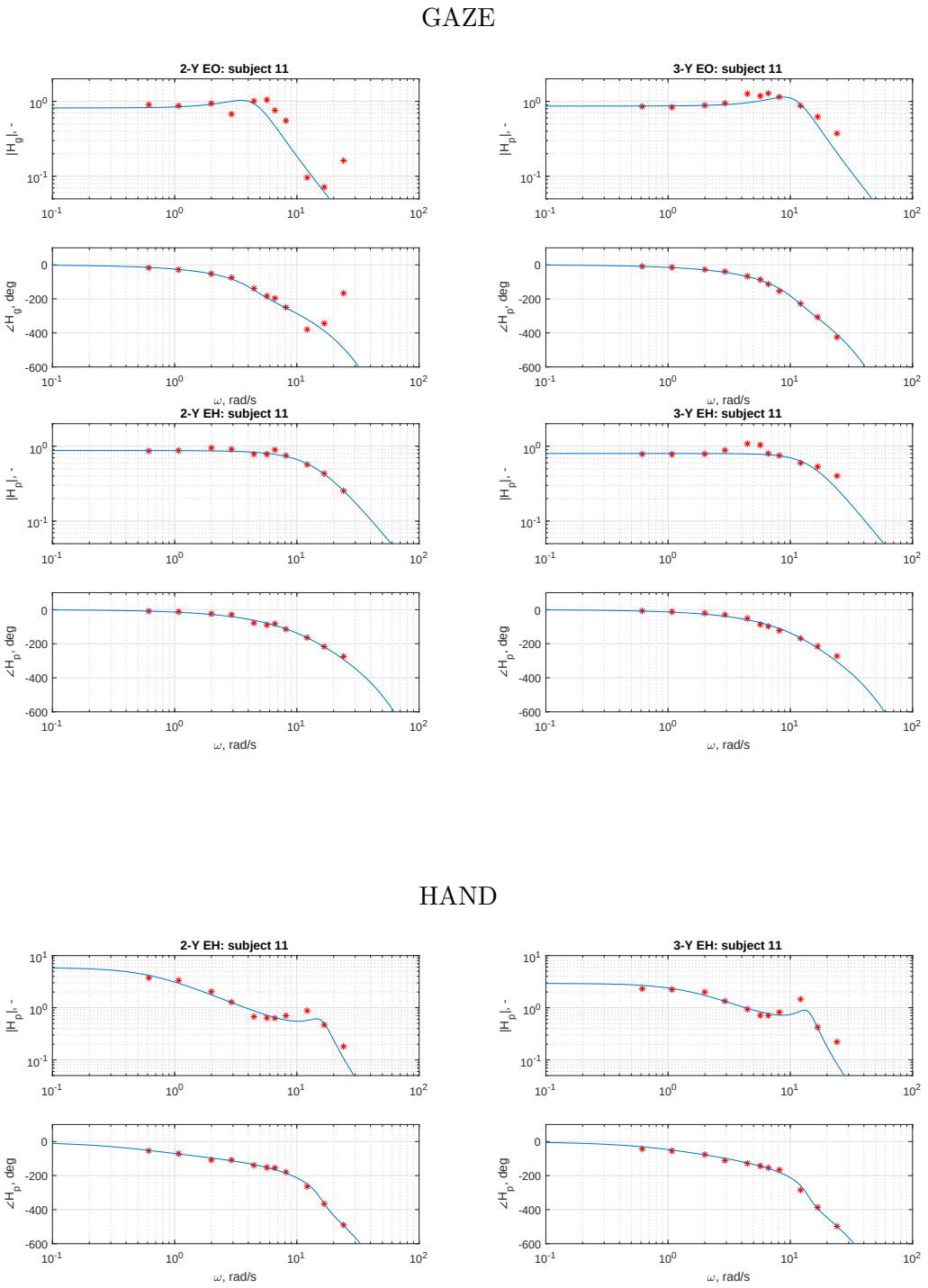

Figure C-11: FRF with fitted models for the gaze dynamics and the hand dynamics of subject 11.

C-1-12 Models Participant 12

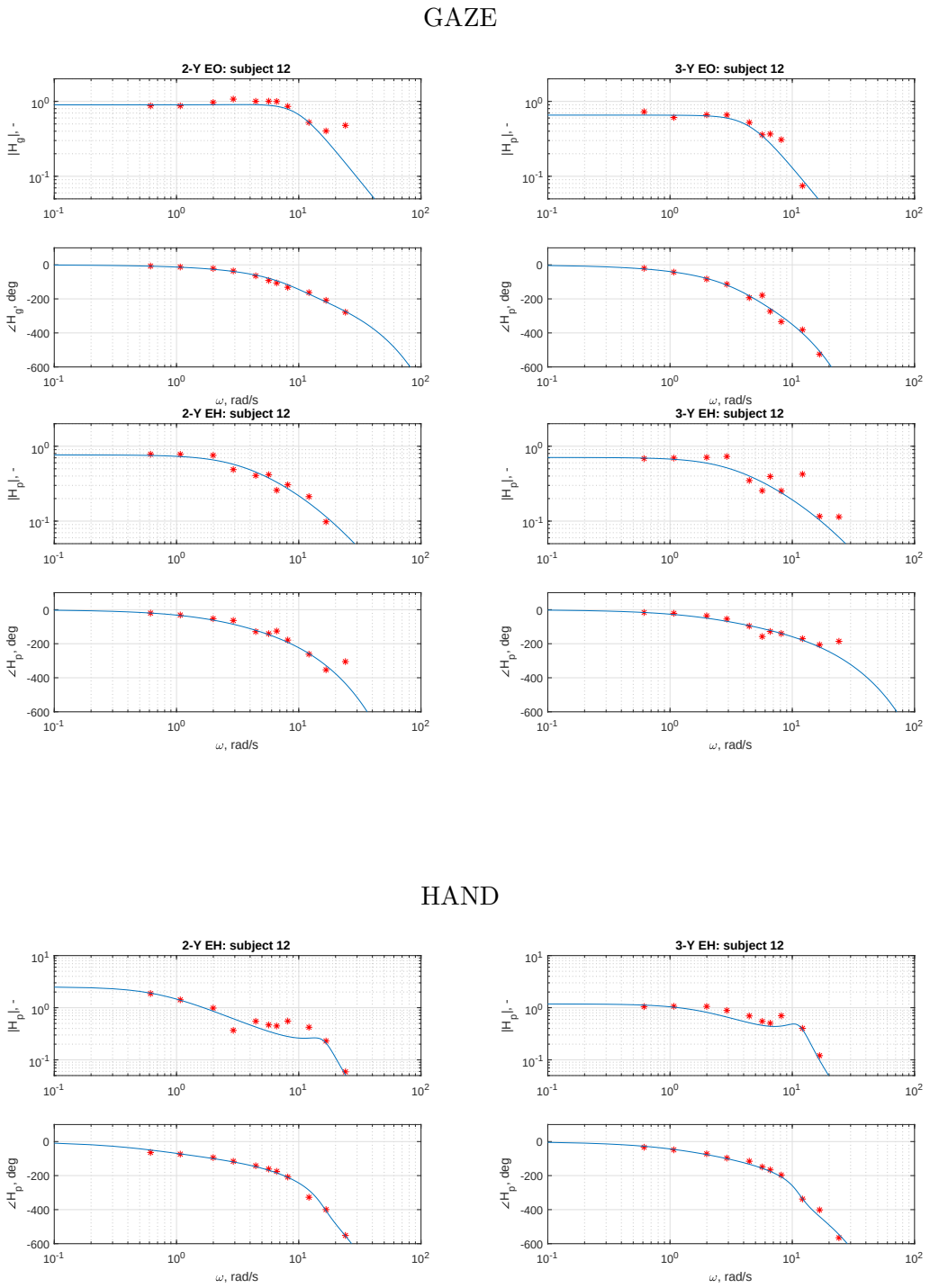

Figure C-12: FRF with fitted models for the gaze dynamics and the hand dynamics of subject 12.

C-1-13 Models Participant 13

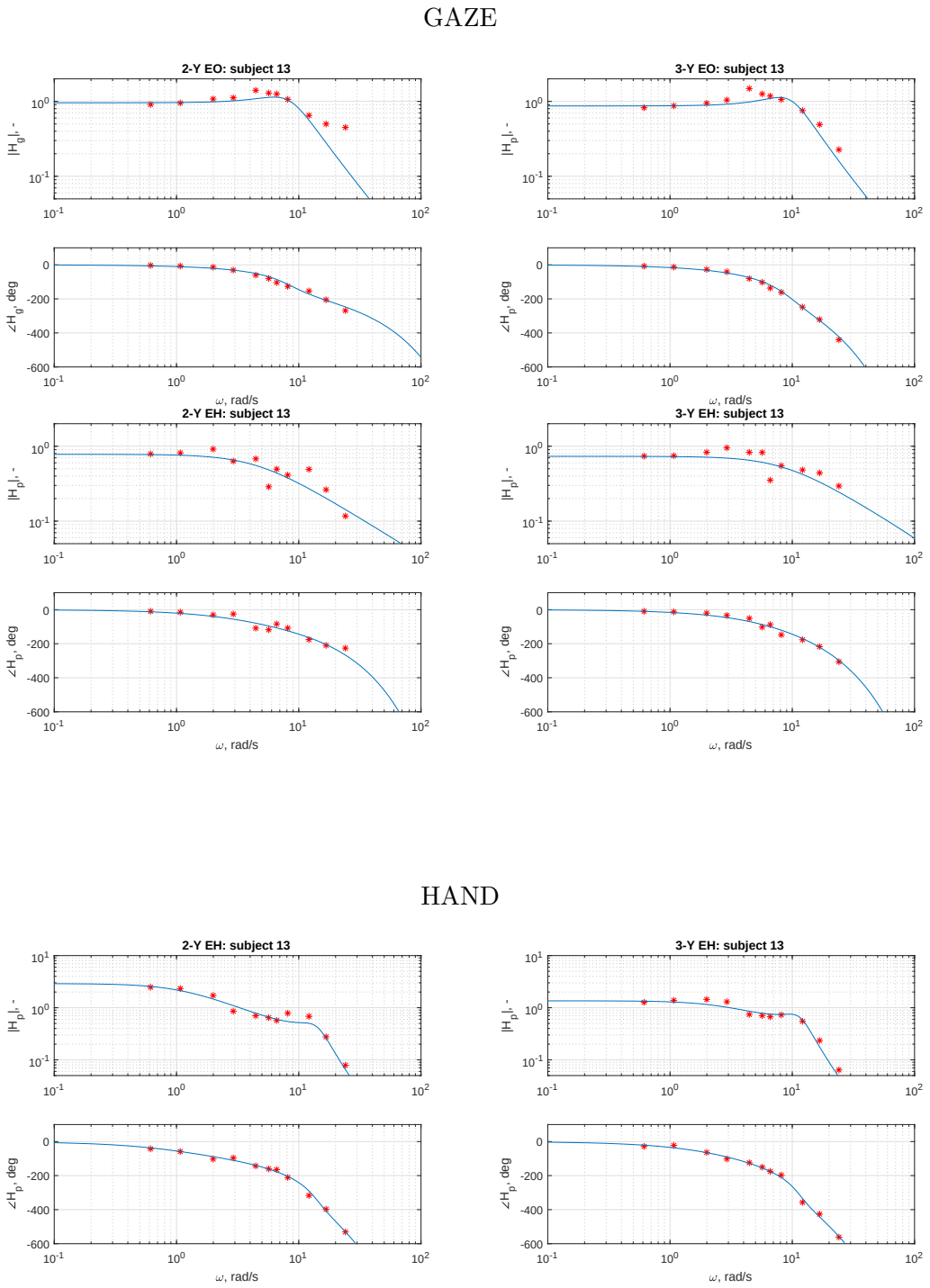

Figure C-13: FRF with fitted models for the gaze dynamics and the hand dynamics of subject 13.

C-1-14 Models Participant 14

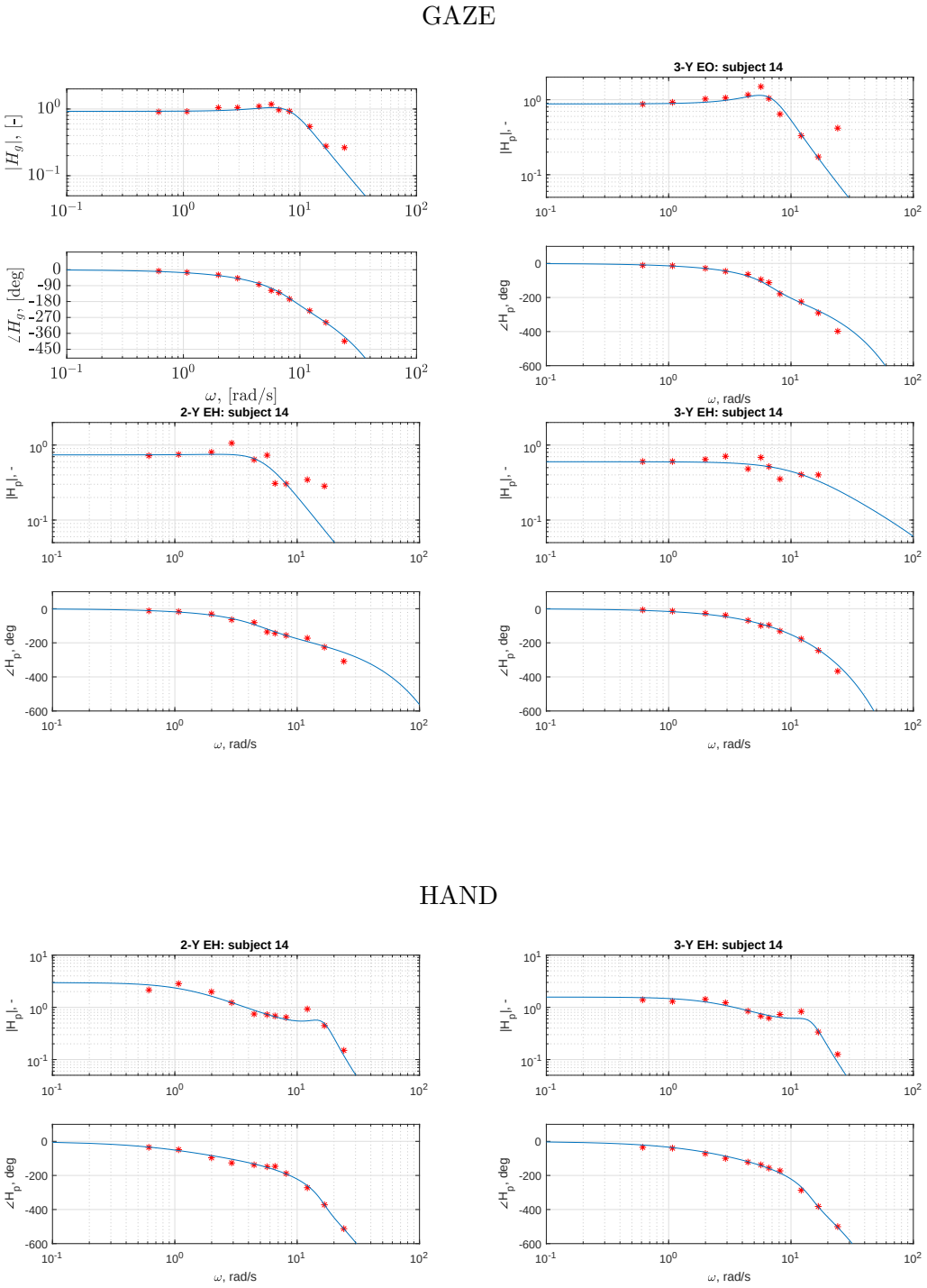

Figure C-14: FRF with fitted models for the gaze dynamics and the hand dynamics of subject 14.

C-1-15 Models Participant 15

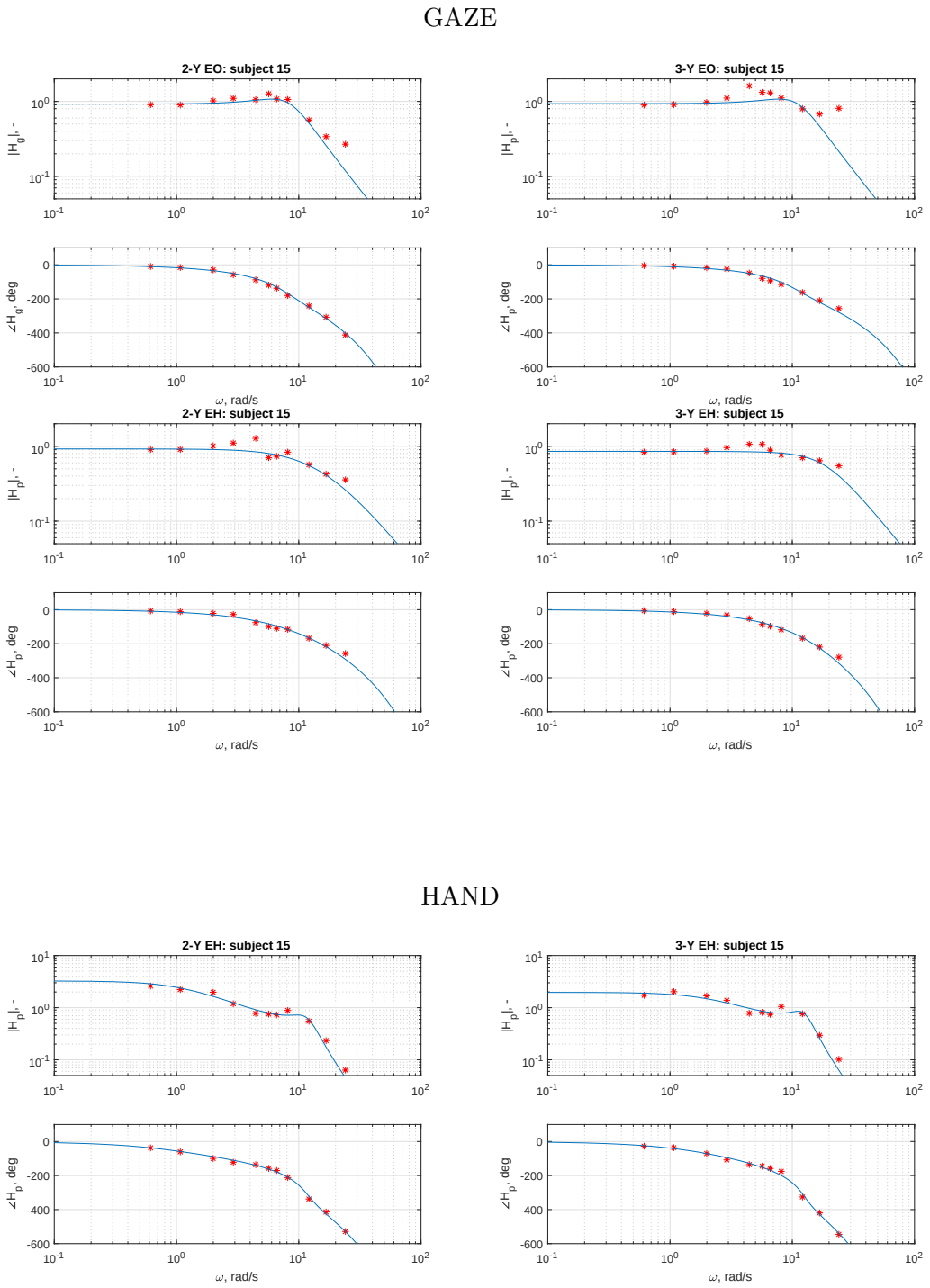

Figure C-15: FRF with fitted models for the gaze dynamics and the hand dynamics of subject 15.

C-1-16 Models Participant 16

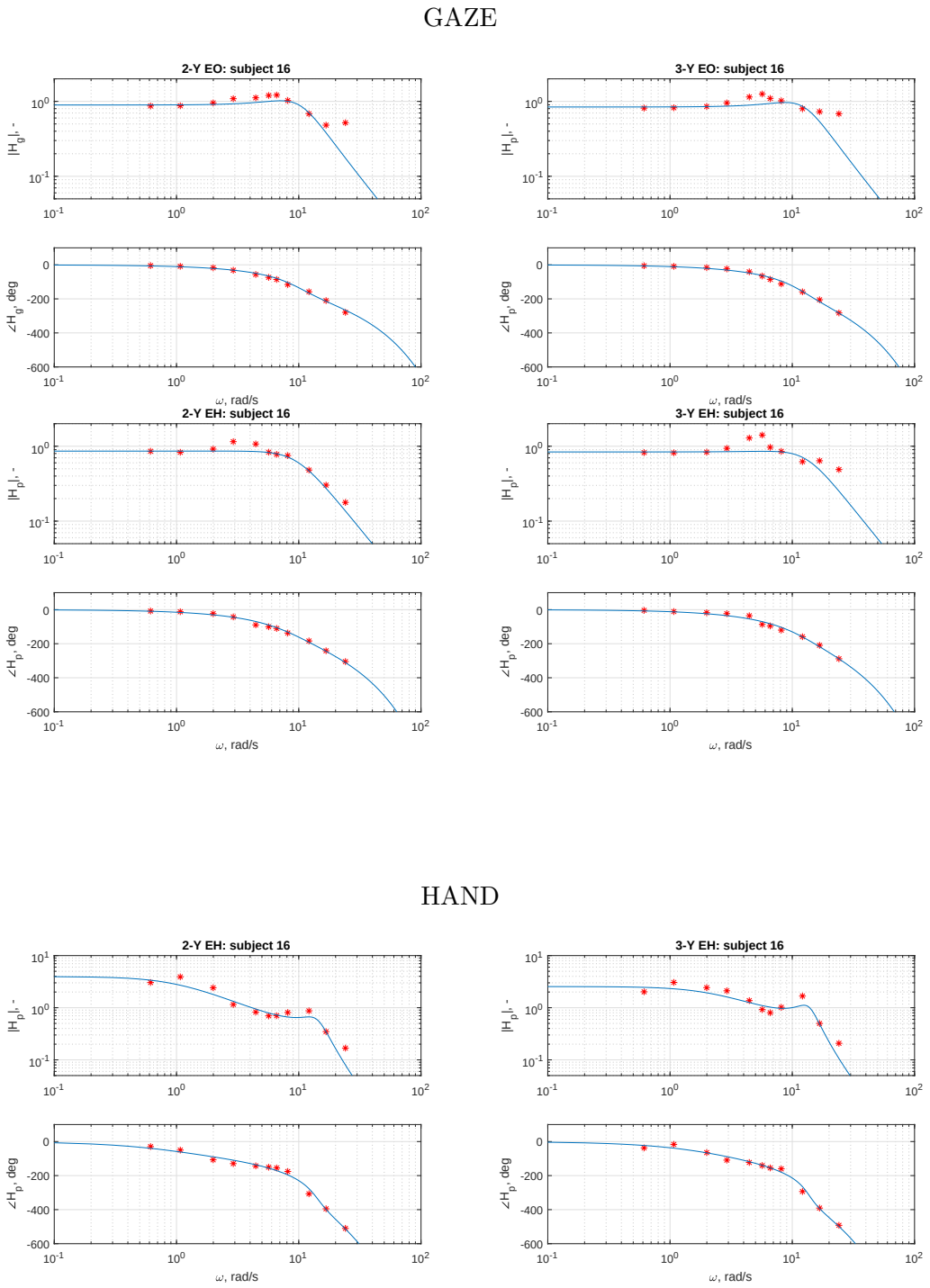

Figure C-16: FRF with fitted models for the gaze dynamics and the hand dynamics of subject 16.

C-1-17 Models Participant 17

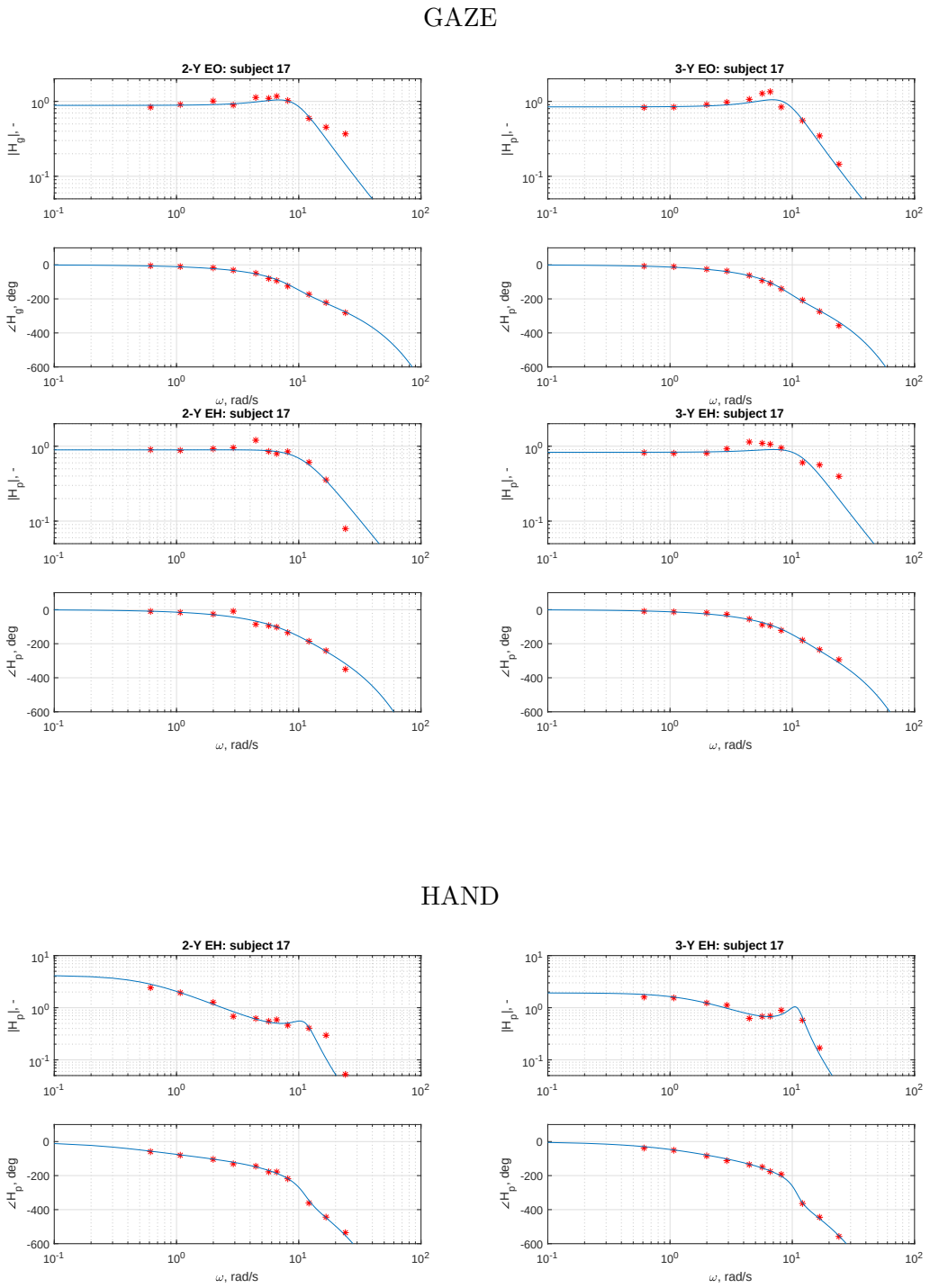

Figure C-17: FRF with fitted models for the gaze dynamics and the hand dynamics of subject 17.

C-1-18 Models Participant 18

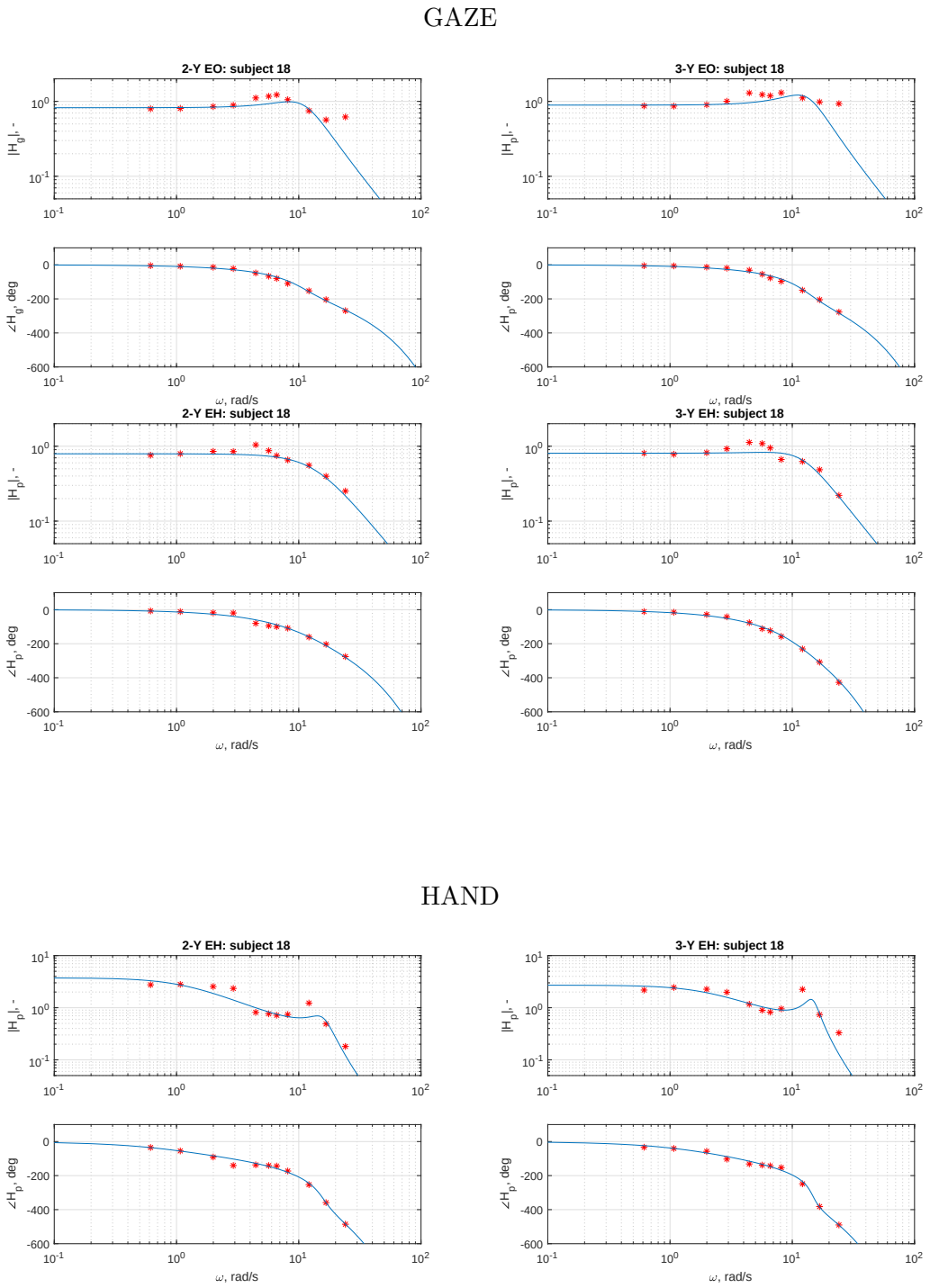

Figure C-18: FRF with fitted models for the gaze dynamics and the hand dynamics of subject 18.

C-1-19 Models Participant 19

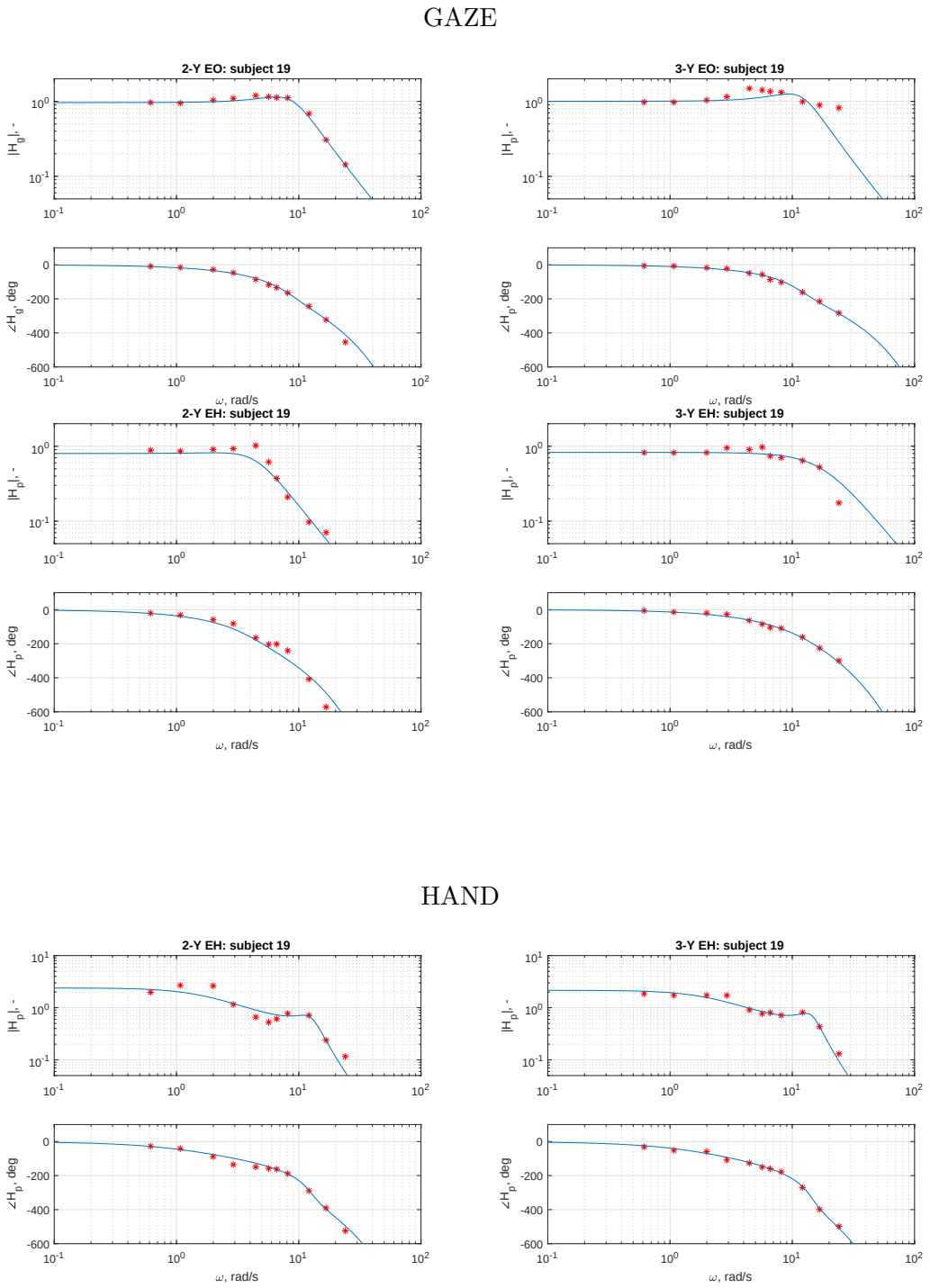

Figure C-19: FRF with fitted models for the gaze dynamics and the hand dynamics of subject 19.

C-1-20 Models Participant 20

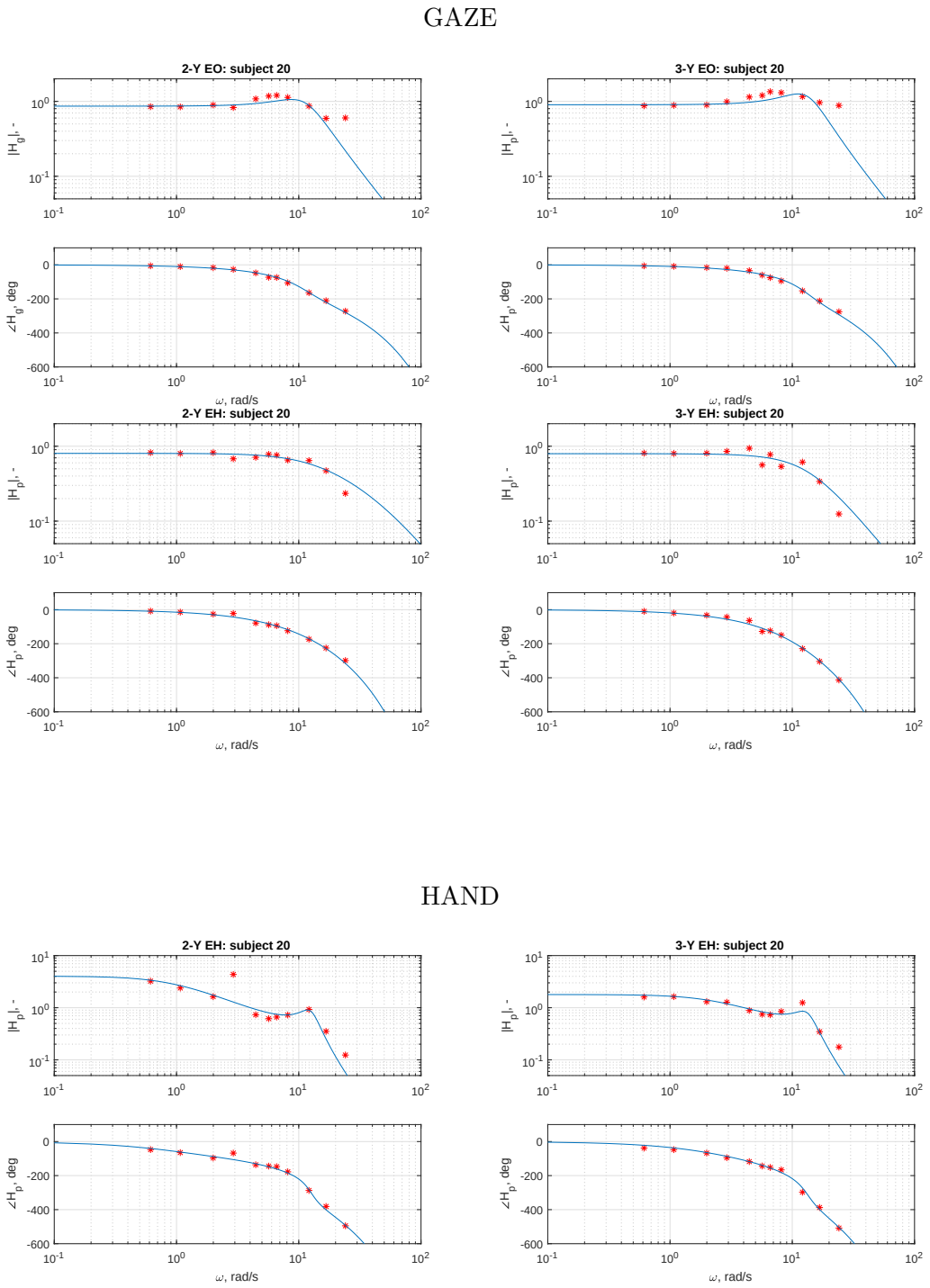

Figure C-20: FRF with fitted models for the gaze dynamics and the hand dynamics of subject 20.

C-2 Older participants

C-2-1 Models Participant 1

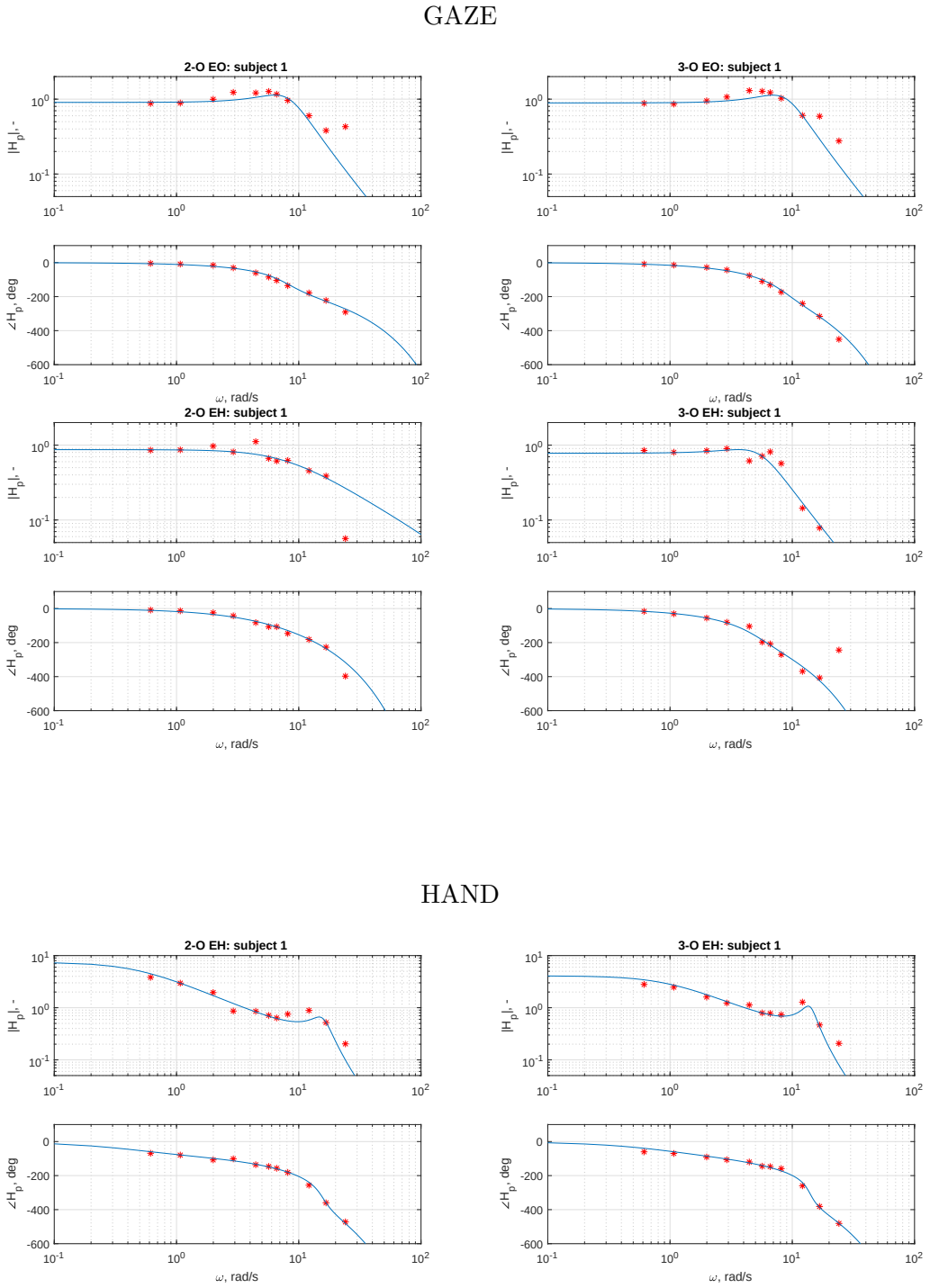

Figure C-21: FRF with fitted models for the gaze dynamics and the hand dynamics of subject 1.

C-2-2 Models Participant 2

GAZE

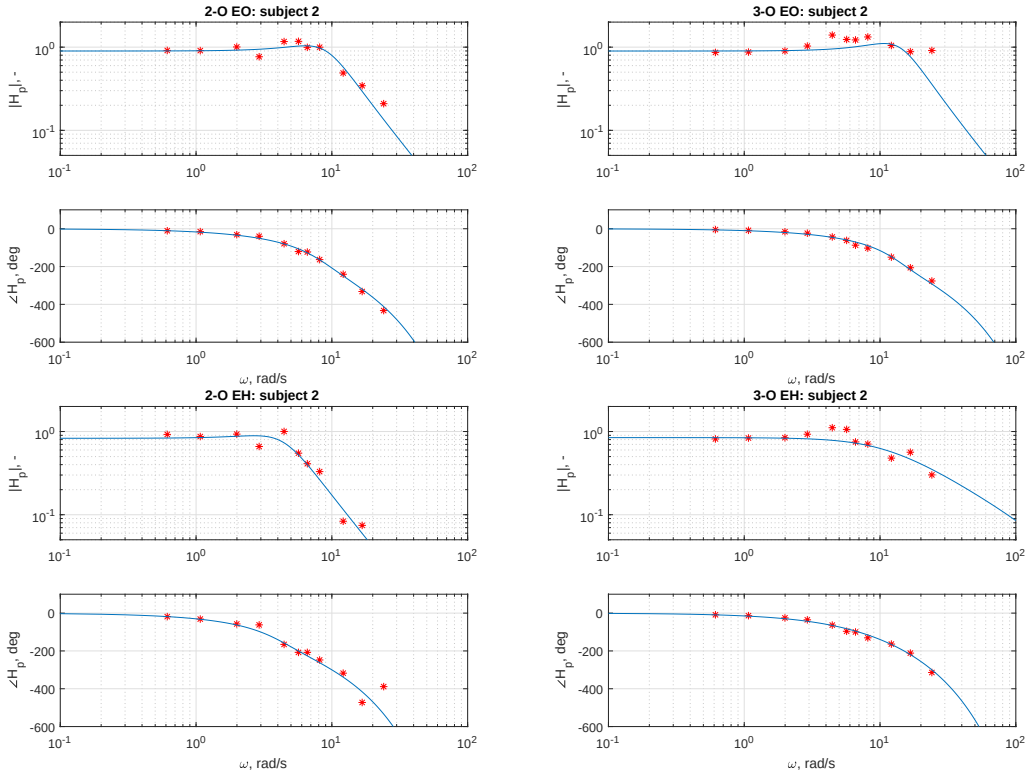

HAND

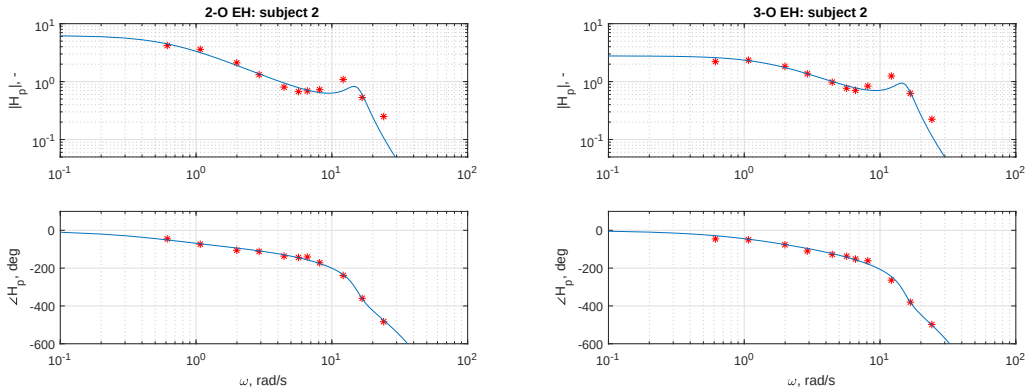

Figure C-22: FRF with fitted models for the gaze dynamics and the hand dynamics of subject 2.

C-2-3 Models Participant 3

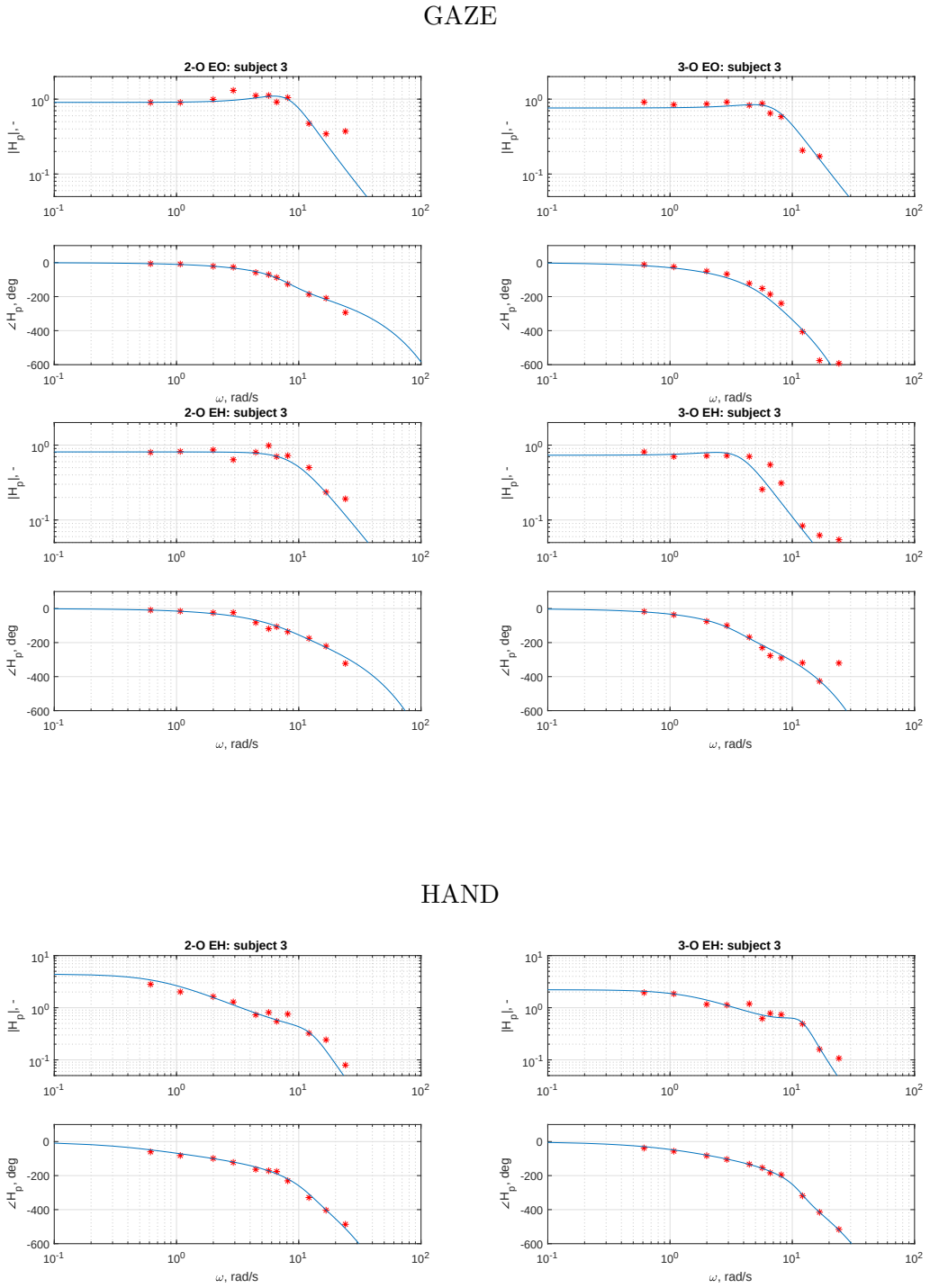

Figure C-23: FRF with fitted models for the gaze dynamics and the hand dynamics of subject 3.

C-2-4 Models Participant 4

GAZE

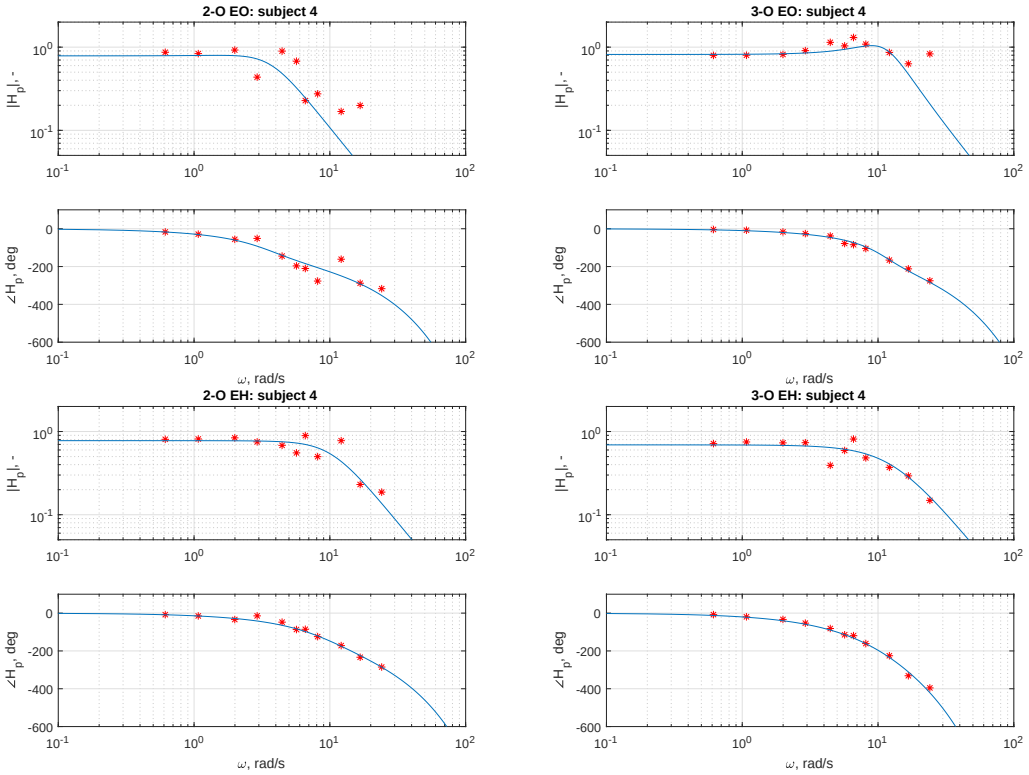

HAND

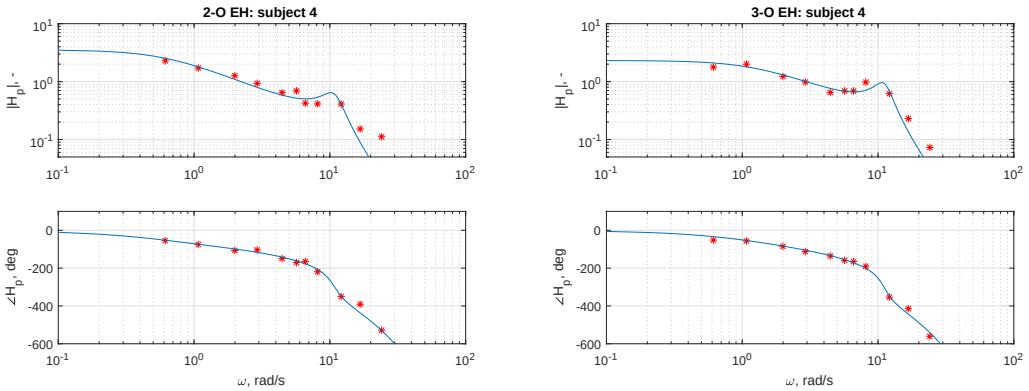

Figure C-24: FRF with fitted models for the gaze dynamics and the hand dynamics of subject 4.

C-2-5 Models Participant 5

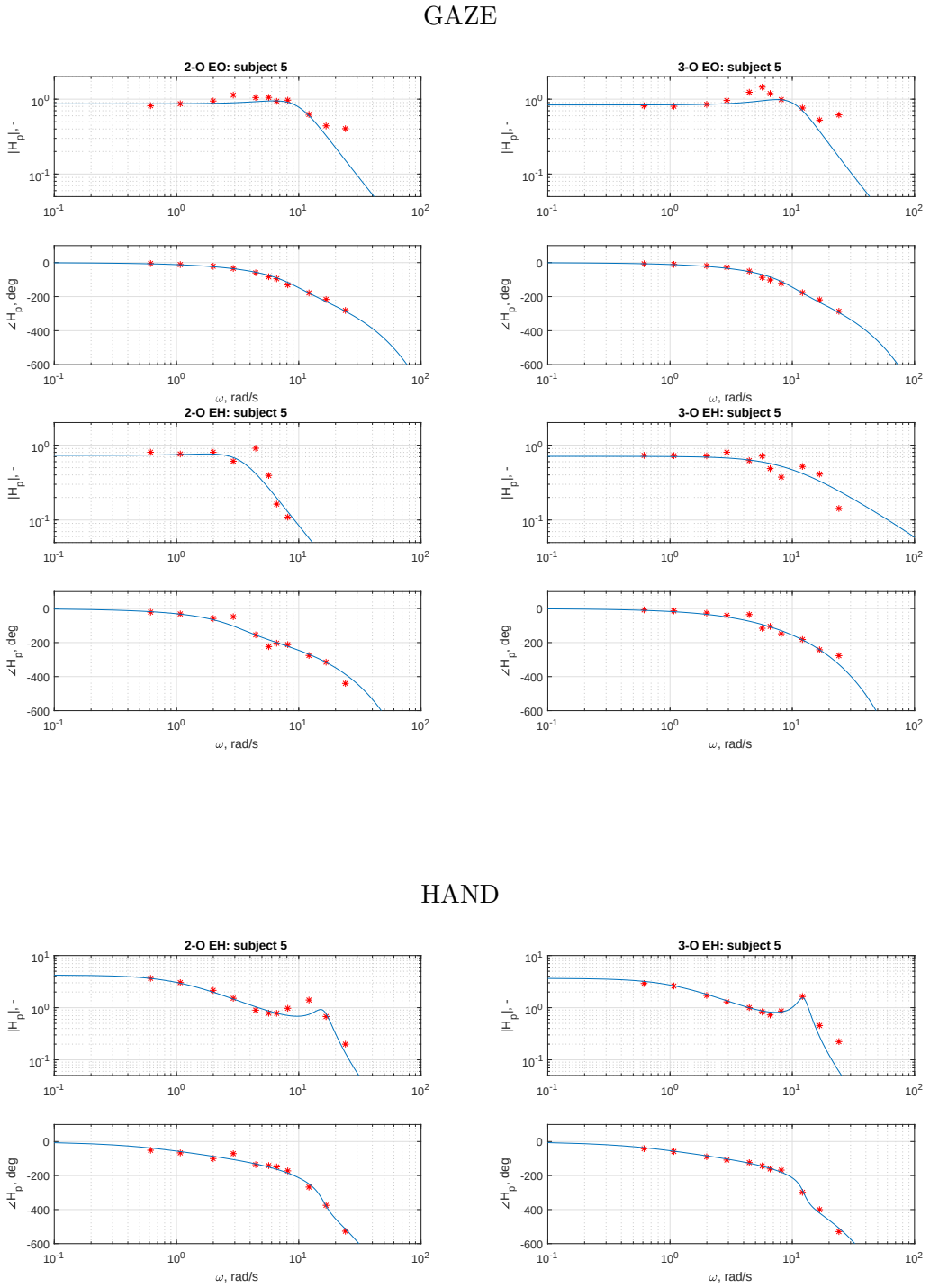

Figure C-25: FRF with fitted models for the gaze dynamics and the hand dynamics of subject 5.

C-2-6 Models Participant 6

GAZE

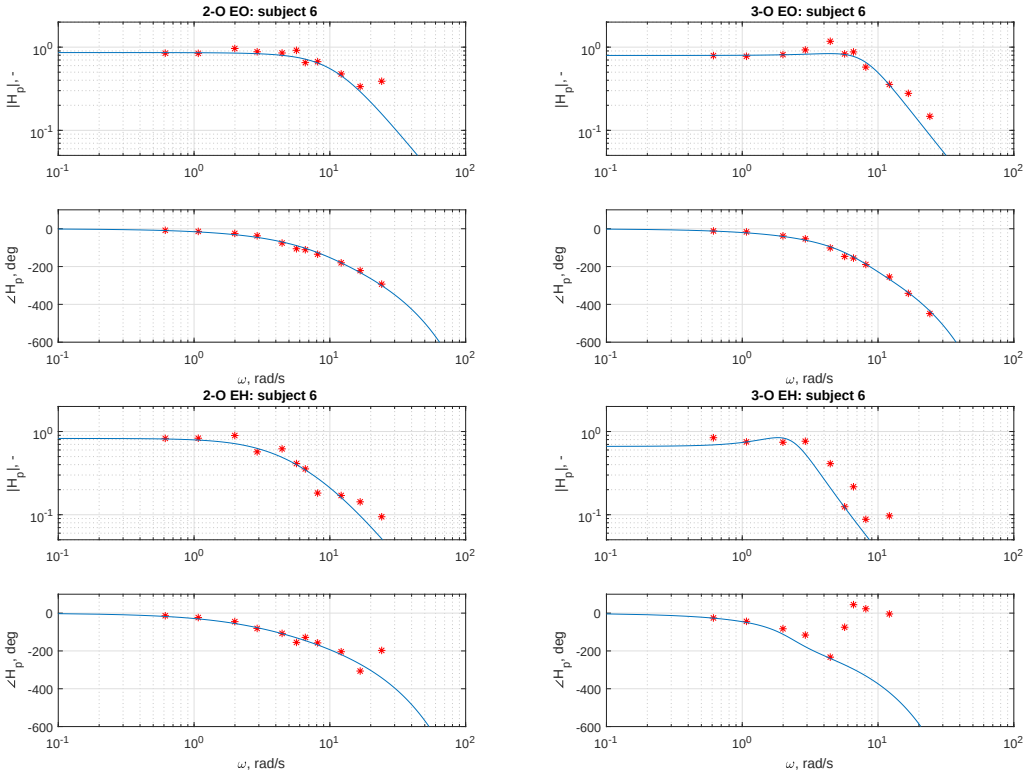

HAND

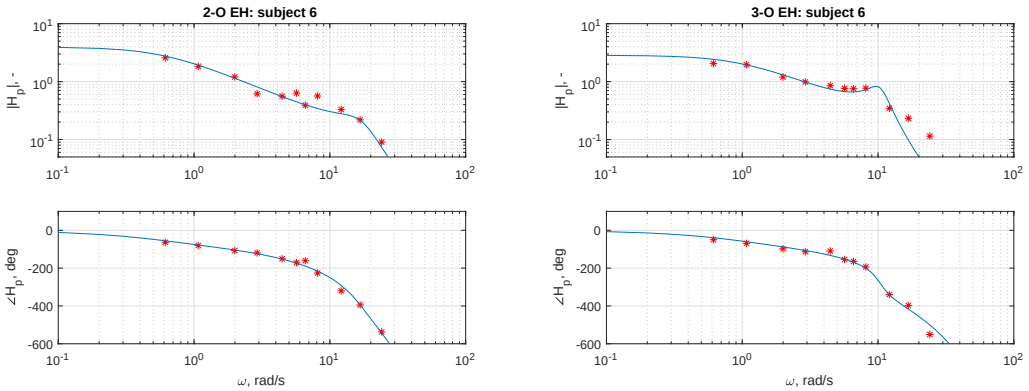

Figure C-26: FRF with fitted models for the gaze dynamics and the hand dynamics of subject 6.

C-2-7 Models Participant 7

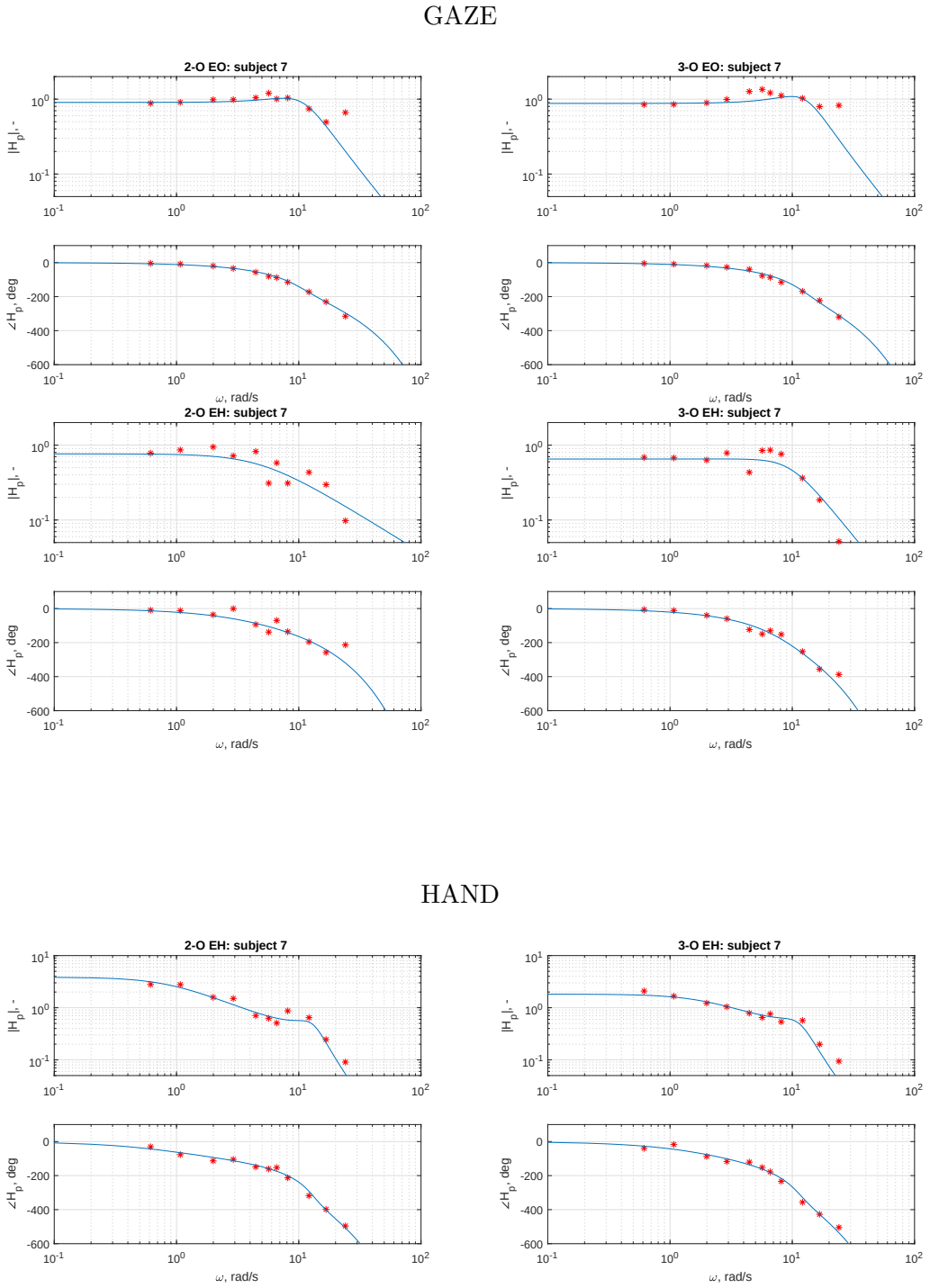

Figure C-27: FRF with fitted models for the gaze dynamics and the hand dynamics of subject 7.

C-2-8 Models Participant 8

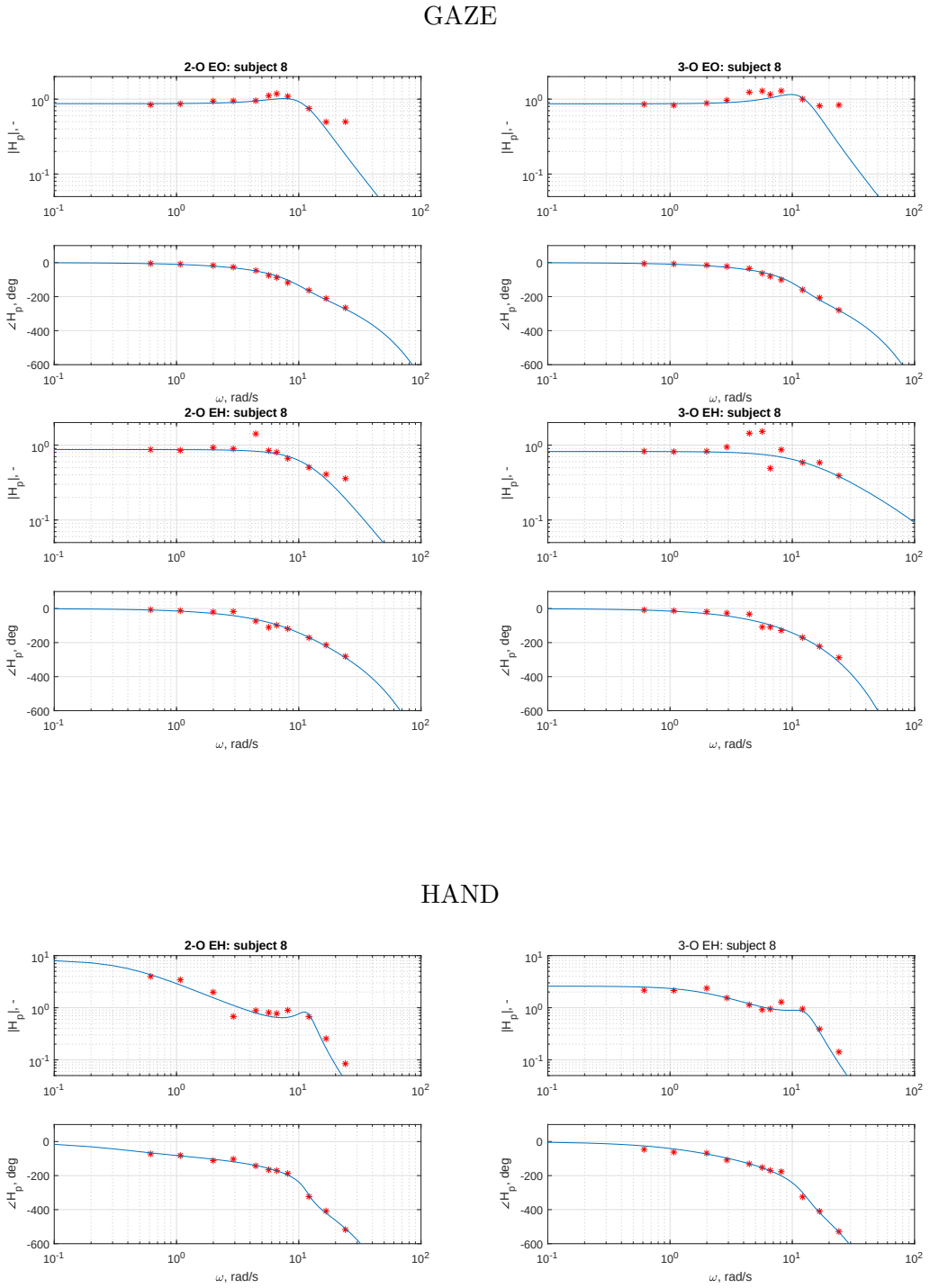

Figure C-28: FRF with fitted models for the gaze dynamics and the hand dynamics of subject 8.

C-2-9 Models Participant 9

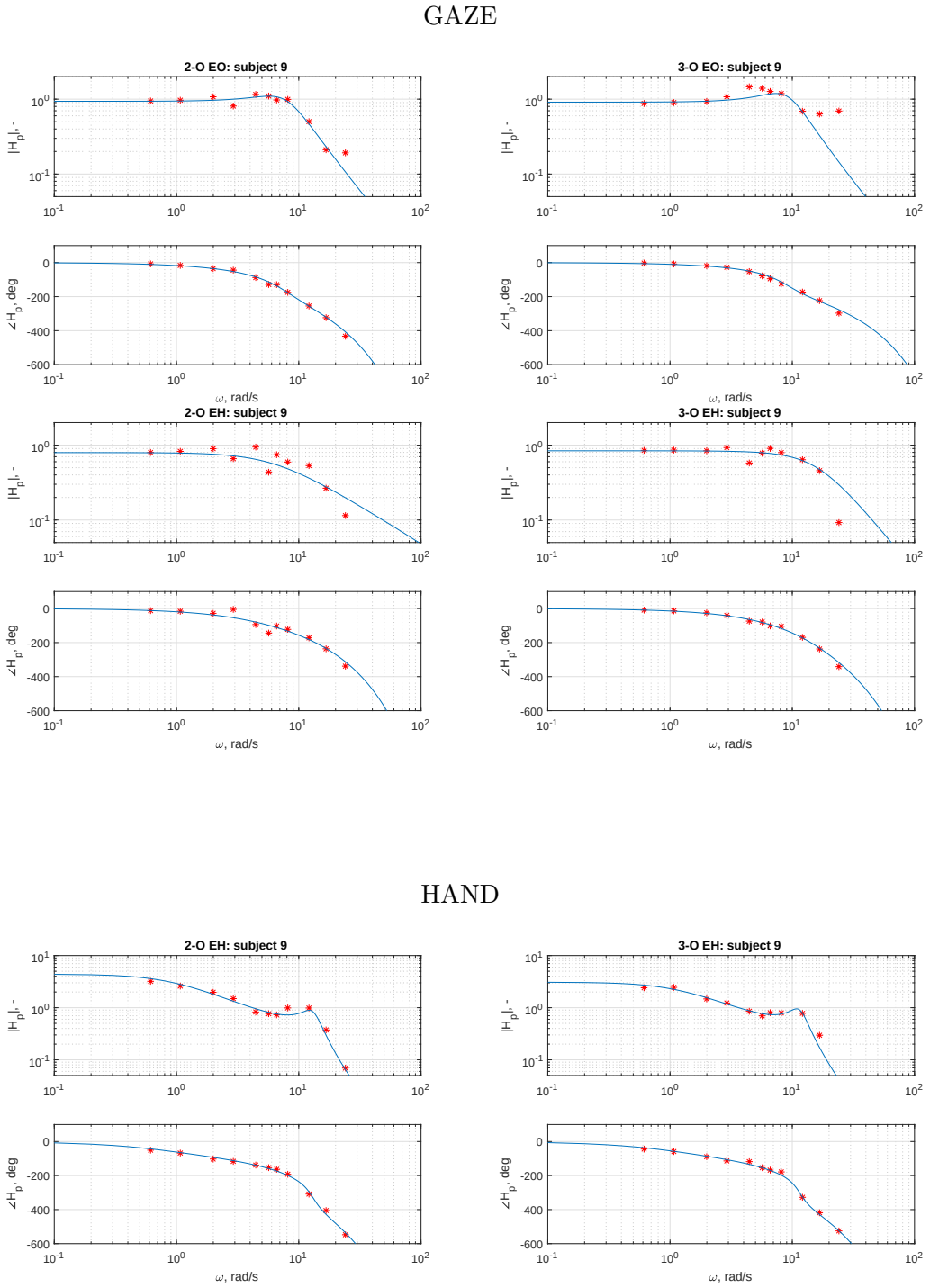

Figure C-29: FRF with fitted models for the gaze dynamics and the hand dynamics of subject 9.

C-2-10 Models Participant 10

GAZE

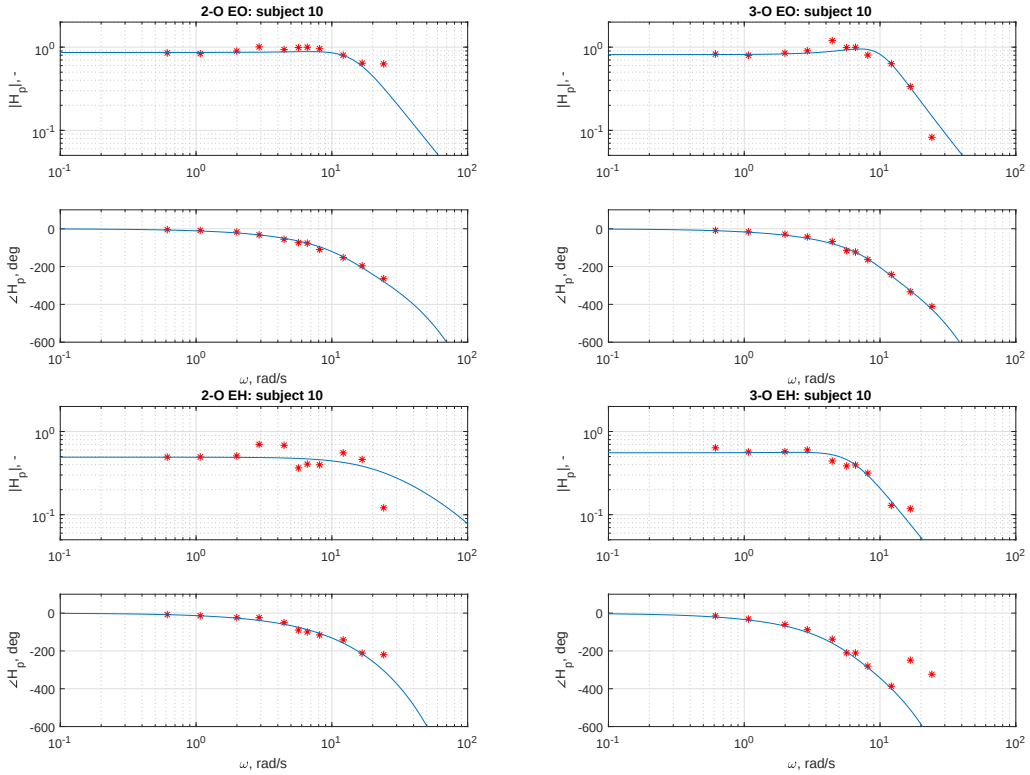

HAND

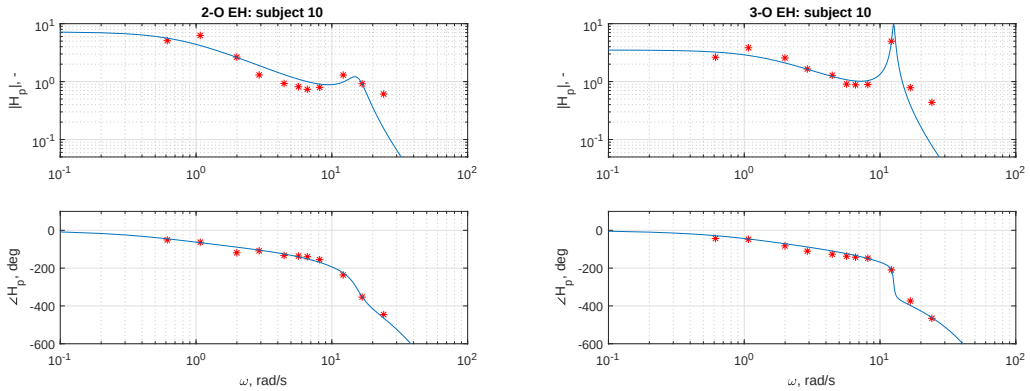

Figure C-30: FRF with fitted models for the gaze dynamics and the hand dynamics of subject 10.

C-2-11 Models Participant 11

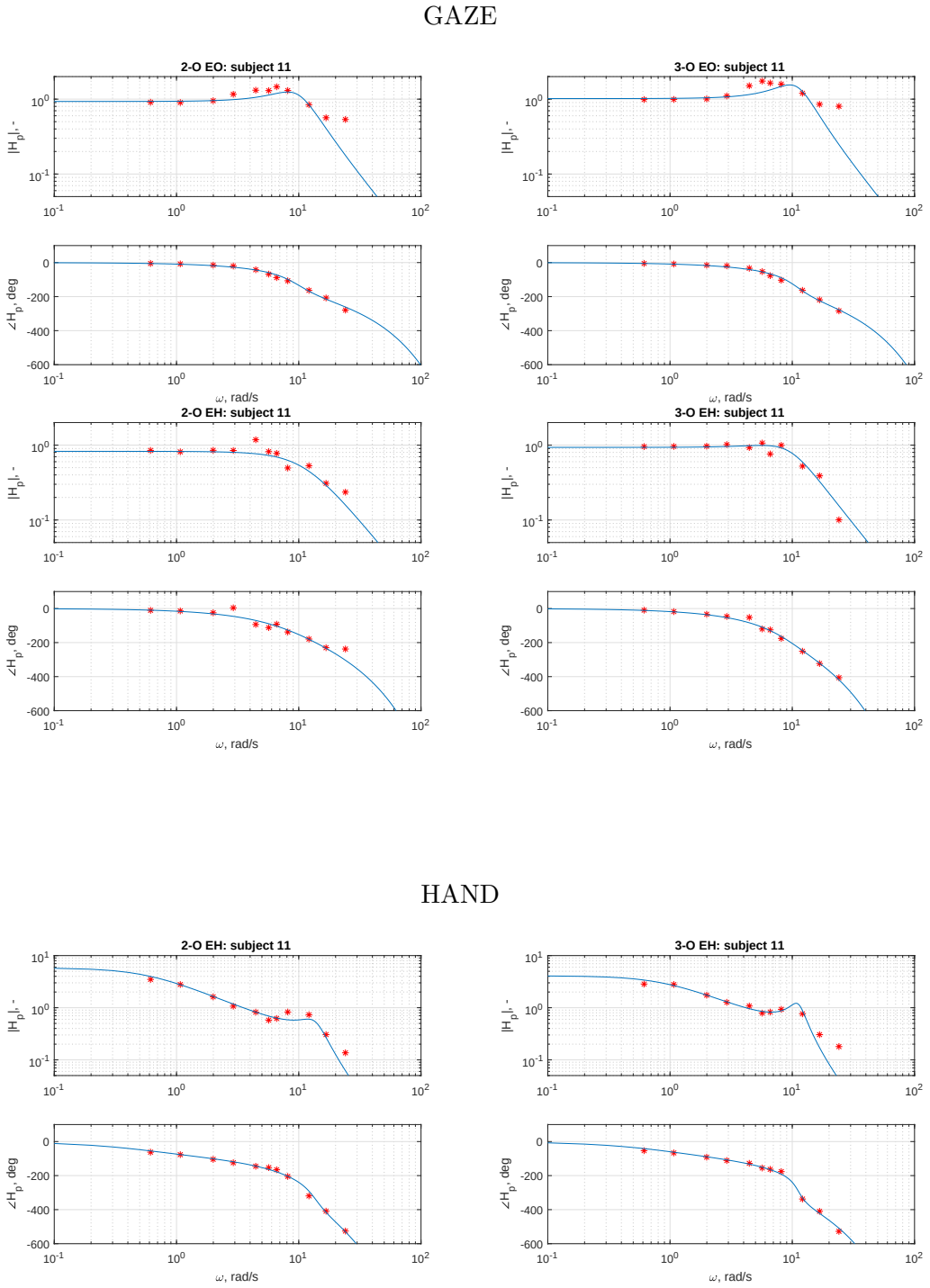

Figure C-31: FRF with fitted models for the gaze dynamics and the hand dynamics of subject 11.

C-2-12 Models Participant 12

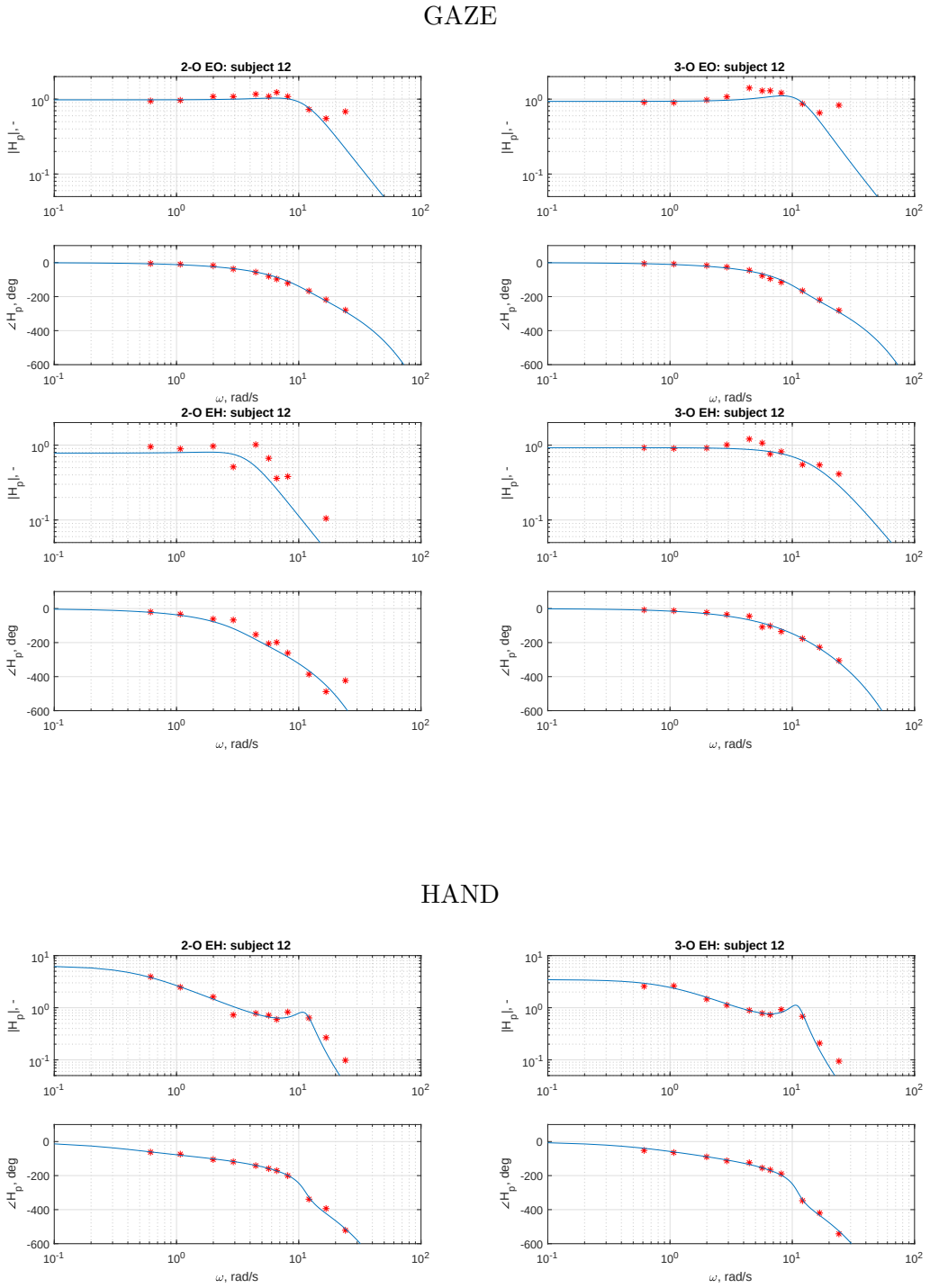

Figure C-32: FRF with fitted models for the gaze dynamics and the hand dynamics of subject 12.

C-2-13 Models Participant 13

GAZE

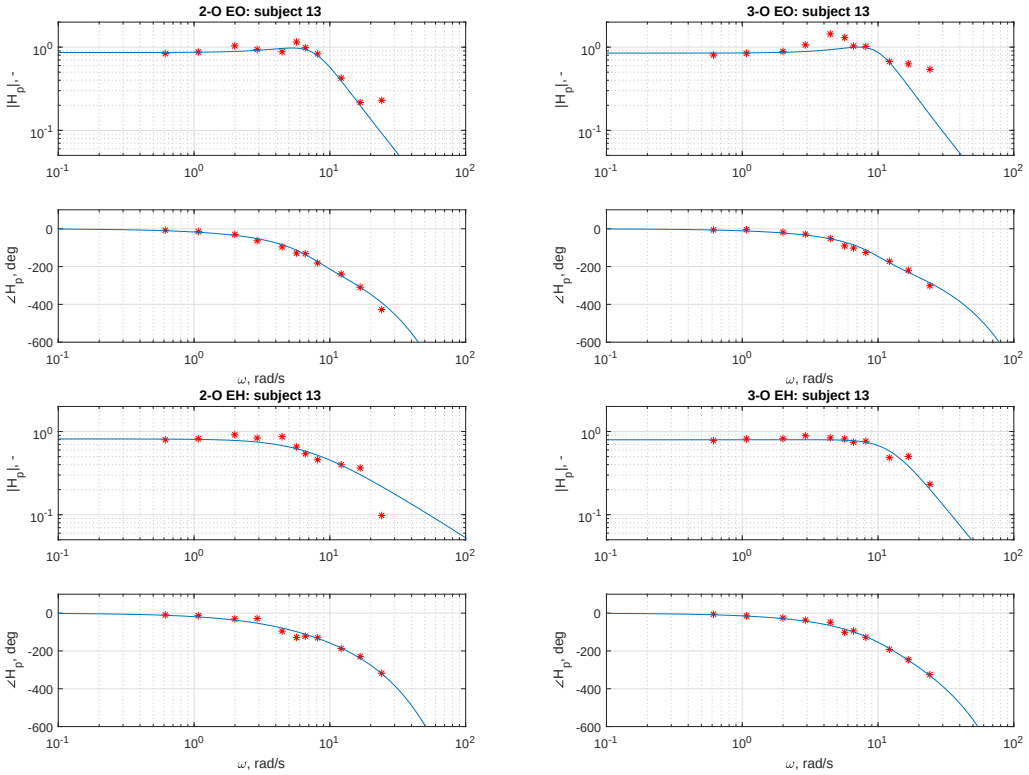

HAND

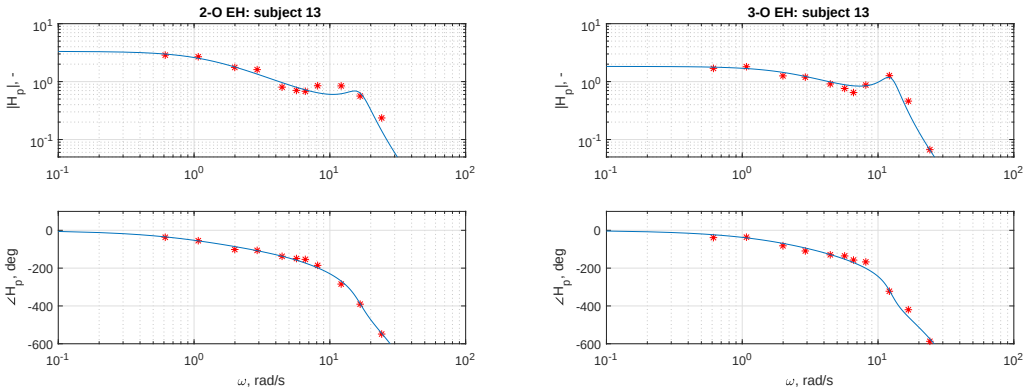

Figure C-33: FRF with fitted models for the gaze dynamics and the hand dynamics of subject 13.

C-2-14 Models Participant 14

GAZE

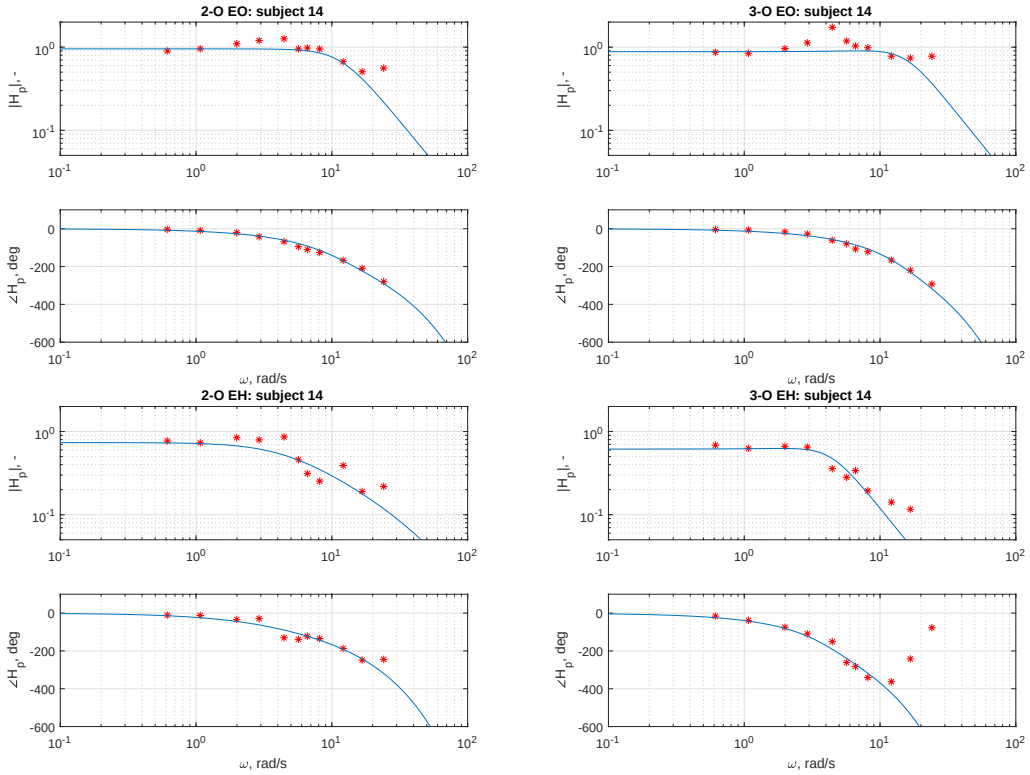

HAND

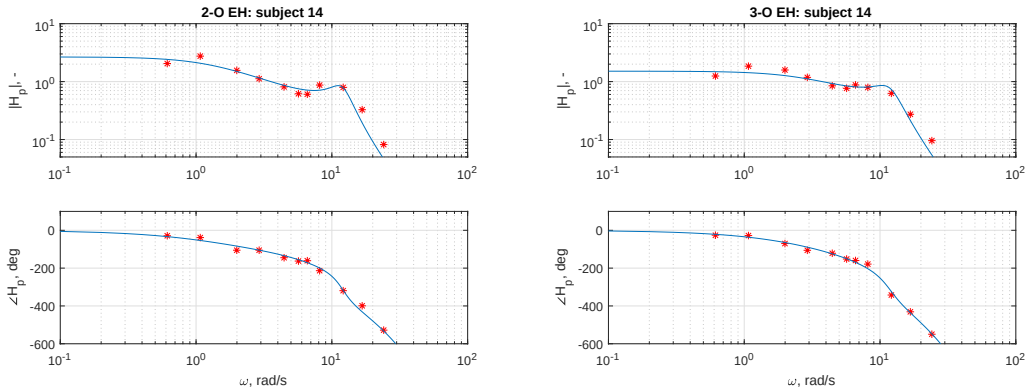

Figure C-34: FRF with fitted models for the gaze dynamics and the hand dynamics of subject 14.

C-2-15 Models Participant 15

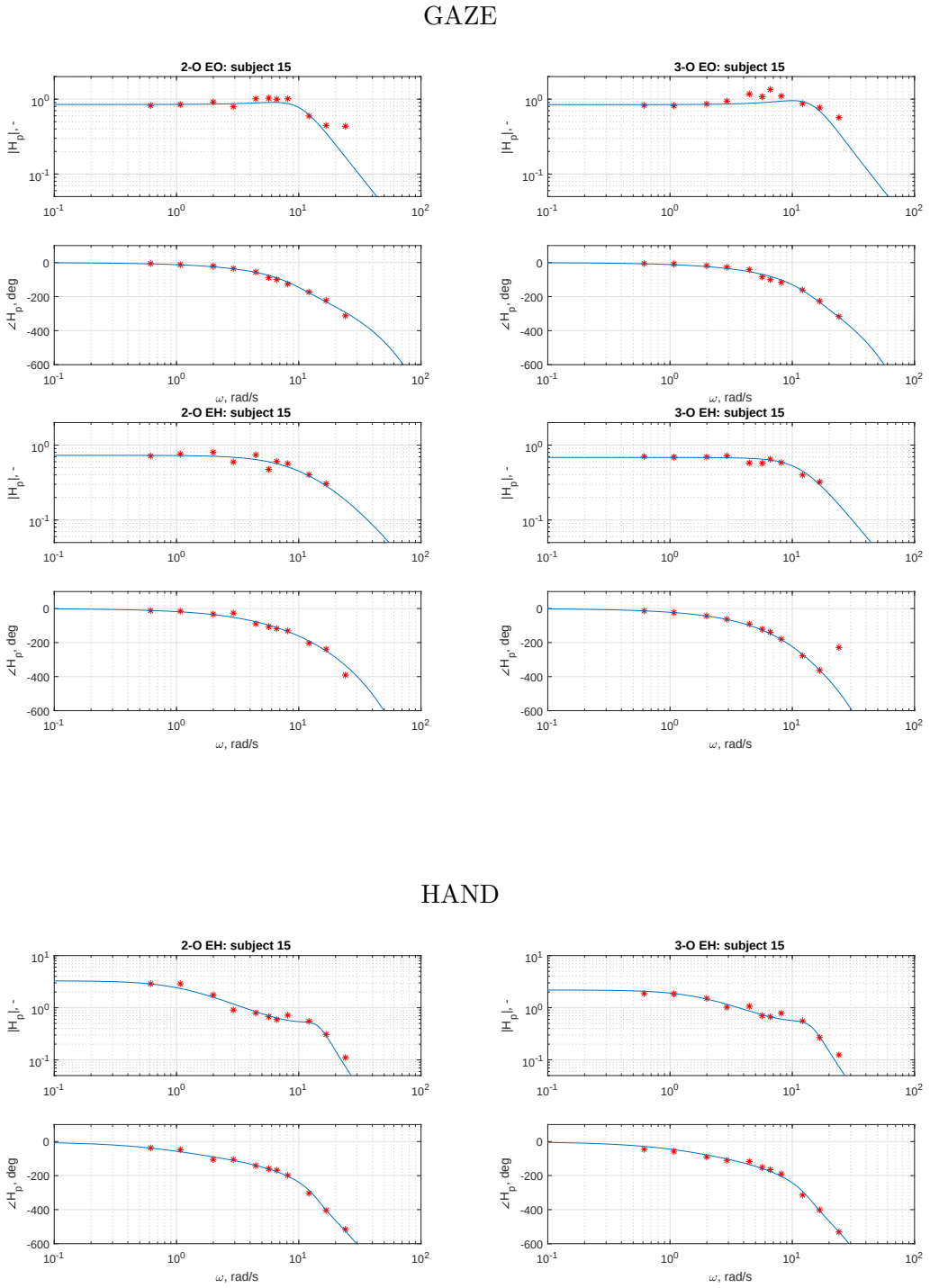

Figure C-35: FRF with fitted models for the gaze dynamics and the hand dynamics of subject 15.

C-2-16 Models Participant 16

GAZE

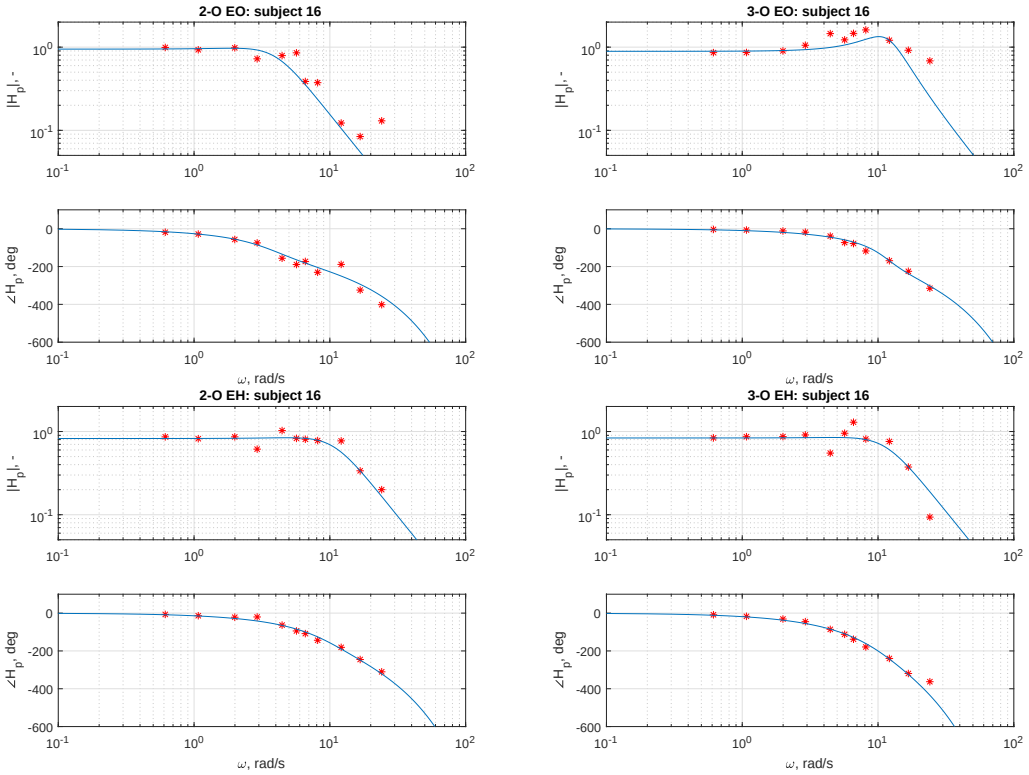

HAND

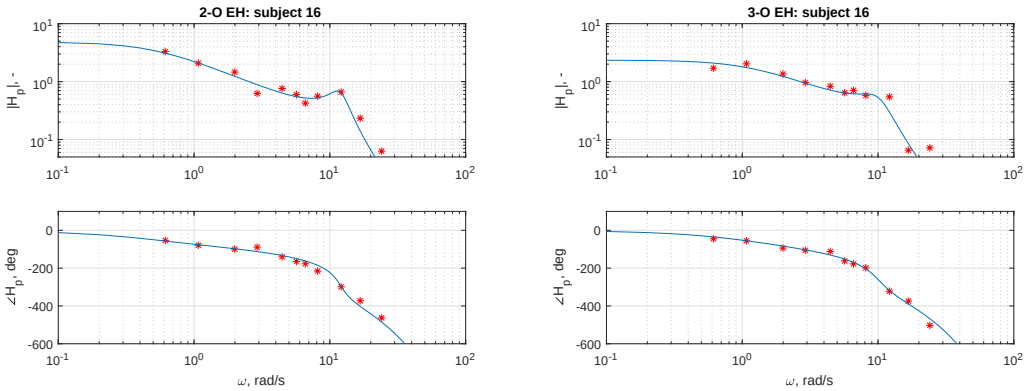

Figure C-36: FRF with fitted models for the gaze dynamics and the hand dynamics of subject 16.

C-2-17 Models Participant 17

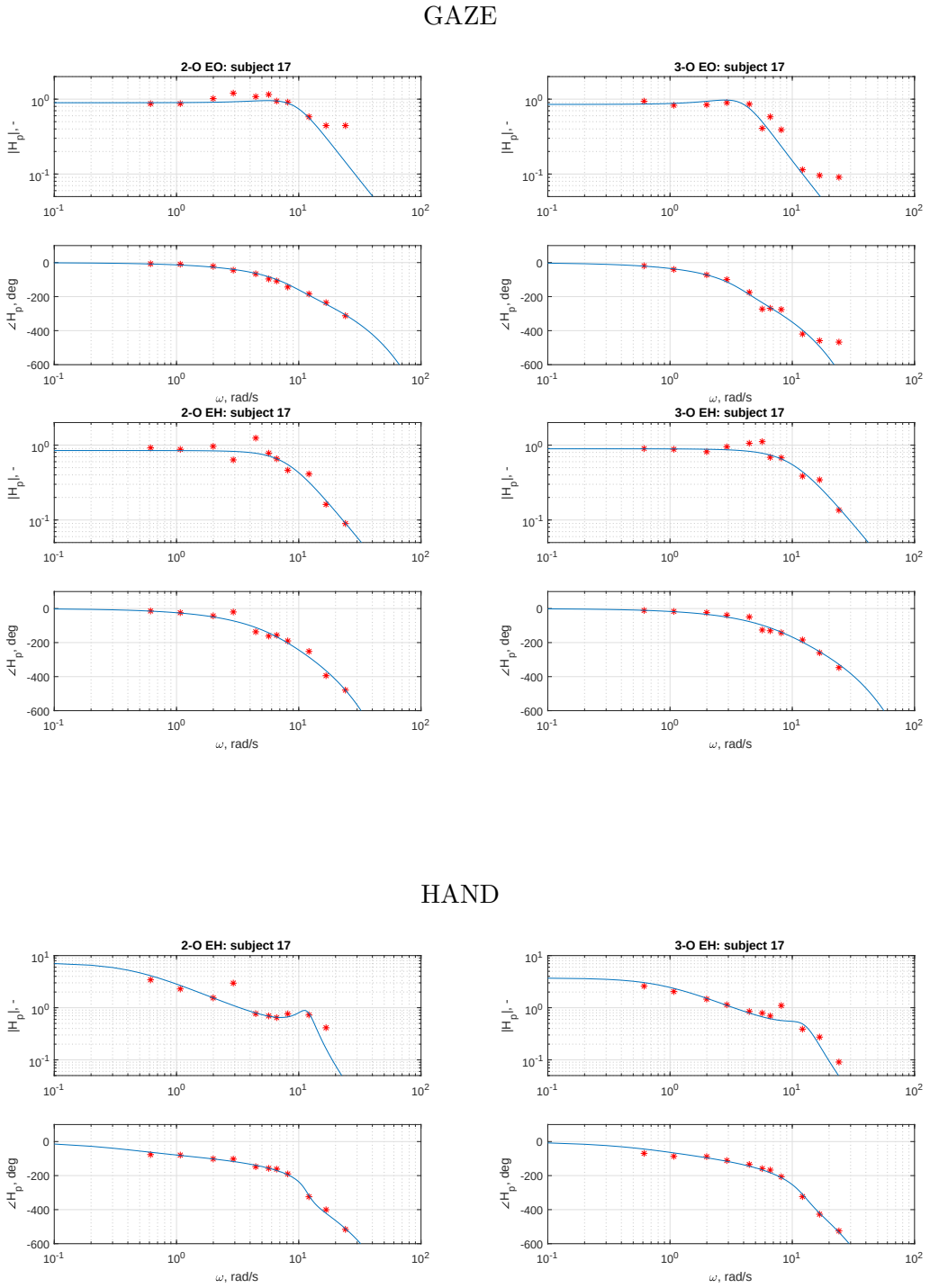

Figure C-37: FRF with fitted models for the gaze dynamics and the hand dynamics of subject 17.

C-2-18 Models Participant 18

GAZE

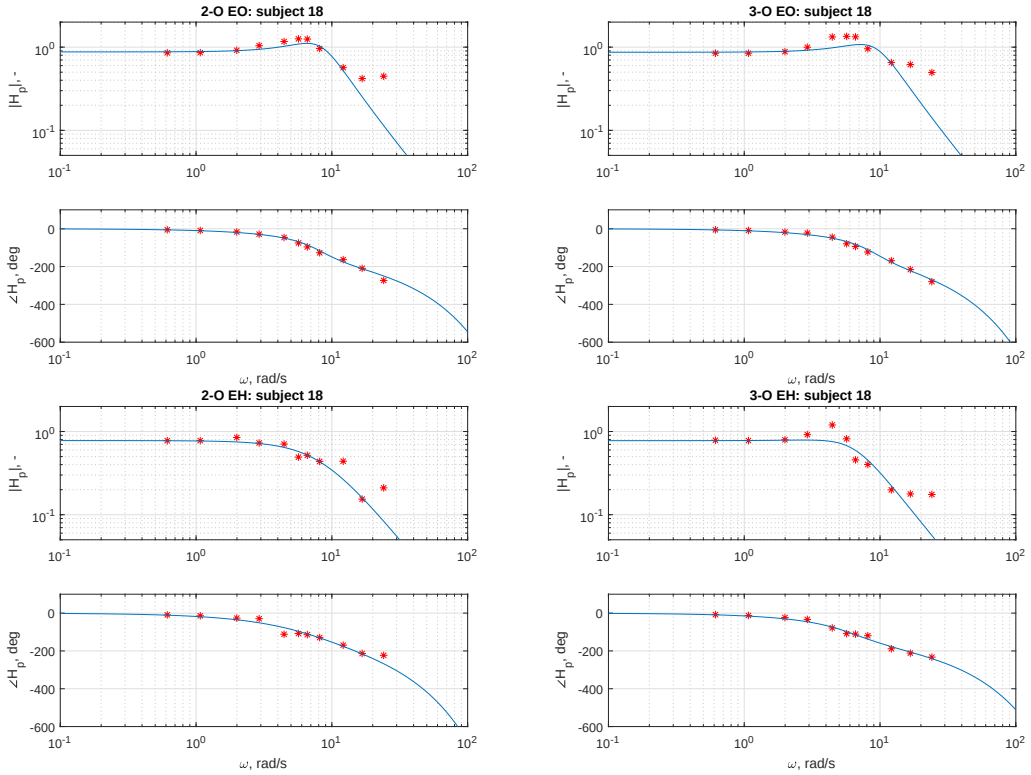

HAND

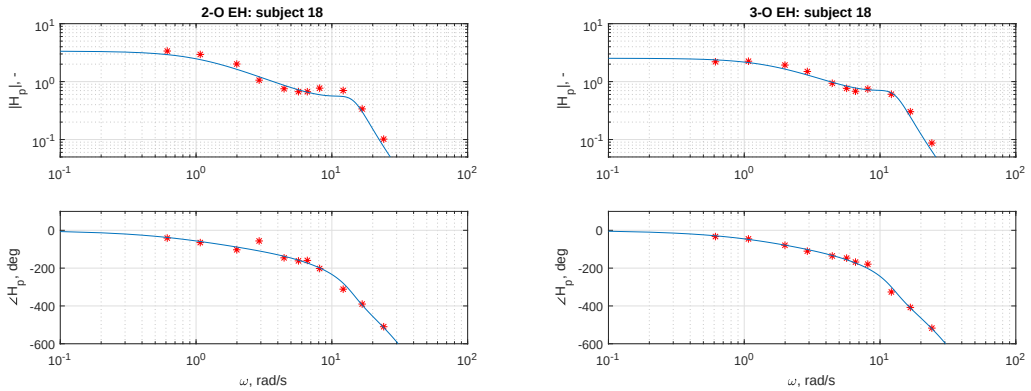

Figure C-38: FRF with fitted models for the gaze dynamics and the hand dynamics of subject 18.

C-2-19 Models Participant 19

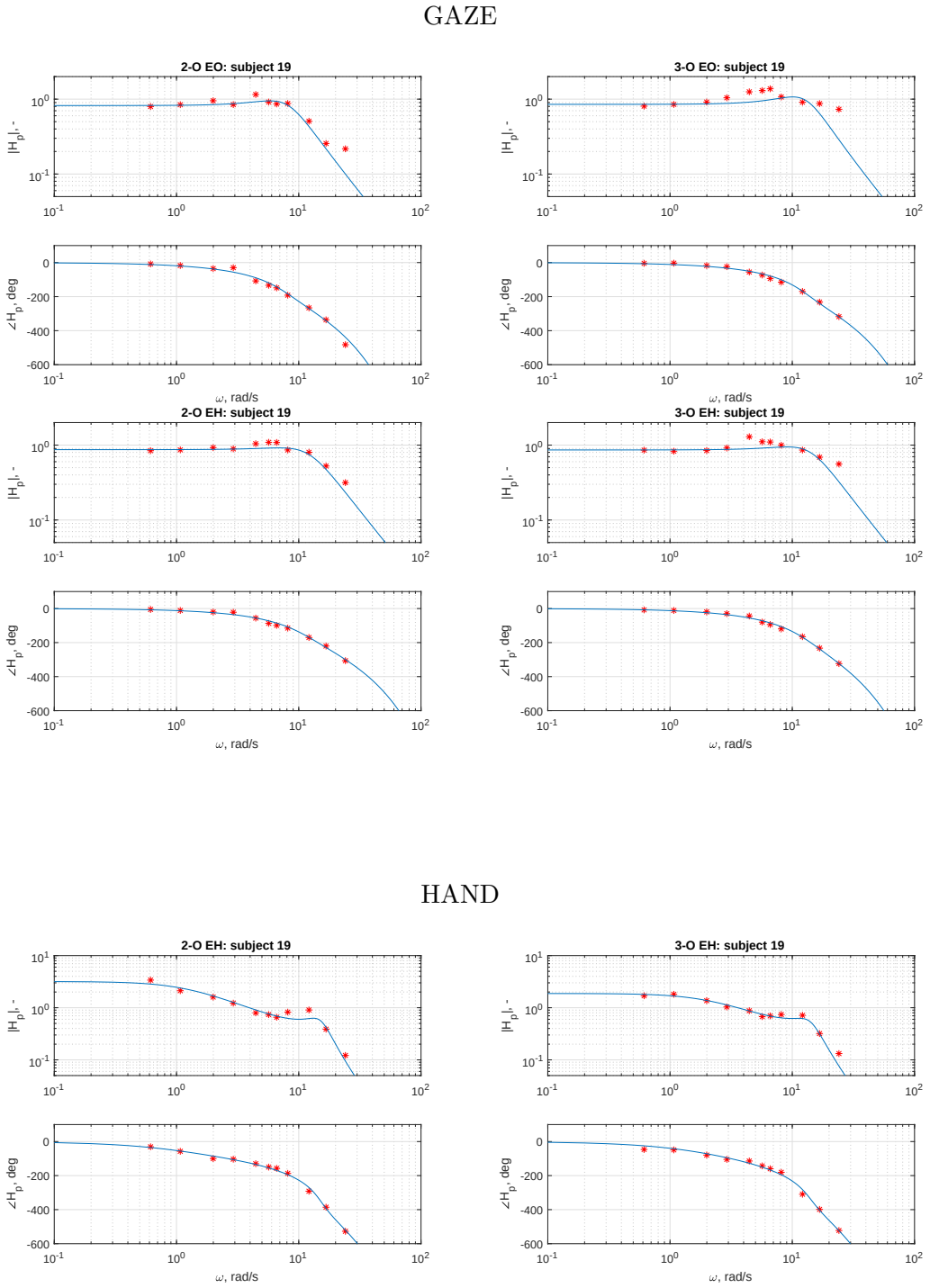

Figure C-39: FRF with fitted models for the gaze dynamics and the hand dynamics of subject 19.

C-2-20 Models Participant 20

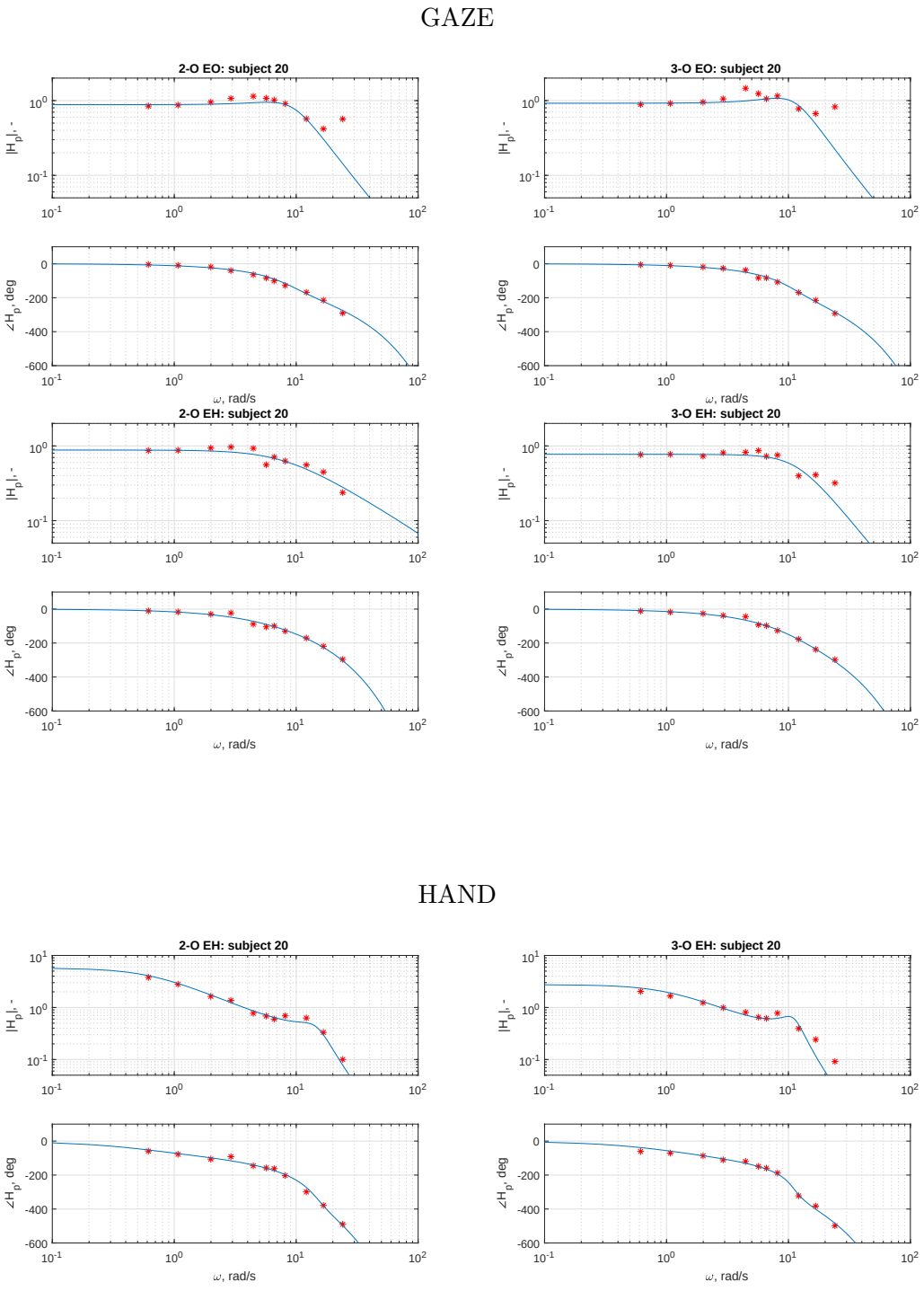

Figure C-40: FRF with fitted models for the gaze dynamics and the hand dynamics of subject 20.

Appendix D

Crossover frequencies and Phase shifts

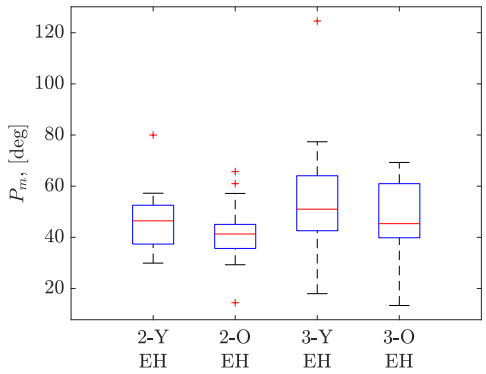

Figure D-1: Phase margin

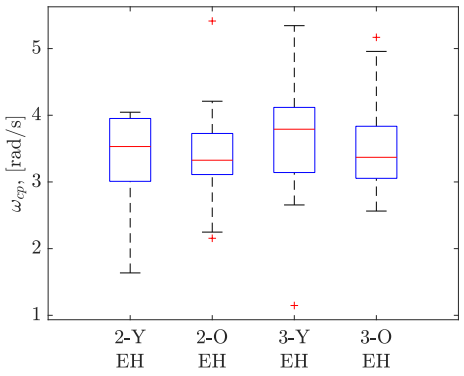

Figure D-2: Crossover frequencies at phase margin

Bibliography

Agrawal, M., & Biswas, A. (2015). Molecular diagnostics of neurodegenerative disorders. *Frontiers in molecular biosciences*, *2*, 54. doi: 10.3389/fmolb.2015.00054

Amin, M. S. (2016). *Vestibuloocular Reflex Testing: Overview, Technique, Impact of Age on the Vestibuloocular Reflex.* Retrieved 2017-11-16, from `https://emedicine.medscape.com/article/1836134-overview`

Ang, B. (2010). *Stereopsis and Binocular Vision - How Both Eyes Work Together.* Retrieved 2017-12-04, from `http://www.vision-and-eye-health.com/stereopsis.html`

Armstrong, R. A. (2011). Visual Symptoms in Parkinson's Disease. *SAGE-Hindawi Access to Research Parkinson's Disease*, *908306*. doi: 10.4061/2011/908306

de Vries, R. (2015). *A tracking task for quantifying loss of motor skills due to parkins's disease* (Unpublished M.Sc. Thesis). Faculty of Aerospace Engineering, Delft University of Technology.

Dowiasch, S., Marx, S., Einhäuser, W., Bremmer, F., Foxe, J. J., Einstein, A., ... Carvalho, N. (2015). Effects of aging on eye movements in the real world. *Frontiers in Neuroscience*. doi: 10.3389/fnhum.2015.00046

Dubois, B., Slachevsky, A., Litvan, I., & Pillon, B. (2000, dec). The FAB: a Frontal Assessment Battery at bedside. *Neurology*, *55*(11), 1621–6. doi: 10.1212/WNL.55.11.1621

Engel, K. C., Anderson, J. H., & Soechting, J. F. (2000). Similarity in the response of smooth pursuit and manual tracking to a change in the direction of target motion. *Journal of Neurophysiology*. doi: 10.1152/jn.2000.84.3.1149

Fahn, S., & Elton, R. (1987). Unified parkinson's disease rating scale. *Recent Developments in Parkinson's Disease*, *2*, 153–163.

Flowers, K. A. (1976). Visual 'closed-loop' and 'open-loop' characteristics of voluntary movement in patients with parkinsonism and intention tremor. *Brain*, *99*(2), 269–310. doi: 10.1093/brain/99.2.269

Folstein, M. F., Folstein, S. E., & McHugh, P. R. (1975). Mini-mental state. a practical method for grading the cognitive state of patients for the clinician. *Journal of psychiatric research*, *12*(3), 189–98. doi: 10.1016/0022-3956(75)90026-6

Fozard, J. L., Vercruyssen, M., Reynolds, S. L., Hancock, P. A., & Quilter, R. E. (1994). Age differences and changes in reaction time: The baltimore longitudinal study of aging. *Journal of Gerontology*, *49*(4), P179–P189. doi: 10.1093/geronj/49.4.P179

Goetz, C. G., Fahn, S., Martinez-Martin, P., Poewe, W., Sampaio, C., Stebbins, G. T., ... LaPelle, N. (2007, jan). Movement Disorder Society-sponsored revision of the Unified Parkinson's Disease Rating Scale (MDS-UPDRS): Process, format, and clinimetric testing plan. *Movement Disorders*, *22*(1), 41–47. doi: 10.1002/mds.21198

Haartsen, Y. (2017). *Quantifying loss of motor skills after cerebellar stroke* (Unpublished preliminary M.Sc. Thesis). Faculty of Aerospace Engineering, Delft University of Technology.

Hanes, D. P., & Wurtz, R. H. (2000). Interaction of the frontal eye field and superior colliculus for saccade generation. *Journal of Neurophysiology*. doi: 10.1152/jn.2001.85.2.804

Hejtmancik, J. F., & Nickerson, J. M. (2017). *Conn's translational neuroscience*. doi: 10.1016/B978-0-12-802381-5.00031-2

Hoehn, M. M., & Yahr, M. D. (1998, feb). Parkinsonism: onset, progression, and mortality. 1967. *Neurology*, *50*(2), 318 and 16 pages following. doi: doi:10.1212/WNL.17.5.427

Khodadadian, S. (2017). *Muscles of the eye.* Retrieved from `https://www.eyedoctorophthalmologistnyc.com/treatment/macular-degeneration/`

Koken, P. W., & Erkelens, C. J. (1991). Influences of hand movements on eye movements in tracking tasks in man. *Experimental Brain Research*, 657–664.

Krauzlis, R. J. (2003). Neuronal Activity in the Rostral Superior Colliculus Related to the Initiation of Pursuit and Saccadic Eye Movements. *The Journal of Neuroscience*.

Krendel, E. S., & McRuer, D. T. (1960). A servomechanisms approach to skill development. *J. Franklin Inst.*. doi: 10.1016/0016-0032(60)90245-3

Kreutzer, J. S., DeLuca, J., & Caplan, B. (2011). *Encyclopedia of Clinical Neuropsychology*. doi: 10.1007/978-0-387-79948-3

Ludwig, C. J. H., Davies, J. R., Eckstein, M. P., & Wurtz, R. H. (2014). Foveal analysis and peripheral selection during active visual sampling. *Psychological and Cognitive Sciences*. doi: 10.1073/pnas.1313553111

Mays, L. E. (1984). Neural control of vergence eye movements: convergence and divergence neurons in midbrain. *Journal of neurophysiology*, *51*(5), 1091–1108. doi: 10.1152/jn.1984.51.5.1091

McRuer, D., Graham, D., Krendel, E., & Reisener, W. (1965). *Human Pilot Dynamics in Compensatory Systems, Theory Models and Experiments with Controlled Element and Forcing Function Variations* (Tech. Rep.). The Franklin Insitute.

McRuer, D. T., & Jex, H. R. (1967). A Review of Quasi-Linear Pilot Models. *IEEE Transactions on Human Factors in Electronics*, *HFE-8 No 3*.

Molitor, R. J., Ko, P. C., & Ally, B. A. (2015). Eye Movements in Alzheimer's Disease. *Journal of Alzheimer's Disease*, *44*, 1–12. doi: 10.3233/JAD-141173

Mulder, M., Pool, D. M., Abbink, D. A., Boer, E. R., Zaal, P. M. T., Drop, F. M., ... van Paassen, M. M. (2017). Manual control cybernetics: State-of-the-art and current trends. *IEEE Transactions on Human-Machine Systems*, 1–18. doi: 10.1109/THMS.2017.2761342

Myers, C. E. (2006). *The cerebellum.* Retrieved from `http://www.memorylossonline.com/glossary/cerebellum.html`

Niehorster, D. C., & Siu, W. W. F. (2015). Manual tracking enhances smooth pursuit eye movements. *Journal of Vision*, *15*(2015), 1–14. doi: 10.1167/15.15.11.doi

Nieuwenhuizen, F. M., Zaal, P. M. T., Mulder, M., Van Paassen, M. M., & Mulder, J. A. (2008). Modeling Human Multichannel Perception and Control Using Linear Time-Invariant Models. *Journal of Guidance, Control and Dynamics*. doi: 10.2514/1.32307

Peters, R. (2006). Ageing and the brain. *Postgrad Med J*, *82*, 84–88. doi: 10.1136/pgmj.2005.036665

Purves, D. (2004). *Neuroscience, 3rd Edition.* Sinauer Associates.

Raz, N. (2004, apr). The aging brain: Structural changes and their implications for cognitive aging. In *New frontiers in cognitive aging* (pp. 115–134). Oxford University Press. doi: 10.1093/acprof:oso/9780198525691.003.0006

Remington, L. A. (2012). Chapter 10 Extraocular Muscles. In *Clinical anatomy and physiology of the visual system* (pp. 182–201). doi: 10.1016/B978-1-4377-1926-0.10010-4

Scarchilli, K., & Vercher, J.-L. (1999). The oculomotor coordination control center takes in account the mechanical properties of the arm. *Exp Brain Res*, *124*, 42–52.

Seidler, R. D., Bernard, J. A., Burutolu, T. B., Fling, B. W., Gordon, M. T., Gwin, J. T., ... Lipps, D. B. (2010). Motor Control and Aging: Links to Age-Related Brain Structural, Functional, and Biochemical Effects. *Neurosci Biobehav Rev*, *34*(5), 721–733. doi: 10.1016/j.neubiorev.2009.10.005

Shibasaki, H., Tsuji, S., & Kuroiwa, Y. (1979). Oculomotor abnormalities in parkinson's disease. *Archives of neurology*, *36 6*, 360-4.

Sparks, D. L. (2002). The Brainstem Control of Saccadic Eye Movements. *Nature*, *3*, 952–964. doi: 10.1038/nrn986

Squire, L. R. (2009). *Oculomotor system: Models.* Retrieved from `http://www.sciencedirect.com/topics/medicine-and-dentistry/oculomotor-system`

Stanley, J., & Swierzewski, M. D. (2015). *Alzheimer's Disease Overview, Brain Anatomy - Alzheimer's Disease - HealthCommunities.com.* Retrieved 2017-11-17, from `http://www.healthcommunities.com/alzheimers-disease/overview-of-alzheimers.shtml`

Swenson, R., Cohen, J., Fadul, C., Jenkyn, L., & Ward, T. (2008). *Extraocular movements.* Retrieved from `https://www.dartmouth.edu/~dons/part_1/chapter_4.html`

The Crankshaft Publishing. (2017). *The visual system (sensory system).* Retrieved from `http://what-when-how.com/neuroscience/visual-system-sensory-system-part-3/`

Thier, P., & Ilg, U. J. (2005). The neural basis of smooth-pursuit eye movements. *Current Opinion in Neurobiology*, *15*, 645–652. doi: 10.1016/j.conb.2005.10.013

Trollor, J. N., & Valenzuela, M. J. (2001). Brain ageing in the new millennium. *Australian and New Zealand Journal of Psychiatry*, *35*, 788-805. doi: 10.1046/j.1440-1614.2001.00969.x

van der El, K., Pool, D. M., Damveld, H. J., van Paassen, M. M., & Mulder, M. (2016). An empirical human controller model for preview tracking tasks. *IEEE Transactons on Cybernetics*, *46*(11).

Waitzman, D. (2017). Oculomotor Systems and Control. In *Conn's translational neuroscience* (pp. 439–465). Elsevier. doi: 10.1016/B978-0-12-802381-5.00032-4

Wang, J. L. (2017). *Biology/electronics-depth perception and 3d movie.* Retrieved from `http://howthingswork.org/biologyelectronics-depth-perception-and-3d-movie/`